Archived version from NCDOCKS Institutional Repository http://libres.uncg.edu/ir/asu/

Appalachian
STATE UNIVERSITY
BOONE, NORTH CAROLINA

Southeastern Geology: Volume 38, No. 1 September 1998

Editor in Chief: S. Duncan Heron, Jr.

Abstract

Academic journal published quarterly by the Department of Geology, Duke University.

Heron, Jr., S. (1998). Southeastern Geology, Vol. 38 No. 1, September 1998. Permission to re-print granted by Duncan Heron via Steve Hageman, Professor of Geology, Dept. of Geological & Environmental Sciences, Appalachian State University.

SOUTHEASTERN GEOLOGY

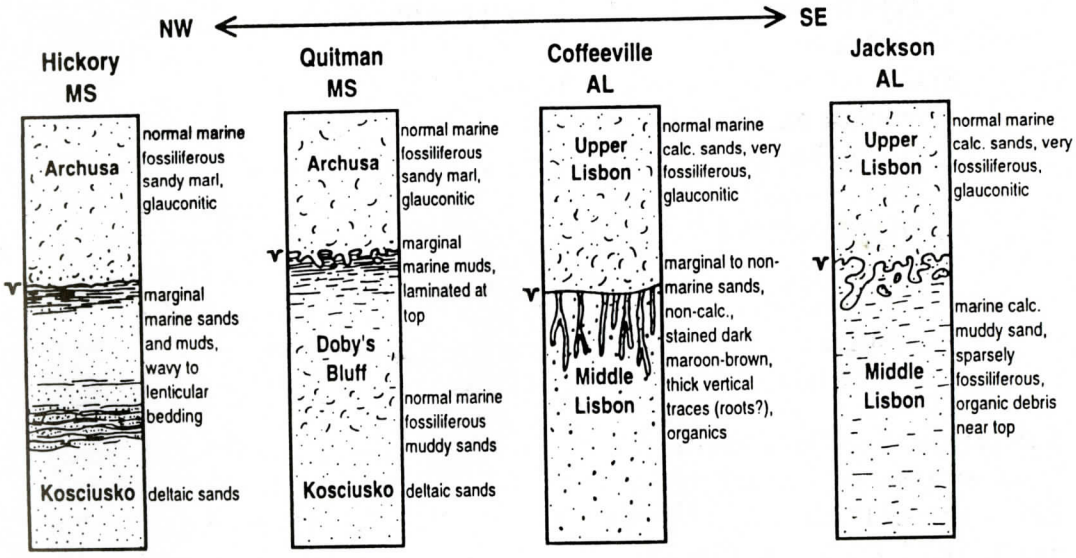

VOL. 38, NO. 1 SEPTEMBER 1998

SOUTHEASTERN GEOLOGY

PUBLISHED

at

DUKE UNIVERSITY

Editor in Chief:

Duncan Heron

This journal publishes the results of original research on all phases of geology, geophysics, geochemistry and environmental geology as related to the Southeast. Send manuscripts to **DUNCAN HERON, DUKE UNIVERSITY, BOX 90233, DURHAM, NORTH CAROLINA 27708-0233**. Phone: 919-684-5321, Fax: 919-684-5833, Email: heron@geo.duke.edu Please observe the following:

1) Type the manuscript with double space lines and submit in duplicate.
2) Cite references and prepare bibliographic lists in accordance with the method found within the pages of this journal.
3) Submit line drawings and complex tables reduced to final publication size (no bigger than 8 x 5 3/8 inches).
4) Make certain that all photographs are sharp, clear, and of good contrast.
5) Stratigraphic terminology should abide by the North American Stratigraphic Code (American Association Petroleum Geologists Bulletin, v. 67, p. 841-875).

Subscriptions to *Southeastern Geology* for volume 38 are: individuals - $18.00 (paid by personal check); corporations and libraries - $24.00; foreign $28. Inquires should be sent to: **SOUTHEASTERN GEOLOGY, DUKE UNIVERSITY, BOX 90233, DURHAM, NORTH CAROLINA 27708-0233**. Make checks payable to: *Southeastern Geology.*

Information about SOUTHEASTERN GEOLOGY is on the World Wide Web including a seachable author-title index 1958-1996. The URL for the Web site is:

http://www.geo.duke.edu/seglgy.htm

SOUTHEASTERN GEOLOGY is a peer review journal.

ISSN 0038-3678

SOUTHEASTERN GEOLOGY

Table of Contents

Volume 38, No. 1

September 1998

SERIALS DEPARTMENT
APPALACHIAN STATE UNIV. LIBRARY
BOONE NC

SOUTHEASTERN GEOLOGY
V. 38, No. 1, September 1998, p. 1-20

SEQUENCE STRATIGRAPHY OF THE MIDDLE EOCENE CLAIBORNE STAGE, US GULF COASTAL PLAIN

LINDA C. IVANY

Museum of Paleontology and Department of Geological Sciences
University of Michigan
1109 Geddes Road, Ann Arbor, MI 48109
ivany@umich.edu

ABSTRACT

I present a stratigraphic analysis of the middle Eocene Claiborne Stage in Alabama and Mississippi based on surface exposures and conducted from the perspective of sequence stratigraphy. Sequences were identified based on observed lithologic transitions, with key surfaces and positions within a sequence often marked also by distinctive trace fossil horizons. Three third order sequences corresponding to the Tallahatta, lower/middle Lisbon, and upper Lisbon (Cook Mountain) Formations were recognized in outcrop-based studies. A previously unrecognized fourth sequence of similar magnitude was identified in the upper part of the upper Lisbon and may correlate with one reported from the subsurface. Smaller scale parasequence development within these sequences is also noted, and may in some cases be useful for correlation. This analysis will allow a better understanding of smaller-scale regional correlations and relative sea-level change through time in the Eastern Gulf Coastal Plain. Some uncertainty remains as to whether the Claiborne cycles are eustatic in origin, but the general agreement of my interpretations with the Haq and others (1987) curve and with workers in Texas and the Atlantic Coastal Plain suggests, with some exceptions, primary control by global sea level fluctuation.

INTRODUCTION

The Gulf Coastal Plain Paleogene section is one of the better known and more intensively studied stratigraphic sections in North America. Many studies based on core and well-log work have been done, yet correlations within and even between some of the major stratigraphic units remain unclear, particularly at the outcrop scale. Some of the outstanding questions and discrepancies may be resolvable with intensive field checking of hypotheses generated from downdip subsurface work.

In the following text, I present a stratigraphic analysis of the middle Eocene Claiborne Stage in the eastern Gulf Coastal Plain based on field studies of surface outcrops in western Alabama and eastern Mississippi (Fig. 1). The analysis is done within the framework of sequence stratigraphy, at least to the extent allowed by the limited surface exposures along strike. Sequences are identified, and position within a sequence is determined, by observed lithologic transitions and distinctive trace fossil horizons. I discuss the agreement of my interpretations with the presumably eustatic Haq and others (1987) curve and others from the Gulf and Atlantic Coast in an effort to distinguish global from regional or local sea-level changes.

METHODS

The division of a stratigraphic section into depositional sequences and their component systems tracts requires the recognition of key, regionally persistent surfaces: sequence boundaries, transgressive surfaces, and maximum flooding surfaces. These are generally surfaces of non-deposition or erosion in proximal shelf settings, and were identified and distinguished in this study using the criteria discussed by Van Wagoner and others (1988), Baum and Vail

Figure 1. Map of Alabama and Mississippi showing pertinent counties and geographic coverage of outcrop localities. In all, over 50 localities were visited for the completion of this study. Some are not represented on this map for sake of clarity.

(1988), and Mancini and Tew (1993).

Sequence boundaries are unconformities and their correlative conformities that separate packages of rock deposited during a single rise and fall of relative sea level change. In shelf settings, sequence-bounding unconformities are generated by relative sea-level fall and are marked by burrowed or bored surfaces, rip-up clasts from the underlying unit, lag deposits, abundant detrital glauconite and/or phosphate, and increasing terrigenous components (*e.g.*, mica, organic matter). Type I sequence boundaries, formed when sea level drops below the level of the shelf edge, involve much erosive scour and incisement of the shelf, and the abrupt transition from relatively deeper-water facies below to shallow or exposed conditions above. Type II boundaries may also involve subaerial exposure, but generally not significant subaerial erosion (Van Wagoner and others, 1990). They are marked by the transition from shallowing sediments below into aggradational or deepening facies above, but without the drastic change of facies seen in Type I boundaries (Van Wagoner and others, 1988). Shelf margin or incised valley deposits are not always present, and in such cases the sequence boundary converges with the transgressive surface.

It is often difficult to distinguish Type I from Type II boundaries in outcrop sections, particularly if one cannot trace the unconformity into deeper facies. For this reason, I have relied on previous workers' conclusions regarding the nature of the sequence boundaries within this supercycle based on their work in the subsurface and other Coastal Plain sections (*e.g.*, Powell and Baum, 1982; Baum and Vail, 1988; Mancini and Tew, 1993).

Transgressive surfaces mark the first substantial rise in relative sea level within a sequence (Van Wagoner and others, 1988), and are identified by burrowed surfaces, rip-up clasts, angular quartz grains, shell lags - often with reworked fossils and shark teeth, and progressively deepening facies above. Initial transgressive deposits often represent slightly higher energy facies than those below the surface, particularly when shelf margin deposits are absent.

The surface of maximum sediment starvation, or maximum flooding surface, is located within the condensed section and is marked by bored and encrusted substrates, much authigenic glauconite, submarine cementation, and an abundance of fine-grained, deep-water depos-

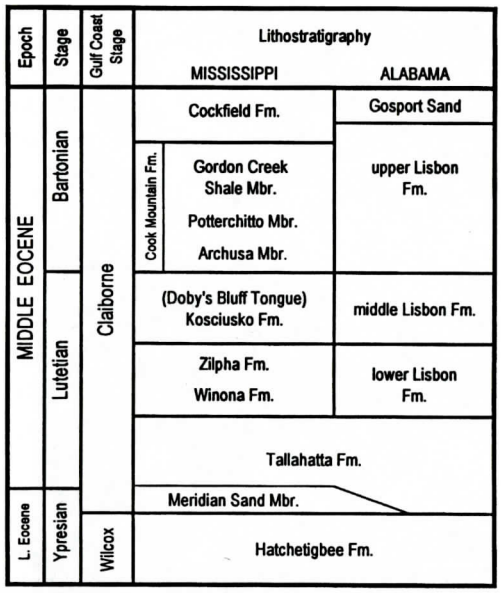

Figure 2. Claiborne Stage lithostratigraphy, showing equivalent units in Alabama and Mississippi.

its. In more proximal settings where the condensed section is not evident, the surface may only be marked by the transition from transgressive to regressive deposits. This surface, and the condensed section in general, is the most useful for stratigraphic correlation as it represents a synchronous time horizon across the shelf and slope and tends to concentrate age-diagnostic fossils (Loutit and others, 1988).

CLAIBORNE STAGE SEQUENCE STRATIGRAPHY

The Claiborne Stage includes the Tallahatta and Lisbon formations and the Gosport Sand in Alabama and their equivalents in Mississippi (Fig. 2). Sediments are generally marine sands and silts deposited in an open shelf setting. Formations become thicker and more proximal from east to west, and hence units in Mississippi are more finely subdivided due to the more pronounced facies changes associated with shallower deposition.

The Claiborne Stage encompasses a single large supercycle in sea-level change (Tb of Powell and Baum, 1982, and Poag and Ward, 1987; Tc of Baum and Vail, 1988, Mancini and Tew, 1993, and Baum and others, 1994). The base of the Claiborne Stage in the Gulf Coast is clearly marked by a Type I unconformity between the Hatchetigbee Formation and the overlying Meridian Sand Member of the Tallahatta Formation, showing erosional truncation of underlying beds and ensuing deposition of nearshore lowstand sands (Fig. 3A). The top of the supercycle, also clearly marked by a Type I unconformity, falls at the contact between the Lisbon Formation and the Gosport Sand (not at the top of the Gosport Sand, which is the uppermost formation of the Claiborne Stage) in Alabama (Fig. 3B), or within the Cockfield Formation in Mississippi at the contact between clean cross-bedded nearshore sands below and lignitic sand above (Mancini and Tew, 1994).

Within the Claiborne Stage supercycle in the Gulf Coast, Baum and Vail (1988) and Baum and others (1994) recognize three third order sequences corresponding to the Tallahatta Formation, lower/middle Lisbon Formation, and upper Lisbon Formation and their equivalents, while Mancini and Tew (1993) recognize a fourth in the middle Lisbon Formation. Third order sequences within the Claiborne Stage are separated by Type II unconformities characterized by heavily burrowed surfaces, and each exhibits (to varying degrees of development) the characteristic transgressive, condensed, and highstand deposits of a standard depositional sequence (*sensu* Van Wagoner, 1988). Sediments are mainly glauconitic calcareous sands, but transgressive systems tracts tend to be more marly while highstand deposits contain more terrigenous muds. Based on this field study, I recognize the three sequences of Baum and Vail (1988) and Baum and others (1994) plus an additional sequence in the upper part of the upper Lisbon Formation that has not previously been identified in Gulf Coast outcrop studies. The middle Lisbon Formation sequence of Mancini and Tew (1993) is clearly present locally but appears to be geographically restricted.

Tallahatta Formation

The TE 2.1 cycle (Baum and Vail, 1988; Mancini and Tew, 1993) of the Tallahatta For-

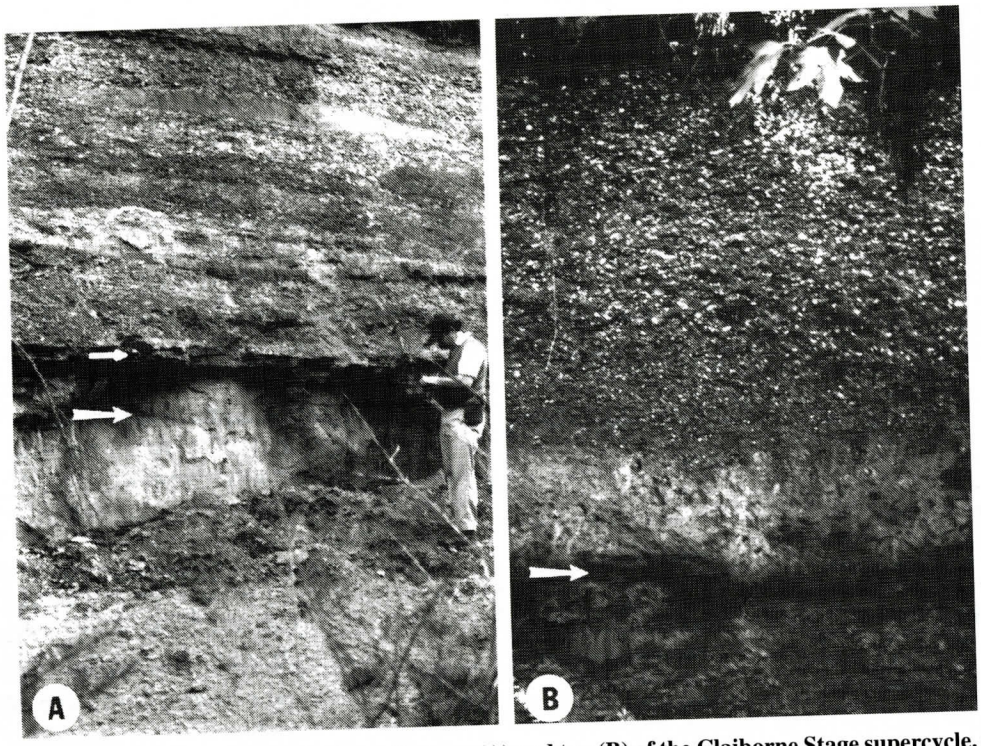

Figure 3. Type I sequence boundaries at the base (A) and top (B) of the Claiborne Stage supercycle. (A) Paul Morris stands at the contact between the fine-grained sands of the Hatchetigbee Formation and the bedded quartz sands of the Meridian Sand. Both units are relatively unconsolidated here and hence weather back beneath the more indurated marine silts and sands of the Tallahatta Formation above. The contact, marked with a thick white arrow, is undulatory and deeply burrowed. The transgressive surface (thin white arrow) is easily discerned at the base of the indurated portion of the section. Locality ACl-13. (B) Contact between the dark gray silty clays at the top of the Lisbon Formation and the overlying lighter colored, extremely fossiliferous, transgressive sands of the Gosport Sand as seen at Little Stave Creek (photo by Ken Schopf). White arrow marks the sequence boundary and contact. Locality ACl-4.

mation begins with the deposition of the Meridian Sand, a medium to fine grained, moderate to well-sorted, white to pale yellow quartz sand that rests on the scoured and undulatory surface of the Hatchetigbee Formation. Deep, branching, near-vertical, sand-filled burrows resembling root traces penetrate at least a meter down from the contact into the Hatchetigbee Formation at Lower Peach Tree, AL (Locality ACl-13; see Appendix A). South of Butler, AL (Locality ACh-16), the contact is marked by thick corkscrew-shaped *Gyrolithes* burrows extending from the Meridian Sand down into the light purple-brown micaceous clayey sand of the Hatchetigbee Formation. The Meridian Sand is cross-bedded on a large scale, with long low-angle foresets characteristic of tabular cross-stratification. Trace fossils of the *Skolithos* ichnofacies are common constituents of the unit (Reynolds,1992). These characteristics are consistent with a shoreface or foreshore depositional environment.

Lowstand sands are capped by a well-defined transgressive surface (Fig. 3A) leading into the marine silts and fine-grained sands of the Tallahatta Formation. At both Butler and Lower Peach Tree, AL (Localities ACh-16 and ACl-13), the transition is abrupt but apparently conformable, for sands grade into silts (former) or are interbedded with them on a decimeter scale for up to 1 meter of stratigraphic thickness (latter). The transgressive surface is characterized

by the spiral burrow *Gyrolithes* and elaborate networks of *Thalassinoides* (see Fig. 9A). Burrows are generally well-cemented and stained orange-brown, likely from oxidation of iron-bearing heavy minerals in the Meridian Sand (mostly ilmenite; Reynolds, 1992) or glauconite in the Tallahatta Formation.

The Tallahatta Formation is atypical for the Claiborne, and indeed for the entire Gulf Coast Paleogene, because of the abundance of very fine grained, indurated, biosiliceous (diatomaceous) sediment locally called *buhrstone*, suggesting highly productive overlying waters (Laws and Thayer, 1992). The predominance of such fine-grained, hemipelagic deposits suggests that the deepest water conditions for the entire Claiborne interval were reached during Tallahatta time, with deposition likely on the outer shelf during maximum transgression. Upwelling of nutrient-rich waters along the shelf edge may have facilitated diatom production and led to the accumulation of buhrstone. The first signs of global cooling at this time also may have changed the solubility of silica in the oceans, leading to the "silica burp" proposed by McGowran (1989). The Tallahatta Formation burhstone may be a reflection of this phenomenon.

Buhrstone is more prevalent in the lower and middle part of the formation, in the transgressive systems tract and condensed interval, while highstand deposits tend to contain more terrigenous silts and sands. The Tallahatta Formation is bedded on a centimeter to decimeter thick scale in most outcrops and bioturbation is extensive, characterized by centimeter-scale and larger horizontal and oblique, often backfilled burrows. Less indurated, sandier interbeds tend to exhibit more bioturbation than silicified layers, but this may be due to enhanced visibility of burrows caused by differential weathering. Buhrstone beds capped by cm-scale burrowed surfaces that separate them from overlying coarse, indurated, glauconitic sand layers are relatively common throughout, suggesting small-scale cyclicity in relative sea-level change and short hiatuses in deposition. Macrofossils are present, both as isolated shells in presumed life position (*e.g.*, the bivalve *Anodontia*) and as thin shelly pavements (particularly in the top third of the section exposed at Meridian, MS, Locality MLa-4), but originally aragonitic shells are always moldic.

At the top of the Tallahatta in eastern Mississippi, marine sands and silts grade into marginal marine laminated mudrock below the contact with weathered iron-stained Winona (lower Lisbon) Formation sands. The transition from marine into marginal marine is well-exposed at the Meridian, MS, outcrop (Locality MLa-4), where it is characterized by the loss of bioturbation and body fossils, a shift to gray, chippy to papery-laminated mudstone overlain by yellow-stained laminated clay, and the presence of *Gyrolithes* burrows. All observed exposures preserving the contact with the overlying Winona Formation are deeply weathered due to more recent oxidation of iron in the Winona; nevertheless, the contact appears not to be erosional. The transgressive surface at the Meridian outcrop (Locality MLa-4) is coincident with the sequence boundary and marked by a red cemented ironstone bed at the base of the Winona Formation sand. Sediment in the ironstone is mostly fine to medium grained sand, with some very coarse-grained quartz sand stringers and dark red mud rip-up clasts. Glauconite was likely abundant in its original state, providing the iron that later oxidized and stained the unit red.

In Alabama, however, the contact is expressed in several different ways. At Little Stave Creek, the top of the Tallahatta Formation is extremely hard, fine-grained, brown-black buhrstone irregularly scoured and capped by very coarse-grained, glauconitic, fossiliferous, marly, indurated sand of the lower Lisbon Formation (Locality ACl-4; Fig. 4). The contact is bored to a depth of about a decimeter by cm-wide *Thalassinoides*-like tubes filled with the overlying sediment. The lithology of the overlying sediment and the presence of burrows suggests that the transgressive surface is coincident with the sequence boundary at this locality. Remnants of shelf margin sediments may be present in a thin layer above the sequence boundary (G. Baum, pers. comm., 1998), but grain size and glauconite abundance decrease

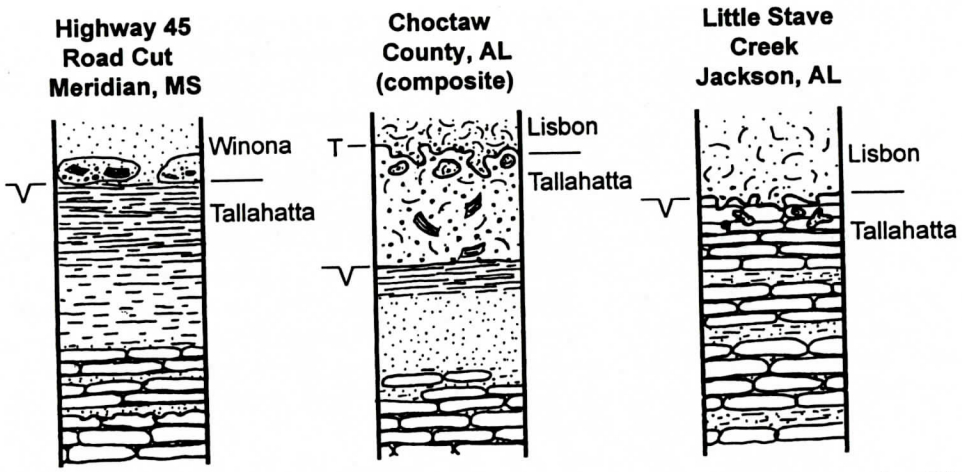

Figure 4. Schematic showing the variation in lithology at the top of the Tallahatta Formation. (A) The section near Meridian, MS (Locality MLa-4), showing a near-conformable transition from marine to marginal marine sediments in the Tallahatta Formation highstand systems tract, then into the overlying Winona Formation sands; (B) a composite of several sections near Souwilpa Creek in Choctaw Co., AL, showing localized shelf margin sands (Localities ACh-7,19,21,22); (C) the section at Little Stave Creek, Jackson, AL, showing burrowed sequence boundary and coincident transgressive surface (Locality ACl-4). The Tallahatta-Lisbon Formation contact falls at the sequence boundary in A and C. Copeland (1968) places the contact at the level of the transgressive surface in section B. Columns represent roughly 2 meters of section; lowermost lithologic symbol in each section (ovoid blocks) is for buhrstone. V marks the sequence boundary, T marks the transgressive surface

rapidly within only a few decimeters of the formation contact.

At a number of localities in the vicinity of Souwilpa Creek south of Gilbertown AL, the contact is associated with a variety of lithologies (Localities ACh-7,19,21,22; Fig. 4). The top of the Tallahatta here is characterized by a massive, indurated, coarse to very coarse-grained, glauconite greensand containing Tallahatta index fossils (*e.g., Cubitostrea perplicata*), underlain by about a decimeter of olive gray and dark gray, finely interlaminated clay, in turn underlain by at least a half meter of slightly glauconitic, indurated, (cross?)laminated, fine-grained quartz sand (in particular, Localities ACh-7, 21). All of this appears to be stratigraphically above the typical Tallahatta Formation buhrstone (exposed at Locality ACh-19). I suggest that the sand and clay represent the upper part of the highstand systems tract, similar to deposits in Mississippi. I place the sequence boundary at the top of the laminated clay, immediately below the greensand. This fossiliferous greensand itself is at least a meter thick at Souwilpa Creek (Locality ACh-7), capped by a heavily burrowed surface (*Thalassinoides* networks) and overlain by typical lower Lisbon Formation fossiliferous, glauconitic, marly sands (Fig. 4). There is no evidence for deepening within the greensand. Quartz grains are very coarse-grained and angular, fossils are distributed randomly with no preferred orientation, and glauconite grains are mature, black, and detrital. I infer the greensand to be a localized remnant of shallow-water, high-energy, shelf margin deposits, and the burrowed contact on top of the greensand to be the transgressive surface. The greensand contains rip-ups of olive gray clay, suggesting that erosional scour and reworking of underlying sediment was extensive in places within the local area. The presence of the rip-ups, very coarse-grained sand, abundant *Protoscutella mississippiensis* (a sand dollar), and a large number of callianassid shrimp claws supports a shallow water, high-energy origin for this unit.

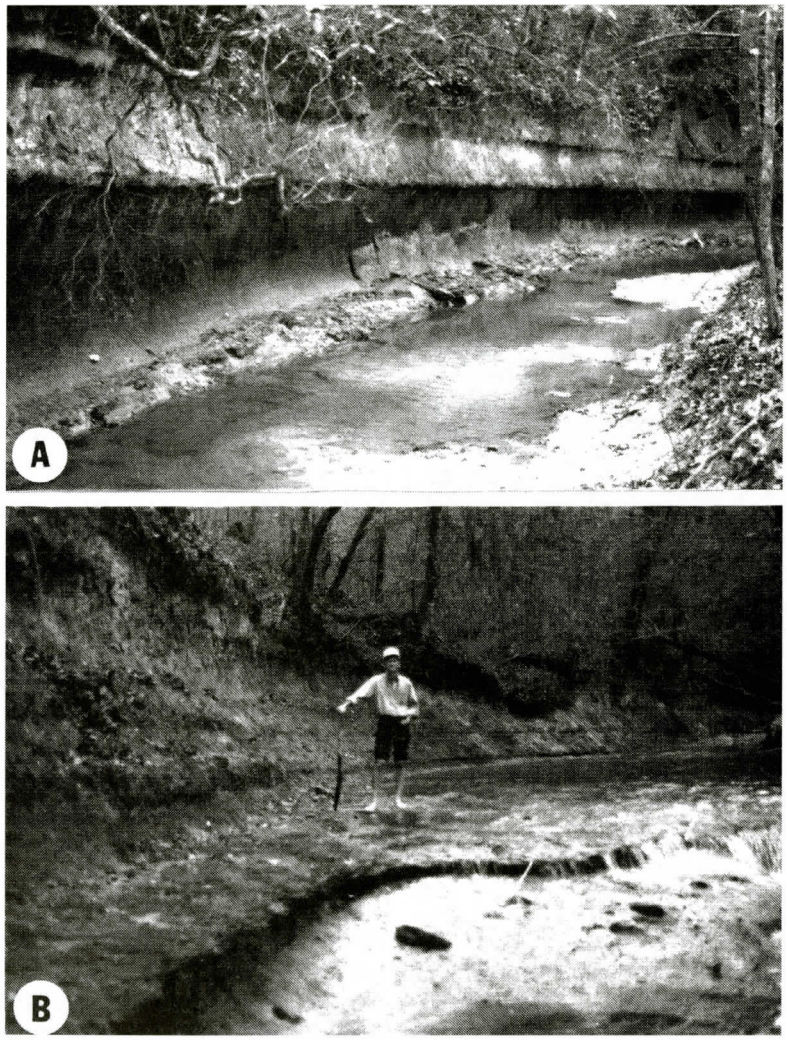

Figure 5. Evidence for smaller scale cyclicity manifested as indurated ledges within third order sequences in the Claiborne Stage supercycle. (A) The lower Lisbon Formation on Thompson Creek in Choctaw Co., AL, Locality ACh-20; (B) Sandy Page stands in the upper Lisbon Formation on Puss Cuss Creek, Choctaw Co., AL, Locality ACh-23.

Lower Lisbon Formation

The lower Lisbon Formation depositional cycle begins with fossiliferous, glauconitic, marly, coarse-grained transgressive sands. As discussed above, thin shelf margin deposits may be present locally between the sequence boundary and the transgressive surface, but at most localities (particularly in Mississippi) the two surfaces appear to be coincident. Like other Claiborne units, the formation is thicker and more proximal in Mississippi. In Alabama, the unit remains fully marine throughout (but see below), with thin transgressive deposits topped by thicker (several meters) highstand deposits of fine-grained, moderately glauconitic and fossiliferous, marly sand. Most macrofossils are moldic, but the excellent detail of external molds can allow specific or at least generic identification through silicone casting (Ivany, unpublished data). Evidence of smaller-scale cyclicity in sea-level change is present within

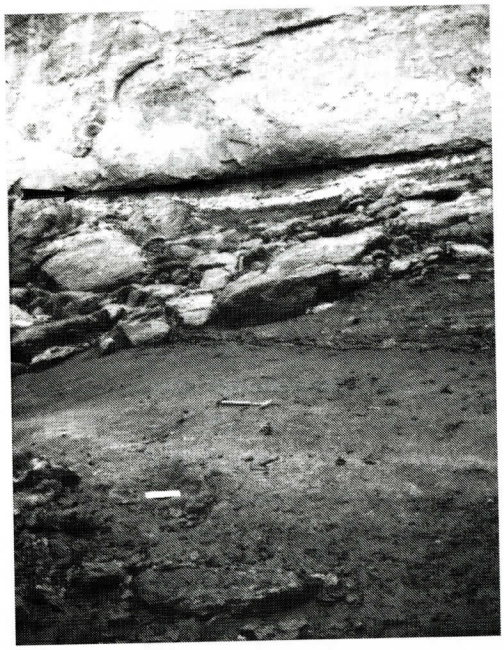

Figure 6. The outcrop at Doby's Bluff on the Chickasawhay River near Quitman, MS (Locality MCl-6). Fossiliferous marine deposits of the middle Lisbon Doby's Bluff tongue of the Kosciusko Formation are overlain by the resistant, light-colored sandy marls of the Archusa Marl Member of the Cook Mountain Formation (upper Lisbon Formation equivalent). The level of the condensed section shell bed is marked by the white sample bag in the foreground; sequence boundary marked with an arrow. Blocks near the base of the cliff are fallen blocks of Archusa Marl.

the lower Lisbon Formation, as can be seen in Figure 5A. Indurated ledges likely reflect relative sea-level stillstands or rises that lead to parasequence development. In Mississippi, transgressive Winona Formation sands record shallow-water marine deposition in an environment much like that seen near the Tallahatta-Lisbon Formation contact in Alabama. Coarse, glauconitic sand with large numbers of *Protoscutella* and callianassid claws co-occur with abraded disarticulated shells of *Cubitostrea lisbonensis* (a lower Lisbon Formation guide fossil). Evidence for diachroneity of the sequence boundary (older in Alabama) may be present, because the same facies and assemblage occurs with *Cubitostrea perplicata*, a Tallahatta Formation guide fossil, in shelf margin sediments and immediately above the transgressive surface (in lowermost Lisbon Formation sediments) in western Alabama (Locality ACh-7). The Winona Formation is succeeded by the highstand deposits of the Zilpha and Kosciusko Formations (carbonaceous clays and sands), recording deltaic or nearshore conditions (Dockery, 1980). These units are not well exposed in surface outcrops. Toulmin (1977) reports nonfossiliferous clay at the top of the lower Lisbon Formation in western Choctaw County, AL (Locality ACh-7), that similarly reflects shallowing and marginal marine conditions during the highstand; these sediments are no longer exposed in outcrop.

"Middle Lisbon" Formation

The middle Lisbon is a problematic unit from both a lithologic and sequence stratigraphic perspective. The name has been used in Alabama to refer to the stratigraphic interval between the highest occurrence of *Cubitostrea lisbonensis* (lower Lisbon Formation guide fossil) and the lowest occurrence of *Cubitostrea sellaeformis* (upper Lisbon Formation guide fossil) (Toulmin, 1977), but at Little Stave Creek (Locality ACl-4) where exposure is good there is no clear sedimentological evidence for delineating the interval[1]. In Mississippi, the name "middle Lisbon" has been applied to deposits of the Kosciusko Formation (Dockery, 1980; Toulmin, 1977). In sequence stratigraphic architecture, the Kosciusko Formation is clearly part of the highstand systems tract of the underlying sequence, and thus correlates with the upper part of the lower Lisbon Formation in Alabama.

1. The only property I could recognize in outcrop that might be interpreted as a diastem of sorts was an increase in glauconite abundance between beds 20 and 21 (of Toulmin, 1962). As the increase in glauconite correlated also with an increase in clay content, it may be more likely that this is the manifestation of the maximum flooding surface for the lower Lisbon sequence.

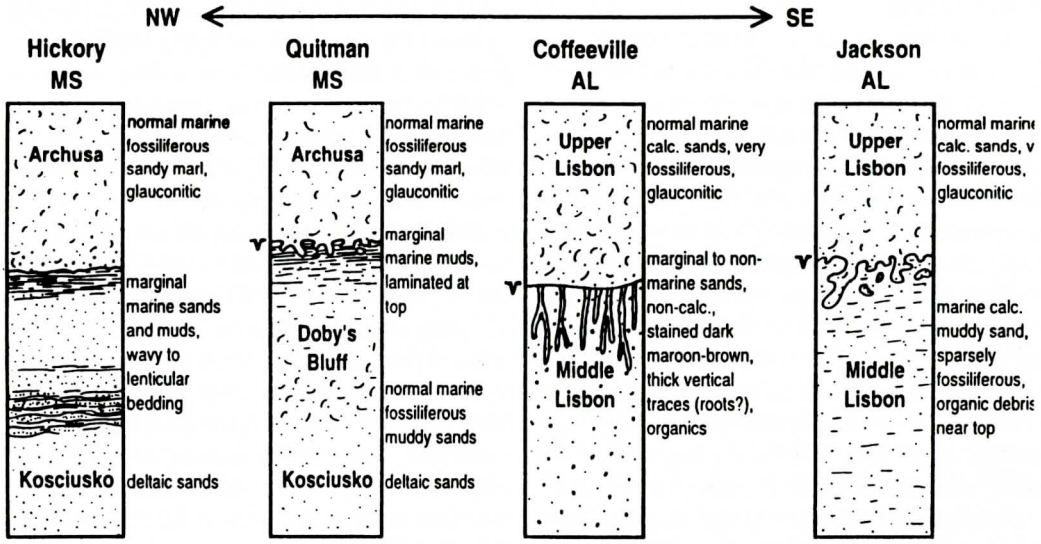

Figure 7. Schematic representation of lithologies at and below the sequence boundary between the middle and upper Lisbon. Only at the Doby's Bluff section is there good evidence for a distinct middle Lisbon Formation depositional cycle; other localities exhibit only highstand deposits from the previous lower Lisbon Formation cycle. Vs mark the sequence boundaries. Vertical scale is relative stratigraphic height, with depicted sections representing on the order of several meters. West to east, Localities MNe-1, MCl-6, ACl-3, ACl-4.

There is no clear evidence for recognizing a separate sequence at Little Stave Creek, and Baum and others (1994) see no evidence for a separate cycle in the more downslope sediments of the Bay Minette core in Alabama.

The problem arises when one considers the fossiliferous marine deposits of the Doby's Bluff tongue of the Kosciusko Formation, exposed on the Chickasawhay River near Quitman, MS (Dockery, 1986) (Locality MCl-6). The Doby's Bluff deposits comprise marine fossiliferous muddy sands, including what appears to be a condensed section shell bed, that grade up into marginal marine crudely laminated silts and clays (Fig. 6). This unit lies between the lignitic sands of the Kosciusko Formation below (Dockery, 1980) and the overlying marine fossiliferous Archusa Member of the Cook Mountain (upper Lisbon) Formation, hence, at this locality, a complete depositional sequence is clearly present. Mancini and Tew (1993) recognize the middle Lisbon as a distinct third order sequence based on these observations.

In my own work based solely on surficial outcrops, however, I have been unable to find convincing evidence for a distinct middle Lisbon Formation sequence elsewhere (Fig. 7). In sections to the west at Hickory, MS (Locality MNe-1), the upper Lisbon Formation sequence overlies unconsolidated wavy-bedded quartz sand and carbonaceous laminated clays, suggesting very nearshore tidal flat and beach deposition. I interpret these sediments as part of the Kosciusko Formation, hence the Doby's Bluff Tongue is not present. To the east, at Coffeeville, AL (Locality ACl-3), south of the US 84 bridge over the Tombigbee River, movement along a fault has exposed the base of the upper Lisbon Formation sequence on the upthrown block. Sediment below the sequence boundary is coarse-grained lignitic sand with large pieces of organic debris, presumably terrestrial, disseminated throughout. This is likely equivalent to the Kosciusko Formation in Mississippi. This sand is probably positioned stratigraphically above the clay reported by Toulmin (1977) near the top of the lower Lisbon Formation, hence the Zilpha-Kosciusko facies transition in highstand deposits to the west is likewise present in western Alabama, directly below the upper Lis-

bon sequence.

In nearly all exposed sections, therefore, upper Lisbon marine fossiliferous marly sands disconformably overlie lignitic or wavy-bedded marginal marine sands and clays with no marine intermediary; in the down-dip section at Little Stave Creek, Jackson AL, the evidence for a separate sequence is equivocal to poor. Given these observations and the lack of a reported sequence in down-dip core studies (Baum and others, 1994), I therefore suggest that the Doby's Bluff tongue is a local, autocyclically derived sequence and does not reflect a eustatic change in sea level. The unit may represent deposition in an interdistributary bay within the Kosciusko delta system. The character of the invertebrate fauna (relatively low diversity, very few corals or echinoids, many grazing and carnivorous gastropods), the presence of thin winnowed storm beds, and the predominance of detrital mud suggests a potentially brackish, nearshore, quiet water setting.

The possibility that erosion along the upper Lisbon Formation transgressive surface removed a distinct middle Lisbon Formation sequence everywhere but at Doby's Bluff cannot, however, be entirely ruled out. In fact, the sharp edges and circular cross sections of burrows extending down from the contact (see below) at all localities except Doby's Bluff indicate that underlying sediment had been compacted and dewatered by the time the burrows were emplaced, suggesting that some erosion of overlying material had occurred prior to deposition of the upper Lisbon Formation. At Doby's Bluff, burrow edges are diffuse and cross sections are often slightly flattened, suggesting that sediment was still somewhat soft when Archusa Marl deposition began, hence very little time (or rock) is missing at the unconformity.

Upper Lisbon Formation

The contact between the middle and the upper Lisbon Formation is a Type II sequence boundary (Baum and Vail, 1988), apparently coincident with the transgressive surface everywhere it could be examined. It is clearly demarcated by an extensively burrowed, erosive contact between underlying marginal marine sands and/or clays and the highly fossiliferous, glauconitic, marly sands above. Depth of bioturbation below the contact seems to be correlated with the degree to which the underlying sediments are marine. Thick (3-10 cm in diameter) *Thalassinoides* burrows extend into the underlying sediment for at least a half meter at Little Stave Creek (Locality ACl-4), where the underlying sediment is still bioturbated and fossiliferous (although perhaps salinity stressed, as inferred from the relatively low-diversity fauna of small molluscs). At Doby's Bluff (Locality MCl-6), burrows extend about 20 cm into the underlying unit, which is composed of gray, silty, occasionally laminated muds, suggesting marginal marine conditions. At Hickory, MS (Locality MNe-1), where underlying sediments indicate very nearshore to beach depositon (see above), depth of bioturbation is only a few centimeters, and burrows are much thinner (<1cm in diameter). The significance of this relationship, if any, remains unclear. It may be a function of the clay content and hence cohesiveness of the underlying sediment. An exception to the trend occurs at Coffeeville, AL (Locality ACl-3), where burrows are very deep, vertical, bifurcating, and filled with the same dark maroon-black organic-stained sand that surrounds them. These characteristics suggest root traces, not sublittoral *Thalassinoides* burrows, therefore in this locality the nearshore sands may have been overprinted by subareal exposure and terrestrial or perhaps mangrove vegetation. The sea-level drop associated with the formation of this sequence boundary is clearly the most significant to occur within the Tc supercycle.

The upper Lisbon Formation cycle is much thicker than the lower (and/or middle) Lisbon Formation cycle (on the order of 30 m vs. 5-6 m in outcrop). In Mississippi, the transgressive portion of the sequence (the Archusa Marl Member of the Cook Mountain Formation) is unusually thick and well-developed, characterized by highly fossiliferous, glauconitic, sandy marls. The maximum flooding surface near the base of the Potterchitto Member is highly glauconitic, locally indurated, and marked by an abundance of large bored and encrusted oysters

(*Cubitostrea sellaeformis*, Fig. 9C; Locality MCl-5). This is in turn overlain by muddy, gray-green, glauconitic sands of the Potterchitto, locally containing a diverse and abundant marine assemblage (*e.g.*, Locality MCl-5 near Quitman, MS). Moving upsection, marine deposits give way to marginal marine, laminated, organic-rich, sulfur-stained clays of the Gordon Greek Shale Member. Surfaces of laminae contain tiny fragments of vascular plant debris, presumed terrestrial in origin. No invertebrates were recovered save for a few tiny, moldic, nuculid bivalves, but very small-scale (mm or less) bioturbation may be present within laminae. Clays are overlain by cross-bedded, reddish-orange, quartz sands of the Cockfield Formation, representing tidal or beach deposition. *Skolithos* escape burrows have been reported from the Cockfield (Toulmin, 1977), supporting the inferred depositional environment. The Potterchitto and Gordon Creek members of the Cook Mountain Formation together with the Cockfield Formation represent a conformable shallowing-upwards sequence (but see next section) that comprises the highstand systems tract in Mississippi (especially visible at localities MCl-1, MCl-2, MCL-5, and MNe-2).

The upper Lisbon Formation section in Alabama begins with extremely fossiliferous, orange-brown, medium-grained sand that overlies the sequence boundary and fills the burrow networks below. The sand contains abundant very coarse-grained pelletal detrital glauconite and large fragments of organic debris, including pieces of branches 1-3 cm in diameter. The transgressive deposits are generally characterized by shell beds and compact, fine-grained, fossiliferous marly sands. Shell beds at Coffeeville, AL, appear to be more transported due to greater amounts of breakage and abrasion. Hence, the Coffeeville shells were probably deposited in more shallow water than those at Little Stave Creek or Barrytown, AL (Locality ACh-8). The Barrytown outcrop, inferred to be just above the transgressive surface due to the presence of very coarse quartz and glauconite grains and large clasts of organic material at its base, has produced some of the finest upper Lisbon Formation fossils, in terms of both diversity and quality of preservation. At least two distinct, diverse oyster (*Cubitostrea sellaeformis*) beds are present at both Little Stave and Coffeeville within the transgressive deposits. Establishment of oyster beds likely also reflects parasequence development in that oysters prefer a low influx of clastic material and are therefore more likely to thrive during relative stillstands or rises in sea level.

The condensed interval in Alabama represents much deeper-water deposition than that in Mississippi. Here, the lithology is a compact, homogeneous, silty, tan to blue-gray clay that weathers to irregular blocks. The clay is several meters thick and becomes progressively more micaceous and silty toward the top. Macrofossils are only present near the top, and then in very low abundance, suggesting that the bulk of the clay was deposited well below the photic zone. The presence of a well-developed condensed interval in the upper Lisbon Formation cycle, both in Alabama and Mississippi, indicates that maximum water depths for the entire Lisbon Formation were reached during this time.

At Little Stave Creek, the transition into highstand deposits represented by shallower-water fossiliferous sediments occurs gradually over about a meter and a half of section. At the more proximal section at Coffeeville, however, a deeply-burrowed depositional hiatus separates bioturbated silty clay below from fine-grained fossiliferous sand above. If this clay is indeed correlative to that at Little Stave Creek, then initial shallowing occurred relatively rapidly at this locality. The diastem also suggests that shallowing was not simply the result of filling of accommodation space, but instead reflects either a eustatic change or a rapid change in base level due perhaps to movement of salt diapirs.

The highstand systems tract is comprised of a series of stacked parasequences made especially visible at Coffeeville Landing by a succession of indurated sandy ledges, which separate softer and more fossiliferous sandy units on a scale of 2-3 meters each (see also Fig. 5B). The undersides of ledges are generally marked by extensive horizontal burrow net-

works that weather out differentially. At least four distinct oyster beds, each containing a diverse marine assemblage, are present in highstand deposits at Little Stave and Coffeeville, once again suggesting parasequence development. That both localities share the same number of oyster beds suggests the possibility that these parasequences may be regionally persistent and hence useful for correlation. Within parasequences, there is evidence for even smaller-scale changes in relative sea-level as indicated by variations in both burrow density and the amount of shelly material within successive half-meter stratigraphic intervals. Cyclic increases in both these parameters are likely correlated with decreases in sedimentation rate, associated either with stillstands or rising relative sea-level, or, more likely, local shifts in the center of deposition.

The top of the upper Lisbon Formation in Alabama, as in Mississippi, is characterized by a transition into marginal marine bioturbated and then laminated mudstones and clays, but water depths did not decrease to the extent that the non-marine components were deposited. These mudstones are best observed at Little Stave Creek, where the uppermost mudstone is silty, crudely laminated but still bioturbated on a small scale, and contains bits of organic matter, and at an outcrop several miles SE of Evansboro, AL (Locality ACh-24), where this facies is succeeded by laminated clays with bits of organic debris along yellow-stained parting planes similar to the Gordon Creek Shale Member in Mississippi.

Figure 8. Burrowed type II sequence boundary (marked with an arrow) at the base of the newly-identified sequence within the upper Lisbon Formation at the outcrop SE of Evansboro, AL. Locality ACh-24.

A New Upper Lisbon Formation Sequence

A previously unrecognized fourth (or fifth, if one accepts the middle Lisbon Formation cycle) third-order sequence within the Claiborne Stage supercycle is seen near the top of the upper Lisbon Formation in a number of localities. At Little Stave Creek, a heavily burrowed surface (*Thalassinoides*, 1-2 cm diameter, 20-30 cm deep) about 8 m below the contact with the overlying Gosport Sand marks the transgressive surface, separating fine-grained muddy sand below from the very glauconitic and shell-rich sand above. This sand fines upward, becoming muddy and micaceous (as described above). A similar pattern is seen at the Evansboro outcrop (Fig. 8). At this locality, transgressive sediments also contain well-preserved specimens of *Teredolites*, the calcareous tubes of a wood-boring bivalve (see Fig. 9B). Its position here is consistent with Savrda (1991a,b), who notes that *Teredolites* is especially common in the transgressive portions of Gulf Coast sequences. Vascular tissue of the wood into which the bivalves were boring is still intact, suggesting proximity to land at the time of deposition. In Newton, MS (Locality MNe-2), a sharp contact exists about 1 meter below the top of the Potterchitto Member between olive gray, clayey, slightly micaceous, glauconitic sand below and dark reddish-brown, very glauconitic, coarse-

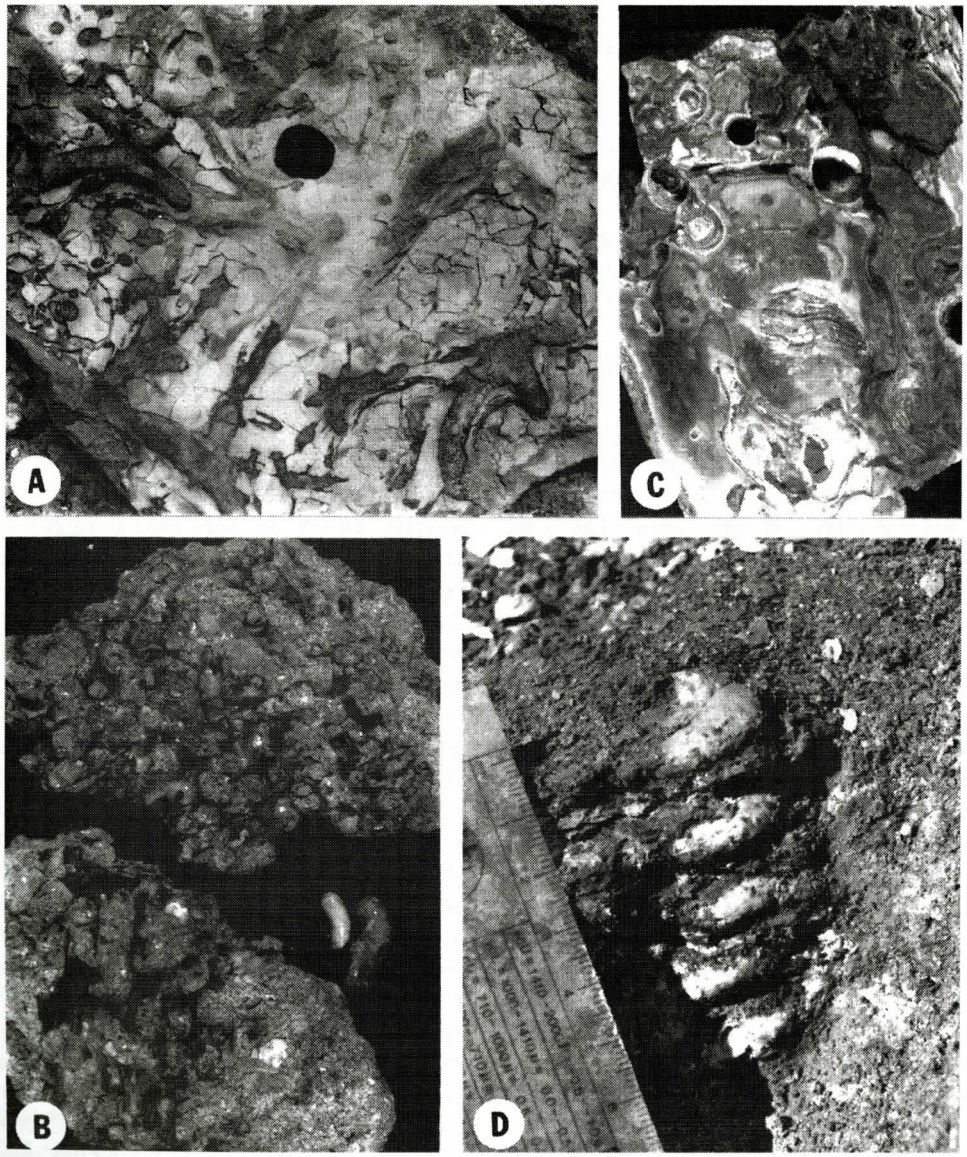

Figure 9. (A) *Thalassinoides* burrow network from near the transgressive surface between the Meridian Sand and the Tallahatta Formation, US 45 roadcut south of Meridian, MS, Locality MLa-4; lens cap is 6 cm in diameter; (B) *Teredolites* borings into wood recovered just above the transgressive surface of the new sequence in the upper Lisbon Formation, SE of Evansboro, AL, Locality ACh-24. Upper sample shows cross-section of calcite linings of tubes produced by the boring bivalves, lower sample shows remnants of woody tissue crossed by borings, and to the right are dissected calcite linings of tubes showing retrusive caps produced near the ends of bores probably in response to overcrowding, signaling a switch to filter-feeding mode of life (Savrda and Smith, 1996); smallest tube is 1 cm long; (C) Pholadid clam borings in the shell of *Cubitostrea sellaeformis* from the inferred surface of maximum transgression near the base of the Potterchitto Member of the Cook Mountain (upper Lisbon) Formation at Shiloh Road, Quitman, MS, Locality MCl-5; oyster is 9 cm in longest dimension; (D) *Gyrolithes* corkscrew burrow from the top of the Tallahatta Formation immediately below the transition into marginal marine laminated clays at the US 45 roadcut south of Meridian, MS, Locality MLa-4.

grained, muddy sand above. The overlying sand contains rip-up clasts of the olive clay. The contact is marked by a zone of dark brick-red cemented *Thalassinoides* burrows 2-3 cm in diameter and extending up to 30 cm below the contact. The presence of a similar zone of iron-stained, cemented *Thalassinoides* below the top of the Potterchitto Member in Quitman, MS (Locality MCl-5), suggests the same phenomenon, but a distinct lithologic contact could not be identified.

The upper Lisbon Formation depositional cycles are capped by a Type I sequence boundary and the initiation of the next major supercycle (Td of Baum and Vail, 1988, and Mancini and Tew, 1993). In western Alabama, the sequence boundary is deeply burrowed and overlain by the Gosport Sand, a highly fossiliferous and glauconitic sand with limited areal extent. In Mississippi, the sequence boundary is placed at the level of an unconformity within the Cockfield Formation (Mancini and Tew, 1994) that separates cross-bedded quartz sands below from lignitic sands and lignite above. The shelly sands of the Gosport Sand are interpreted to be the transgressive systems tract of the next third order cycle, while the upper half of the Cockfield Member signifies terrestrial colonization of nearshore sands and marshy conditions during the highstand (Mancini and Tew, 1994). Lignitic clays and sands occasionally bearing leaf compressions occur near the top of the Gosport Sand at Claiborne Bluff and likely represent the correlate to the upper Cockfield Member.

ARE THE CLAIBORNE STAGE CYCLES EUSTATIC?

I recognize four major (third order) sequences within the Claiborne Stage supercycle: one each corresponding to the Tallahatta and lower/middle Lisbon Formations, and two within the upper Lisbon Formation (Fig. 10). Comparison of these cycles with the eustatic sea-level curve of Haq and others (1987) and with other sections in the Gulf and Atlantic Coastal Plain helps to determine the geographic extent of sea-level changes seen in this portion of the Gulf Coast.

Correlation with the eustatic curve suggests that a given cycle is global in its extent, while mismatches generally require regional or local explanations based on tectonism or shifting depocenters within alluvial systems (Posamentier and Allen, 1993). A strong cautionary note must be sounded, of course, because construction of the Paleogene portion of the Haq and others (1987) eustatic curve is based in part on data from the Gulf Coast (only the section at Little Stave Creek was mentioned specifically for the middle Eocene; Haq and others, 1988). Agreement between my interpretations and the Haq and others curve may therefore not be as meaningful as one would like. However, the eustatic curve also includes Paleogene data from a large number of basins in western Europe, Australia, New Zealand, and the Atlantic Coastal Plain (Haq and others, 1988). Reported patterns of cyclicity are therefore likely to be more than simply regional.

I found evidence for only a single third order cycle in the Tallahatta Formation. The Haq and others curve shows 2 cycles (TA 3.1 and TA 3.2), based in part on the Lutetian Stage section in the Paris Basin (Haq et al., 1988). Other workers in the Gulf Coast uniformly recognize only one cycle in the Tallahatta Formation (Baum and Vail, 1988; Mancini and Tew, 1993; Baum and others, 1994; Yancey and Davidoff, 1994), a pattern that appears to hold true in the Atlantic Coastal Plain as well (Powell and Baum, 1982). The discrepancy may be because evidence for the second cycle has yet to be found, or because regional processes effectively swamped the eustatic signal during this time in southeastern North America.

In agreement with Baum and Vail (1988) and Baum and others (1994), I suggest that the lower and middle Lisbon formations together represent a single cycle of sea-level change in the Gulf Coast. While Mancini and Tew (1993) use the marine sequence at Doby's Bluff to justify a distinct middle Lisbon sequence separate from the lower Lisbon, I was unable to find outcrop evidence of this cycle anywhere else along strike between Hickory, MS, and Jackson, AL. The Haq and others (1987) curve *does* show a

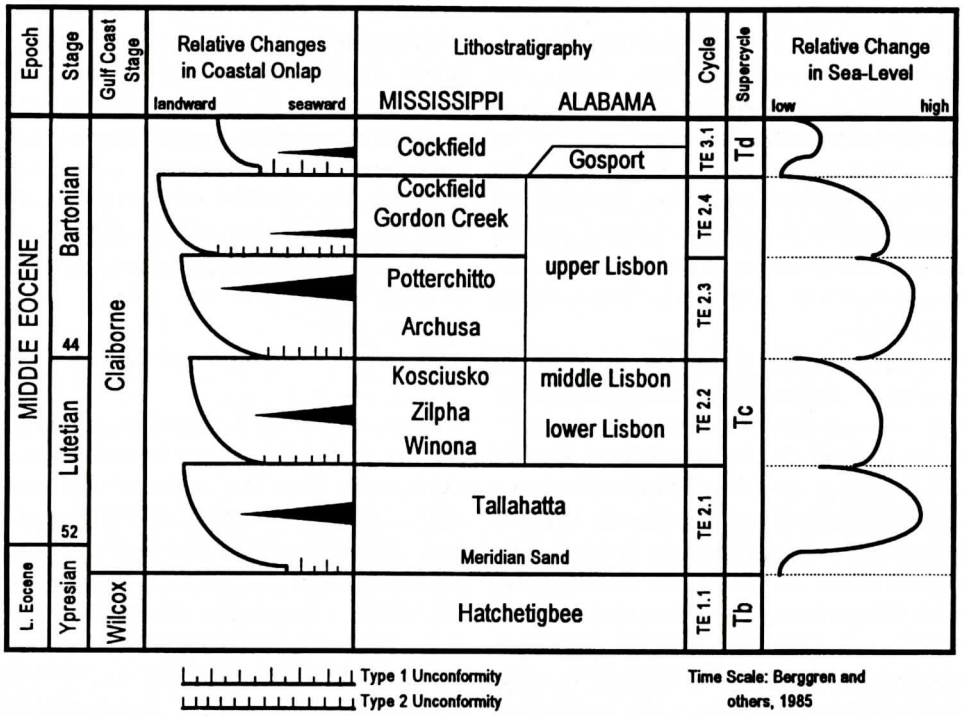

Figure 10. Sequence stratigraphy of the Claiborne Stage as derived from this study. Black triangles represent condensed intervals, sea-level curve is relative. Vertical scale is relative stratigraphic position. After Baum and Vail (1988).

separate eustatic sequence that is correlative with the middle Lisbon. However, because (as mentioned above) outcrops from the Gulf Coast in Alabama and Mississippi were used to construct the Paleogene portion of the sea-level curve, it is quite possible that the Doby's Bluff section played a significant role in that construction — Doby's Bluff offers the only highly visible outcrop of the middle Lisbon Formation in the region, hence it is likely that the Haq group took it into consideration. My suggestion that the middle Lisbon cycle is not eustatic is therefore not necessarily weakened by the presence of a cycle in the Haq curve. Powell and Baum (1982), working in Atlantic and Gulf coast sections, do not report a separate sequence correlating with the middle Lisbon Formation in either area, nor do Zullo and Harris (1987) in North Carolina, but Yancey and Davidoff (1994) recognize a distinct middle Lisbon cycle in the subsurface of Texas. The evidence for one versus two cycles is therefore equivocal at this point in time. Subsurface data may help to resolve the uncertainty.

Mancini and Tew (1993), Baum and Vail (1988), and Baum and others (1994) each report a single third-order cycle from the upper Lisbon Formation in Alabama. I have found evidence for a second, regionally persistent cycle of similar magnitude in the upper part of the upper Lisbon Formation. Haq and others (1987) report two third order sequences within the Bartonian (upper Lisbon interval), as do Hull (1992) from subsurface work in Texas and Louisiana, and Yancey and Davidoff (1994) also from Texas. This may be the more proximal expression of the phenomenon they observe in the subsurface. Powell and Baum (1982) report a sequence in the upper Castle Hayne Limestone from North Carolina that falls between units correlating to the upper Lisbon Formation and the Gosport Sand. It is possible that this sequence, not represented in South Carolina sections, may correlate with that seen in the Gulf

Coast near the top of the upper Lisbon Formation. Robinson (1996) notes the presence of upper Lisbon foraminiferans above a sequence boundary in the Bay Minette core from Alabama identified by Baum and others (1994) as the Lisbon/Gosport contact. The sequence boundary recognized within the upper Lisbon Formation in this study may correlate with the boundary seen by Baum and others (1994), and hence provide a resolution to Robinson's foraminiferan data.

Overall, my interpretations of sea-level change in the eastern Gulf Coast agree relatively well with the eustatic curve and studies from the central Gulf (Texas) and Atlantic Coasts. There is general agreement about the presence of only a single third-order cycle in the Tallahatta Formation, but more attention should be paid to the lower and middle Lisbon Formation before deciding whether one or two cycles characterize the interval. The recognition of two sequences in the upper Lisbon Formation agrees with the eustatic curve, the Texas curve, and potentially that based on North Carolina sections, favoring eustatic control for both.

SUMMARY

Field work in the eastern Gulf Coastal Plain Claiborne Stage reveals four major third order sequences within Tc supercycle of Baum and Vail (1988) and Mancini and Tew (1993): one each corresponding to the Tallahatta and lower/middle Lisbon Formations, and two within the upper Lisbon Formation. The middle Lisbon cycle as evidenced at Doby's Bluff, MS, is considered local and autocyclic, not eustatic in origin. The newly identified cycle in the upper part of the upper Lisbon Formation may correlate to one recognized earlier in the subsurface and present in the eustatic sea level curve, and so is tentatively identified here as a fourth third-order sequence. Cyclicity is manifested on a number of different scales, as evidenced by parasequence development and smaller scale variability within parasequences. Parasequences are marked by indurated ledges, small-scale burrowed surfaces, and oyster beds, some of which may be regionally correlative. Water depths reached a maximum during Tallahatta Formation deposition, and again deepened substantially during deposition of the upper Lisbon Formation; the most significant drop in sea level occurred between the middle and upper Lisbon Formation cycles. The general agreement of my interpretations with the Haq and others (1987) eustatic curve suggests that the third order cycles in the Claiborne Stage reflect global changes in sea level.

ACKNOWLEDGMENTS

Many thanks go to Peg Yacobucci, David Goldsmith, and Paul Morris for assistance in the field, and to Nick Tew (Geological Survey of Alabama) and David Dockery (Mississippi Bureau of Geology) for insightful comments on Claiborne Stage stratigraphy. Sandy Page (USDA-NRCS, Choctaw Co. Soil Survey) is especially thanked for showing me new outcrops in and around Choctaw County, AL, for helpful discussions regarding the Tallahatta-Lisbon contact, and for proving to me that good vegetarian food *can* be found in Jackson, AL. Nick Tew, Ernest Mancini and Gerald Baum read the manuscript and provided many helpful suggestions and comments. Thanks to Bonnie Miljour for assistance with graphics, and to Ken Schopf for the photo of the Lisbon-Gosport contact. Thanks also to Bobby Fagan and Pee Wee Waltman for a boat trip down the Tombigbee River (and, thankfully, back up again in one piece) for stratigraphic description and collection along the river banks. This work was supported by a dissertation fellowship from the American Association of University Women and research grants from the Paleontological Society, the Geological Society of America, and the Department of Earth and Planetary Sciences at Harvard University. Thanks also to support from the Michigan Society of Fellows and a National Science Foundation Postdoctoral Research Fellowship.

REFERENCES CITED

Bandy, O.L., 1949, Eocene and Oligocene foraminifera from Little Stave Creek, Clarke County, Alabama: *Bulletin of American Paleontology*, v. 32, p. 5-209.

Baum, G.R. and Vail, P.R., 1988. Sequence stratigraphic concepts applied to Paleogene outcrops, Gulf and Atlantic basins, *in* Wilgus, C.W., Hastings, B.S., Kendall, C.G. St.C., Posamentier, H.W., Ross, C.A., and Van Wagoner, J.C. (eds.) *Sea-Level Changes: An Integrated Approach*, SEPM Special Publication No. 42, p. 309-327.

Baum, J.S., Baum, G.R., Thompson, P.R., and Humphrey, J.D., 1994. Stable isotopic evidence for relative and eustatic sea-level changes in Eocene to Oligocene carbonates, Baldwin County, Alabama: *Geological Society of America Bulletin*, v. 106, p. 824-89.

Berggren, W. A., Kent, D.V., Flynn, J.J., and Van Couvering, J.A., 1985. Cenozoic geochrononology: *Geological Society of America Bulletin*, v. 96, 1407-1418.

Copeland, C.W., 1966. Facies changes in the Alabama Tertiary: *Alabama Geological Society Field Trip Guidebook*, v. 4, 103 p.

Copeland, C.W., 1968. *Geology of the Alabama Coastal Plain*: Geological Survey of Alabama Circular 47, 97 p.

Dockery, D.T., 1980. The Invertebrate Macropaleontology of the Clarke County, Mississippi, Area: *Mississippi Department of Natural Resources Bureau of Geology*, Bulletin 122, p. 1-387.

Dockery, D.T., 1986. Dobys Bluff tongue of the Kosciusko Formation and the Archusa Marl Member of the Cook Mountain Formation at Dobys Bluff on the Chickasawhay River, Clarke County, Mississippi: *GSA Centennial Field Guide - Southeastern Section*, p. 379-382.

Foster, V.M., 1940. Lauderdale County mineral resources: *Mississippi State Geological Survey Bulletin*, v. 41.

Haq, B.U., Hardenbol, J., and Vail, P.R., 1987. Chronology of fluctuating sea levels since the Triassic: *Science*, v. 235, p. 1156-1167.

Haq, B.U., Hardenbol, J., and Vail, P.R., 1988. Mesozoic and Cenozoic chronostratigraphy and cycles of sea-level change, *in* Wilgus, C.W., Hastings, B.S., Kendall, C.G. St.C., Posamentier, H.W., Ross, C.A., and Van Wagoner, J.C. (eds.) *Sea-Level Changes: An Integrated Approach*, SEPM Special Publication No. 42, p. 71-108.

Hull, R.A., 1992. Origin of regressive-transgressive sequences in the Claiborne Group: *Gulf Coast Association of Geological Societies Transactions*, v. 42, p. 811.

Ivany, L.C., 1997. *Faunal Stability and Environmental Change in the Middle Eocene Gulf Coastal Plain*: Ph.D. Dissertation, Harvard University, 221 p.

Jones, D.S., 1967. Geology of the coastal plain of Alabama: *Geological Society of America Field Trip Guidebook*, v. 80, 113 p.

Knight, J.E., Offeman, I.D., and Landry, R.M, 1977. Fossils and Localities of the Claiborne Group (Eocene) of Texas: *Texas Paleontology Series*, v. 1, p. 57.

Laws, R.A., and Thayer, P.A., 1992. Origin and diagenesis of Middle Eocene diatomite, Tallahatta Formation, southwest Alabama: *Gulf Coast Association of Geological Societies Transactions*, v. 42, p. 517-527.

Loutit, T.S., Hardenbol, J., and Vail, P.R., 1988, Condensed sections: the key to age determination and correlation of continental margin sequences, *in* Wilgus, C.W., Hastings, B.S., Kendall, C.G. St.C., Posamentier, H.W., Ross, C.A., and Van Wagoner, J.C. (eds.) *Sea-Level Changes: An Integrated Approach*, SEPM Special Publication No. 42, p. 183-213.

Mancini, E.A., and Tew, B.H., 1993. Sequence stratigraphy of Paleogene strata of the eastern limb of the Mississippi Embayment - Guidebook for Field Trip #8: *American Association of Petroleum Geologists Annual Convention*, New Orleans, LA: Gulf Section, SEPM, p. 68.

Mancini, E.A., and Tew, B.H., 1994. Claiborne-Jackson Group contact (Eocene) in Alabama and Mississippi: *Gulf Coast Association of Geological Societies Transactions*, v. 44, p. 431-439.

McGowran, B., 1989. Silica burp in the Eocene ocean: *Geology*, v. 17, p. 857-860.

Poag, C.W., and Ward, L.W., 1987. Cenozoic unconformities and depositional supersequences of North Atlantic continental margins: testing the Vail model: *Geology*, v. 15, p. 159-162.

Posamentier, H.W., and Allen, G.P., 1993. Variability of the sequence stratigraphic model: effects of local basinal factors: *Sedimentary Geology*, v. 86, p. 91-109.

Powell, R.J., and Baum, G.R., 1982. Eocene biostratigraphy of South Carolina and its relationship to Gulf Coastal Plain zonations and global changes of coastal onlap: *Geological Society of America Bulletin*, v. 93, p. 1099-1108.

Reynolds, W.R., 1992. The heavy mineral population within the beach sand facies of the Meridian Sand exposed in Mississippi: *Gulf Coast Association of Geological Societies Transactions*, v. 42, p. 633-646.

Robinson, E., 1996. Stable isotopic evidence for relative and eustatic sea-level changes in Eocene to Oligocene carbonates, Baldwin County, Alabama: Discussion: *Geological Society of America Bulletin*, v. 108, p. 117-119.

Savrda, C.E., 1991a. Ichnology in sequence stratigraphic studies: an example from the Lower Paleocene of Alabama: *Palaios*, v. 6, p. 39-53.

Savrda, C.E., 1991b. *Teredolites*, wood substrates, and sea-level dynamics: *Geology*, v. 19, p. 905-908.

Savrda, C.E., and Smith, M.W., 1996. Behavioral implications of branching and tube-lining in *Teredolites*: *Ichnos*, v. 4, p. 191-198.

Siesser, W.G., 1983. Paleogene calcareous nannoplankton biostratigraphy: Mississippi, Alabama and Tennessee: *Mississippi Department of Natural Resources Bulletin*, v. 125, p. 1-61.

Smith, E.A., Johnson, L.C., and Daniel W. Langdon, J., 1894. Report of the geology of the coastal plain of Alabama: *Geological Survey of Alabama Special Report 6*, 759 p.

Toulmin, L.D., 1962. Geology of the Hatchetigbee anticline area, southwestern Alabama: *Gulf Coast SEPM Guidebook*, p. 1-46.

Toulmin, L.D., 1977. *Stratigraphic Distribution of Paleocene and Eocene Fossils in the Eastern Gulf Coast Region, Volumes 1 and 2*: Geological Survey of Alabama Monograph 13, 602 p.

Toulmin, L.D., LaMoreaux, P.E., and Lanphere, C.R., 1951. Geology and ground-water resources of Choctaw County, Alabama: *Geological Survey of Alabama Special Report*, v. 21.

Van Wagoner, J.C., Posamentier, H.W., Mitchum, R.M., Vail, P.R., Sarg, J.F., Loutit, T.S., and Hardenbol, J., 1988. An overview of the fundamentals of sequence stratigraphy and key definitions, *in* Wilgus, C.W., Hastings, B.S., Kendall, C.G. St.C., Posamentier, H.W., Ross, C.A., and Van Wagoner, J.C. (eds.) *Sea-Level Changes: An Integrated Approach*, SEPM Special Publication No. 42, p. 39-45.

Van Wagoner, J.C., Mitchum, R.M., Campion, K.M., and Rahmanian, V.D., 1990. *Siliciclastic Sequence Stratigraphy in Well Logs, Cores, and Outcrops: Concepts for High-resolution Correlation of Time and Facies*: AAPG Methods in Exploration Series, No. 7, 55 p.

Yancey, T.E., and Davidoff, A.J., 1994. Paleogene sequence stratigraphy of the Brazos River section, Texas: *Gulf Coast Association of Geological Societies Fieldtrip Guidebook*, v. 44th Annual Meeting, p. 1-104.

Zachos, L.G., 1993. Occurrence of the spatangoid echinoid *Maretia arguta* (Clark) in the Middle Eocene of Texas: *Journal of Paleontology*, v. 67., p. 148-150.

Zullo, V.A., and Harris, W.B., 1987. Sequence stratigraphy, biostratigraphy, and correlation of Eocene through lower Miocene strata in North Carolina: *Cushman Foundation for Foraminiferal Research, Special Publication 24*, p. 197-214.

Appendix A. Locality Register for outcrops examined during this study.

Note: Localities are labeled following the scheme of Toulmin (1977). Original Toulmin site identifications are used whenever possible for Alabama localities and many new sites were added to the original Toulmin list (Ivany, 1997). Many sites in Mississippi were listed in Dockery (1980), and references are made to his locality numbers when applicable. New localities not previously described (to my knowledge) are indicated with an asterisk.

ALABAMA

Choctaw County

ACh-7 Tallahatta Fm. (top); Lower Lisbon
Road cut on east side of AL highway 17, south side of valley of Souwilpa Creek, about 4 miles south of Gilbertown; E½, Sec. 19, T. 10 N., R. 3 W.

ACh-8 Upper Lisbon Fm. (lower)
Road cut on west side of road .1 mile south of bridge over Souwilpa Creek, and on east side of road about .1-.2 miles south of bridge, on county route 21 about 1 mile south of junction with county route 14 in Barrytown, AL; W ½, SW ¼, Sec. 24, T. 10 N., R. 3 W.

ACh-8a* Lisbon Fm. (middle?)
Stream cut exposure under county road 21 bridge over Souwilpa Creek, about 1 mile south of junction with county road 14 in Barrytown; NW ¼, SW ¼, Sec. 24, T. 10 N., R. 3 W.

ACh-9 couldn't find outcrop (Gosport Sand; Moodys Branch)
Road cut on old US 84 (old paved road to Isney), 3.9 miles west of Silas; N ½, Sec. 4, T. 9 N., R. 4 W.

ACh-10 Moodys Branch Fm.
Road cut on both sides of county road 14, 3.9 miles west of Gilbertown; SE ¼, Sec. 28, T. 1 N., R. 4 W.

ACh-13 outcrop no longer exists (Lower Lisbon)
Mill Creek, 1½ miles south of Gilbertown on AL highway 17; NE ¼, Sec. 7, T.10 N., R. 3 W.

ACh-16 Hatchetigbee Fm. (top); Meridian Sand; Tallahatta Fm (lower)
Road cut on west side of AL highway 17, about 5.5 miles south of Butler, 11.5 miles north of Gilbertown; N½, Sec.10, T. 12 N., R. 3 W.

ACh-18 Moodys Branch Fm.
Low road cut on north side of US highway 84, 3.5 miles west of junction with AL highway 17 at Bolinger and Silas, AL; middle of Sec. 4, T. 9 N., R. 4 W.

ACh-19* Tallahatta Fm. (near top)
Creek-bed exposure on SE side of bridge over Little Souwilpa Creek on county road 8 (left fork, dirt road), about 1.3 miles west of AL highway 17; E ½, SE ¼, Sec. 24, T 10 N., R. 4 W.

ACh-20* Lower Lisbon Fm.
Stream cut on SW bank of Thompson Creek .3 miles NW of old railroad tracks (now logging road), 1.2 miles N of county road 8 on RR tracks, west of highway 17 and NE of Souwilpa; N ½, SW ¼, SW ¼, Sec. 18, T. 10 N., R. 3 W.

ACh-21* Tallahatta Fm. (top); Lower Lisbon Fm.
Bank exposure facing N toward swampy lake on W side of old railroad tracks, about 1 mile N of county road 8, west of highway 17 and NE of Souwilpa; NW ¼, Sec. 19, T. 10 N., R. 3 W.

ACh-22* Tallahatta Fm.
Creek-bed exposure on Souwilpa Creek, .3 miles E of highway 17 on dirt road, 1.5 miles N of intersection with US 84; SW ¼, NW ¼, Sec. 32, T. 10 N., R. 3 W.

ACh-23* Upper Lisbon Fm.
Stream cut on E bank of Puss Cuss Creek, park 4 miles N of US 84 on county road 39, walk in on hunting club trail, first right fork, stay right at clearing and cross stream; NW ¼, SW ¼, SW ¼, Sec. 18, T. 10 N., R. 4 W.

ACh-24* Upper Lisbon Fm.
Creek-bed and surface exposure at SE end of lake,

on west side of county road 39 SE of Evansboro, AL, 5 miles N of intersection with US 84, park at dirt road S of stream outlet and walk up, to the right, and downhill to stream; W ½, NW ¼, SW ¼, Sec. 7, T. 10 N., R. 4 W.

ACh-25 Tallahatta Fm. (Lower Lisbon reported but was not observed)
Road cut on N side of county road 23 about 4 miles N of Womack Hill, just SW of Tallawampa Creek; (Toulmin and others, 1951); SW ¼, SE ¼, SE ¼, Sec. 27, T. 11 N., R. 2 W.

ACh-26 outcrop no longer exists (Gosport Sand, Moodys Branch)
Road cut on east side of Puss Cuss Creek on county road 14, 3.9 miles west of Gilbertown; (Toulmin and others, 1951); NE ¼, SE ¼, SW ¼, Sec. 28, T. 11 N., R. 4 W.

ACh-27 Gosport Sand; Moodys Branch
Road cut on highway 17, about .25 miles south of Cullomburg; (Toulmin and others, 1951); N ½ of junction of Sec. 31 and 32, T. 9 N., R. 3 W.

ACh-28 very overgrown (Upper Lisbon Fm., Gosport Sand, Moodys Branch)
Stream cut on south bank of Negro Creek and in road cut on county road 13, 3 miles south of Melvin; (Toulmin and others, 1951); NW ¼, Sec. 35, T. 11 N., R. 5 W.

ACh-29 outcrop not found (Hatchetigbee Fm.; Meridian Sand; Tallahatta Fm.; Lisbon Fm.)
Road cut.25 miles west of West Butler on dirt road; (Toulmin and others, 1951); SW ¼, NE ¼, Sec. 25, T. 13 N., R. 4 W.

Clarke County

ACl-3 Middle Lisbon (top), Upper Lisbon, thick section
Coffeeville Landing, left (east) bank of Tombigbee River, section extends from just upstream of landing by Folson Bridge to well south (downstream) of the bridge; 3 fault blocks expose different parts of the section; S ½, Sec. 8, and N ½, Sec. 17, T. 9 N., R. 1 W.

ACl-3a* Upper Lisbon
East side of Tombigbee River about ½ mile upstream (north) of Coffeeville Landing, ½ mile N of US 84 on route 69, turn left, go 3 ½ miles, turn left, go 2 ½ miles on dirt road, walk to river; SW ¼, Sec. 8, T. 9 N., R. 1 W.

ACl-4 Tallahatta Fm.; Lower, Middle and Upper Lisbon Fm.; Gosport Sand; Moodys Branch Fm.
Little Stave Creek, outcrops in banks along length of stream; S ½ Sec. 20, T. 7 N., R. 2 E.

ACl-9 Tallahatta Fm. (lower)
Road cut on highway 69 1.5 miles SW of Campbell; NE ¼, Sec.20, T. 11 N., R. 1 E.

ACl-12 Moodys Branch Fm.
Road cut on US 43, 9.6 miles S of intersection with Highway 5 in Thomasville, 5.8 miles N of Grove Hill; SE ¼, Sec. 34, T. 10 N., R. 3 E.

ACl-13* Hatchetigbee Fm., Meridian Sand, Tallahatta Fm. (lower)
Road cut on south side of county road 35, 5 miles west of Lower Peach Tree; Sec. 19, T. 10 N., R. 5 E.

ACl-13a* Hatchetigbee Fm.
Road cut on north side of county road 35, 4.5 miles west of Lower Peach Tree; Sec. 19, T. 10 N., R. 5 E.

ACl-14 Moodys Branch Fm.
Road cut on US 4, 2 miles N of Grove Hill; (Siesser, 1983); Sec. 22, T. 9 N., R. 3 E.

ACL-15 Tallahatta Fm.
Road cuts along Highway 69 about 1 mile SE of Campbell above Tallahatta Creek; (Copeland, 1968); W ½, NW ¼, Sec. 21, T. 11 N., R. 1 E.

Monroe County

AMo-4 Gosport Sand, Moodys Branch Fm.
Claiborne Bluff, east side of Alabama River, directly under and north of US 84 bridge over river, approach from road to boat ramp; SE ¼, NE ¼, Sec. 25, T. 7 N., R. 5 E, and NE ¼, Sec. 30, T. 7 N., R. 6 E.

AMo-4a Upper Lisbon Fm., Gosport Sand
Claiborne Bluff landslide zone, east side of Alabama River, south of US 84 bridge and lower landing site, approach by boat or turn right on 2nd road SE of US 84 bridge and walk through back of cemetery next to Mount Zion Church and down south side of large gully through woods; SE ¼, Sec. 25, T. 7 N., R. 5 E.

Washington County

AWa-2 Upper Lisbon Fm., Gosport Sand, Moodys Branch Fm.
Bakers Hill on west side of Tombigbee River, ¾ mile north (upstream) of St. Stephens Quarry, south end of Old Lock One Cutoff; T. 7 N., R. 1 W.

LOUISIANA

LNa-1* Weches Fm.
Road cut on west side of I-49 just over a mile south of rt 6 exit, Natchetoches.

MISSISSIPPI

Clarke County

MCl-1 Upper Lisbon (Cook Mt.) Fm., Potterchitto, Gordon Creek, Cockfield Members
Outcrop on N side of highway 513, 1.2 miles west of I-59, west of Enterprise; Dockery #54; SE ¼, NW ¼, NE ¼, Sec. 29, T. 4 N., R. 14 E.

MCl-2 Upper Lisbon (Cook Mt.) Fm., Potterchitto, Gordon Creek, Cockfield Members
Railroad cut on N side of tracks under highway 11 bridge, about 4 miles south of Enterprise; Dockery #55, NE ¼, NE ¼, NW ¼, Sec. 10, T. 3 N., R. 14 E.

MCl-3 Upper Lisbon (Cook Mt.) Fm., Archusa Marl Mbr.
Railroad cut on N and S sides of tracks, about 1 mile

N of highway 11 bridge south of Enterprise; Dockery #s 61 and 62; W ½, NE ¼, Sec. 3, T. 3 N., R. 14 E.

MCl-4 Upper Lisbon (Cook Mt.) Fm., Archusa Marl Mbr.
Archusa Creek Water Park, road cut on east side of Shiloh Road (Co. road 110) just south of park entrance, east of Quitman; Dockery #27; NE ¼, NW ¼, SW ¼, Sec. 7, T. 2 N., R. 16 E.

MCl-5* Upper Lisbon (Cook Mt.) Fm., Potterchitto, Gordon Creek, Cockfield Members
New outcrop on east side of Shiloh Road, 4.3 miles south of intersection with highway 511, SE of Quitman; SW ¼, SW ¼, SW ¼, Sec. 29, T. 2 N., R. 16 E.

MCl-5a* Upper Lisbon (Cook Mt.) Fm., Archusa Marl Mbr.
Stream cut on Fallen Creek, under Shiloh Road bridge, 4 miles south of intersection with highway 511, SE of Quitman; SW ¼, NW ¼, SW ¼, Sec.29, T. 2 N., R. 16 E.

MCl-6 Middle Lisbon, Doby's Bluff Tongue of Kosciusko Fm.; Upper Lisbon (Cook Mt.) Fm., Archusa Marl Mbr.
Doby's Bluff, east side of the Chickasawhay River; Dockery #26; SW ¼, NW ¼, NW ¼, Sec. 18, T. 2 N., R. 16 E.

MCl-7 Lower Lisbon (Winona) Fm.
Stream cut on east bank of Chickasawhay River about ½ mile south of Rt. 513 bridge at Enterprise; Dockery #22; SW ¼, NE ¼, SE ¼, Sec. 24, T. 4 N., R. 14 E.

MCl-8* Lower Lisbon (Winona) Fm.
Stream cut on west bank of Chickasawhay River, directly under Rt. 513 bridge in Enterprise; SW ¼, NE ¼, Sec. 24, T. 4 N., R. 14 E.

Hinds County

MHi-1 Cockfield Mbr.; Moodys Branch Fm., Yazoo Fm.
Riverside Park, Jackson, MS, outcrop in steep ravine along nature trail below a golf course; NE ¼, NW ¼, NW ¼, Sec. 36, T. 6 N., R. 1 E.

Lauderdale County

MLa-1 Tallahatta Fm., Basic City Shale Mbr.
Road cut on US 11 north of Basic City, next to RR tracks, near type section (on RR tracks; Dockery #60); SW ¼, Sec. 33, T. 4 N., R. 15 E.

MLa-2 no outcrop found, very overgrown (Tallahatta Fm.)
Ditch on west side of road 50 ft south of Dunn's Falls, between Arundel and Basic City; Dockery #24; SE ¼, NE ¼, SW ¼, Sec. 21, T. 4 N., R. 15 E.

MLa-3 Tallahatta Fm.
Dunn's Falls, about 2 ½ miles N of highway 11, N of Enterprise (follow signs from hwy 11 or I-59); SE ¼, NE ¼, SW ¼, Sec. 36, T. 5 N., R. 14 E.

MLa-4* Meridian Sand; Tallahatta Fm.; Lower Lisbon (Winona) Fm.
Road cut on west side (also east) of new stretch of highway 45 5.3 miles south of I-20 in Meridian, 1 mile N of junction with Rt. 145 (old Rt. 45);

Newton County

MNe-1* Middle Lisbon (Kosciusko) Fm. (top); Upper Lisbon (Cook Mt.) Fm. Archusa Marl
Road cut on east side of dirt road, about 1 mile S of Hickory on highway 503, turn right on dirt road, about 3/4 mile to top of first hill; SE ¼, NW ¼, SW ¼, Sec. 2, T. 5 N., R. 12 E.

MNe-1a Upper Lisbon (Cook Mt.) Fm. Archusa Marl Mbr.
Road cut on east side of dirt road, about 1 mile S of Hickory on highway 503, turn right on dirt road, about 1 mile down, top of second hill; Dockery #71; SE ¼, NW ¼, SW ¼, Sec. 2, T. 5 N., R. 12 E.

MNe-2 Upper Lisbon (Cook Mt.) Fm. Potterchitto, Gordon Creek, Cockfield Sand Mbrs.
Outcrop behind Citgo gas station on SW corner of intersection of I-20 and highway 15, NE of Newton; Dockery #65; NE ¼, NW ¼, NE ¼, Sec.***, T. 6 N., R. 11 E.

MNe-3 Upper Lisbon (Cook Mt.) Fm. Archusa Marl Mbr.
Stream cut behind Boro's Restaurant, intersection of I-20 and highway 15, NE of Newton; NE ¼, Sec. ***, T. 6 N., R. 11 E.

MNe-4 Tallahatta Fm.; Lower Lisbon (Winona) Fm.
Road cuts along I-20 and highway 80 between Meridian and Newton

SOUTHEASTERN GEOLOGY
V. 38, No. 1, September 1998, p.21-27

AGE AND ISOTOPIC COMPOSITION OF THE APPLING GRANITE, EASTERN GEORGIA

ANN HEATHERINGTON

Department of Geology
University of Florida
Gainesville, FL 32611-7340

ABSTRACT

U-Pb zircon dating of the Appling granite yielded a precise age of 294.2 ± 0.9 Ma, demonstrating that it was emplaced during the latter part of the Alleghanian orogenic event. This is the first radiometric date reported for this pluton. Whole-rock Sr and Nd isotopic data (initial $^{87}Sr/^{86}Sr = 0.70385$; initial $\varepsilon_{Nd} = -0.5$) suggest that the magma was derived from an unenriched source, such as mafic crust and/or lithospheric mantle.

INTRODUCTION

The Appling granite is located in eastern Georgia, U.S.A. (Figure 1). It intrudes the Kiokee Belt, within the Carolina terrane as delineated by Horton and others (1989; 1991), as well as the Savannah River terrane, a portion of the Carolina terrane that Maher and others (1991) proposed as a separate, exotic block. The Appling granite is undeformed and contains two petrographic phases, one a porphyritic phase consisting of biotite granite with large alkali feldspar phenocrysts, and the other a medium-grained biotite-muscovite-garnet granite (Nusbaum and others, 1992). Nusbaum and others (1992) classified the porphyritic phase as an I-type granite and the medium-grained phase as transitional between S- and I-type based on chemical compositions and the criteria of Chappell and White (1974). Although it has not previously been successfully dated, the undeformed nature of Appling granite, and its petrographic similarity to known late Paleozoic southern Appalachian plutons has led to its classification as part of the late Paleozoic (ca. 325-265 Ma) Alleghanian orogenic suite (Fullagar and Butler, 1979; Wenner, 1981).

Over the past 15 to 20 years, there has been considerable speculation in the literature concerning the tectonic environment in which the Alleghanian plutons were emplaced, and how that environment may have evolved over the approximately 60 million year duration of the orogenic event (e.g., Fullagar and Butler, 1979; Sinha and Zietz, 1982; Cook and others, 1983; Dallmeyer and others, 1986; Secor and others, 1986a and 1986b; Hermes and Murray, 1988; Gates and others, 1988; Hatcher, 1989; Sacks and Secor, 1990; Speer and others, 1994; Samson and others, 1995; Speer and Hoff, 1997). Petrogenetic models proposed for Alleghanian plutonism in the southern Appalachians encompass a wide range, in part because the paucity of quality geochronologic data available for the plutons limits time-space-composition analysis of the orogen. These models include: west-dipping subduction that led to the development of a voluminous magmatic arc (Sinha and Zietz, 1982), decompressional crustal melting in a transpressional tectonic regime (Gates and others, 1988; Speer and others, 1994; Speer and Hoff, 1997), intracrustal melting induced by crustal thickening (Cook and others, 1983), and intracrustal melting caused by crustal delamination which was, in turn, induced by crustal thickening (Sacks and Secor, 1990; Nelson, 1992; Samson and others, 1995).

In addition, the age and geochemical composition of the Appling granite, in particular, is relevant to models concerning the origin and thermal history of the Savannah River terrane and its bounding faults (Maher and others, 1994). Results of U-Pb zircon dating and whole-rock Sr and Nd isotopic analysis of the Appling granite show that it was emplaced dur-

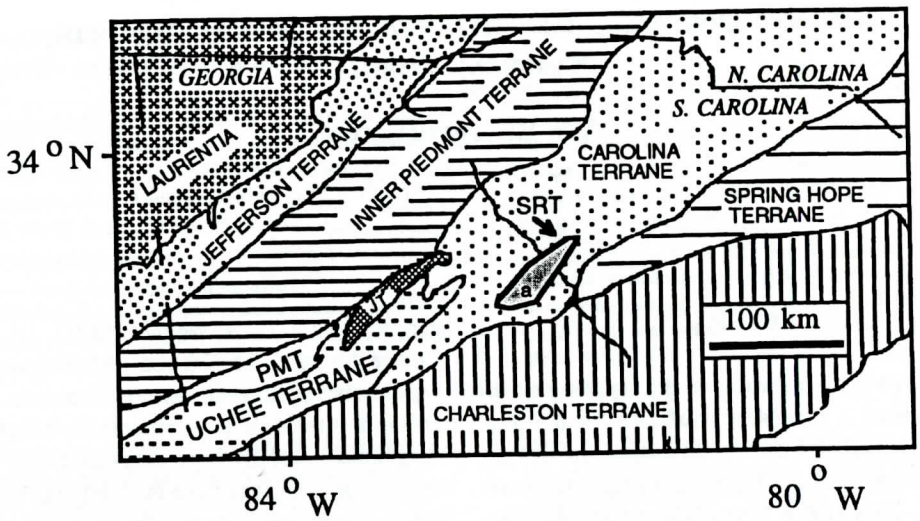

Figure 1. Approximate location of the Appling granite ("a") on a tectonostratigraphic terrane map drawn after Horton and others (1989; 1991). The Appling granite covers 32 square kilometers (Fullagar and Butler, 1979) within the Savannah River terrane. Abbreviations: SRT= Savannah River terrane; JT=Juliette terrane; PMT= Pine Mountain terrane.

ing the latter part of the Alleghanian event and provide additional data to help constrain tectonic and petrogenetic models for the evolution of the Alleghanian orogen and the Savannah River terrane.

SAMPLE AND ANALYTICAL METHODS

The sample analyzed was obtained from the Southern Aggregates Company Dogwood Quarry 3.5 miles east of Appling, GA, on Georgia Rt. 232. The sample is from the porphyritic phase of the pluton as defined by Nusbaum and others (1992). Mineralogy observed in hand sample and thin section consists of large (2-8 cm) K-feldspar phenocrysts (~40% of total volume) in a groundmass of small alkali feldspar crystals (~10%), plagioclase (~20%), biotite, partially altered to chlorite (~5%), quartz (~25%), and sphene (<1%), zircon (<1%), and opaque minerals (<1%).

The whole-rock sample was crushed in a steel jaw crusher, then ground to <50 mesh using a disk mill. A small portion of the coarse crush was powdered in an alumina ceramic mixer mill and reserved for whole-rock analysis. Heavy minerals were separated from the <50 mesh portion by passing the sample over a water table and then though heavy liquids. Zircons were separated from the heavy mineral fraction via magnetic separation followed by hand picking. A considerable amount of pyrite was present in the heavy mineral fraction.

The zircons are clear, euhedral and have a uniform morphology, despite large variations in size. All grains had a high length to width ratio (typically 4:1 to 6:1) and were generally flattened. Lengths ranged from 25 to 500 microns. Zircons were separated according to size and magnetic susceptibilities. Some were air-abraded to remove potentially discordant outer portions of the grains, and all were washed in warm HNO_3 prior to dissolution. A mixed ^{205}Pb-^{235}U spike was added to the zircons before dissolution in purified HF + HNO_3, at 230°C in Teflon capsules contained within a sealed, steel-jacketed Teflon bomb. Separation of Pb and U was achieved via standard HCl chromatography on Dowex 200-400 mesh AG 1-X8 anion exchange resin (Krogh, 1973). Total procedural blanks at UF were 5 to 10 pg for Pb and <1 pg for U.

For whole-rock isotopic analyses, rock powder was dissolved by heating in a sealed Teflon vial for two days at 120° C with purified HF and a few drops of purified HNO_3. Rb, Sr, and rare-earth elements were separated using standard

chromatographic methods on Dowex 50-X12 cation exchange resin. Nd and Sm were separated from the other rare earth elements using HCl elution on quartz columns packed with Teflon beads coated with bis-ethylhexyl phosphoric acid (after Richard and others, 1976). Concentrations of Rb, Sr, Sm and Nd were determined by isotope dilution. Samples analyzed for Sr, Rb, Nd, and Sm were spiked prior to dissolution with ^{87}Rb, ^{84}Sr, ^{149}Sm, and ^{150}Nd tracers in order to determine elemental concentrations. Procedural blanks are less than 30, 80, 200, and 350 picograms for Sm, Nd, Rb, and Sr, respectively.

The elemental separates were analyzed using a VG 354 thermal ionization mass spectrometer at the University of Florida, with the exception of zircon fraction D (Table 1), which was analyzed on a VG Sector 54 spectrometer at MIT (for analytical conditions at MIT, see Bowring and others, 1993). At UF, Rb, Sm, Nd, Pb, and U isotopic ratios were determined in single collector mode, and Sr ratios were determined in dynamic triple collector mode. Lead separates were loaded on single rhenium filaments together with silica gel and phosphoric acid. Lead isotopic compositions were measured using a single Faraday collector with an ion beam intensity of 1×10^{-12} to 1×10^{-11} amps of total Pb and were corrected for -0.065% per amu mass discrimination based on results for NBS 981 (measured $^{207}Pb/^{206}Pb = 0.91396$). Uncertainties in measured isotopic ratios of $^{207}Pb/^{206}Pb$ are <0.07% (2-sigma) based on long-term reproducibility of NBS 981 analyses. Uranium separates were loaded on single rhenium filaments together with graphite and phosphoric acid. Uranium isotopic compositions were measured using a single analog Daly collector with a total beam intensity of 4×10^{-14} to 2×10^{-13} amps. Errors in ages and calculated ratios of $^{207}Pb/^{206}Pb$, $^{235}U/^{207}Pb$, $^{238}U/^{206}Pb$ were determined using methods of Ludwig (1991).

Strontium samples were loaded on tungsten single filaments with tantalum oxide. Data were acquired at a beam intensity of 2 volts total Sr, with corrections for instrumental discrimination made assuming $^{86}Sr/^{88}Sr = 0.1194$. Errors in measured $^{87}Sr/^{86}Sr$ are better than +-0.00002 (2-sigma) based on long-term reproducibility of NBS 987 ($^{87}Sr/^{86}Sr = 0.71024$). Nd and Sm samples were loaded on one side filament of a triple filament array using Re center filaments and Ta side filaments. Data were acquired at a beam intensity of 1.2 V total Nd, with corrections for instrumental discrimination made assuming $^{146}Nd/^{144}Nd = 0.7219$. Errors in measured $^{143}Nd/^{144}Nd$ are better than 0.00002 (2-sigma) based on long-term reproducibility of the La Jolla Nd standard ($^{143}Nd/^{144}Nd = 0.511836$). $^{143}Nd/^{144}Nd$ values (ε_{Nd}) are cited as parts in 10^4 deviation from CHUR (chondritic uniform reservoir) defined by present-day $^{143}Nd/^{144}Nd = 0.512638$ and $^{147}Sm/^{144}Nd = 0.1967$ (Jacobsen and Wasserburg, 1980).

RESULTS

Geochronology

U-Pb dates were obtained for eight fractions of zircon of varying size and magnetic susceptibility designated with the letters "A" through "H" in Table 1. Results are also shown on a Tera-Wasserberg plot (Figure 2, generated using software of Ludwig (1990)). (For young zircons such as these, where little growth of ^{207}Pb has occurred, a Tera-Wasserberg plot is more relevant than a conventional concordia plot (Tera and Wasserburg, 1973 and 1974)). The smallest of these fractions (fraction D, Table 1) consisted of fourteen individual zircon grains weighing a total of 0.009 mg. It was not possible to analyze individual grains because of their low Pb abundances. In Mesoproterozoic or younger rocks containing zircons of moderate U-content, ages based on the $^{206}Pb/^{238}U$ system are generally preferred over those produced using either the $^{207}Pb/^{235}U$ system or the combination of the two systems ($^{207}Pb/^{206}Pb$). This is a consequence of the low abundance of ^{207}Pb, which results in low beam intensities for this isotope and lower precision for ages involving the $^{207}Pb/^{235}U$ system. The $^{206}Pb/^{238}U$ ages are more precise and provide more useful minimum ages. Three $^{206}Pb/^{238}U$ ages were concordant within 2-sigma error (Figure 2). These ages were: 293.2 ± 4.2 Ma (fraction A), 292 ± 1.7 Ma

Table 1. U-Pb geochronologic data.

Fraction	Grain Size (microns)	**Magnetic Properties	Air-abraded?	Weight (mg)	U (ppm)	Pb (ppm)	measured $^{206}Pb/^{204}Pb$	$^{207}Pb/^{235}U$	$^{206}Pb/^{238}U$	$^{207}Pb/^{206}Pb$	$^{206}Pb/^{238}U$ Age (Ma)
A	<75	m 1°	yes	0.027	769.5	39.1	583.4	0.3352	0.04653	0.05225	293.2 ± 4.2
B	<75	m 1°	no	0.57	1152.6	56.7	5465	0.3406	0.04703	0.05252	296.3 ± 4.4
C	<75	m 1°	no	0.3	1130.1	54.5	6993	0.3327	0.04634	0.05208	292.0 ± 1.7
D†	<75	m 1°	yes	0.009	563.1	30.5	469.8	0.3358	0.04663	0.05223	293.8 ± 0.7
E	<75	m 0°	no	0.75	854.8	40.4	11765	0.3268	0.04520	0.05244	*285.0 ± 3.9
F	>150	nm 1°	yes	0.03	870.5	42.8	1030	0.3437	0.04701	0.05303	296.1 ± 1.5
G	>150	m 1°	no	0.35	871.8	41.3	14095	0.3388	0.04664	0.05269	293.9 ± 1.6
H	>150	m 4°	no	0.15	724.3	31.6	2457	0.3225	0.04406	0.05309	*277.9 ± 1.1
											mean = 294.2 ± 0.9

† analyzed at MIT

* values not used in computing average age

**m=magnetic; nm=nonmagnetic. Degrees refer to side tilt on Franz magnetic separator.

Age errors are 2-sigma

(fraction C), and 293.8 ± 0.7 Ma (fraction D) (Table 1). Two fractions, E (285.0 ± 3.9 Ma) and H (277.9 ± 1.1 Ma), yielded ages significantly younger than the others, possibly as a result of post-crystallization loss of lead. Fraction H had a high magnetic susceptibility, consistent with lattice damage and post-crystallization lead loss. The average $^{206}Pb/^{238}U$ age of the six fractions with the oldest ages was 294.2 ± 0.9 Ma, which agrees, within 2-sigma error, with the ages of the three concordant fractions. No obvious indications of inherited components or other primary chronologic heterogeneities are present in the data.

Whole-Rock Isotopic Analysis

Initial isotopic ratios for the Appling granite are: $^{87}Sr/^{86}Sr = 0.70385$; $\varepsilon_{Nd} = -0.5$ (Table 2). Samson and others (1995) previously reported initial $^{87}Sr/^{86}Sr$ ratios of 0.7038 to 0.7049 for this pluton using estimated ages of 325 and 275

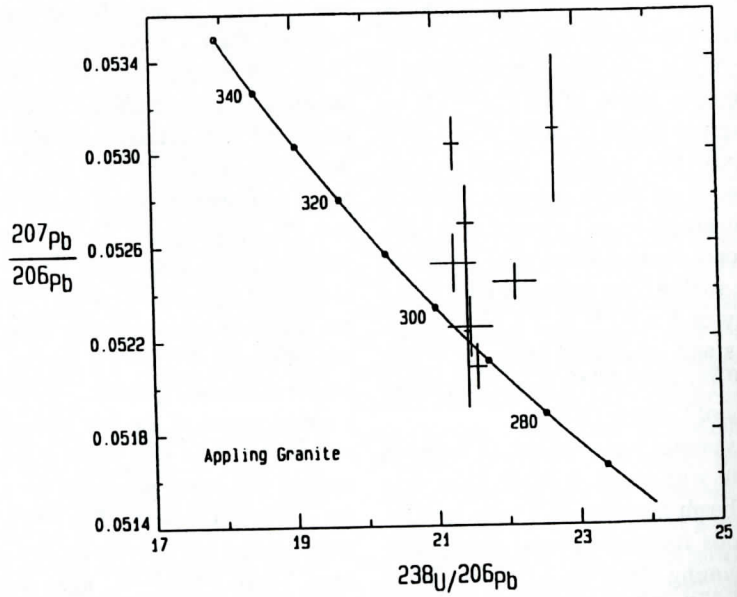

Figure 2. Tera-Wasserburg plot of U-Pb zircon data. Ages along concordia curve are given in Ma. Error bars are 2-sigma.

Table 2. Whole-rock isotopic data.

$^{87}Sr/^{86}Sr$ (present)	0.71158
Rb (ppm) †	183
Sr (ppm) †	287
$^{87}Rb/^{86}Sr$	1.848
$^{87}Sr/^{86}Sr$ (294 Ma)	0.70385
$^{143}Nd/^{144}Nd$	0.512433
Nd (ppm) †	42
Sm (ppm) †	7.2
$^{147}Sm/^{144}Nd$	0.10309
ε Nd (present)	-4.0
$^{143}Nd/^{144}Nd$ (294 Ma)	0.51223
ε Nd (294 Ma)	-0.5
T_{DM}*	853 Ma

†Concentration (ppm) determined by isotope dilution

* Depleted mantle model age calculated using the model of Depaolo (1981)

Ma, respectively, and an initial ε_{Nd} of +0.5 using an estimated age of 300 Ma. Recalculation of Samson and others' data to 294 Ma, and adjustment for interlaboratory differences in measured $^{143}Nd/^{144}Nd$ ratios for the LaJolla standard produces initial ratios of $^{87}Sr/^{86}Sr$ = 0.70444 and ε_{Nd} = +0.1. The ε_{Nd} value is the same as that reported here within quoted 2-sigma errors. The $^{87}Sr/^{86}Sr$ ratio is slightly higher than the value reported here; the difference may indicate a degree of source heterogeneity within the pluton, which is not uncommon for large granitic bodies, including the Alleghanian plutons (e.g., Leake, 1990; Fullagar and Butler, 1979).

These initial $^{87}Sr/^{86}Sr$ values of 0.70385 (this work) and 0.70444 (recalculated from Samson and others, 1995) are some of the lowest reported for Alleghanian plutons of the southern Appalachians (c.f. data of Fullagar and Butler, 1979; Sampson and others, 1995). Coupled with the initial ε_{Nd} values of -0.5 (this work) and +0.1 (recalculated from Samson and others, 1995), they are consistent with derivation of the Appling granite magma from relatively non-radiogenic crust and/or mantle. Near-zero initial ε_{Nd} values and initial $^{87}Sr/^{86}Sr$ ratios < 0.706 are typical of the majority of Alleghanian plutons within the Carolina terrane and Kiokee belts, in contrast with plutons of the Inner Piedmont terrane, which have negative initial ε_{Nd} values and initial $^{87}Sr/^{86}Sr$ ratios > 0.706 (Samson and others, 1995).

DISCUSSION AND CONCLUSIONS

The U-Pb zircon data indicate a crystallization age of 294.2 ± 0.9 Ma for the Appling granite. Speer and others' (1994) compilation of reported ages for Alleghanian plutons suggests a bimodal age distribution (300-282 Ma and 326-305 Ma). Within this grouping, the Appling granite belongs to the younger set, which represents a second pulse of magmatic activity within the Alleghanian event. Additional quality geochronologic data for other Alleghanian plutons must be gathered in order to determine whether the bimodality is real, or an artifact of the available data, as Speer and others (1994) cautioned.

The Appling granite is younger than the U-Pb age of 317 ± 4 reported for two, somewhat discordant, zircon fractions from the Edgefield granite, also located within the Savannah River terrane (Dallmeyer and others, 1986). The Edgefield granite contains a weak foliation and was interpreted to have been emplaced prior to the regional D_2 foliation event (Lake Murray deformation: 295-315 Ma, Snoke and others, 1980; Dallmeyer and others 1986; and Secor and others, 1986a and 1986b). The measured U-Pb age for the Appling granite indicates it postdates the D_2 event and is within the upper end of the age range reported for the subsequent D_3 event (Clarks Hill deformation: 285-295, Snoke et al, 1980; Dallmeyer and others, 1986; and Secor and others, 1986a and 1986b). The D_3 event produced map-scale folds, outcrop scale folds, and crinkle lineations. It was the last deformational event to affect the part of the Savannah River terrane in which the Appling granite is located (Maher and others, 1991). The absence of deformational fabric within the Appling granite suggests that the lower limit for the age range of the D_3 event within the Savannah River terrane may be closer to 294 Ma.

The whole-rock isotopic data indicate deriva-

tion of the Appling granite magmas from a relatively unenriched source, with a near-bulk earth composition. This may support indications of a sub-lithospheric mantle contribution to the magma at the time of its genesis, with subsequent contamination by a more enriched lithospheric component. The data are also consistent, however, with magma derivation by partial melting of mafic, unenriched crust and/or lithospheric mantle. Wenner (1981) measured a low $\delta\ ^{18}O$ of +6 for the Appling granite, and similarly low values (+8.2 to +5.5) for the majority of plutons of Charlotte-Slate belt (Carolina terrane) and Kiokee belt. He proposed that these plutons were derived from mafic sources. This hypothesis is consistent with the present results, with the findings of Sacks and others (1989), who suggested that the lithologies composing the Savannah River terrane were metamorphosed and migmatized ophiolites from a mid-ocean ridge setting, and with the ideas of Samson and others (1995), who hypothesized on the basis of radiogenic isotope data that the Kiokee belt contains a large amount of juvenile crust.

ACKNOWLEDGMENTS

The author thanks Sam Bowring for use of mass spectrometry facilities at MIT, Southern Aggregates Company for quarry access, and Michael Smith for field assistance. Comments by Paul Fullagar and Robert Nusbaum improved the manuscript. This work was supported by NSF grant EAR-9206119.

REFERENCES CITED

Bowring, S.A., Grotzinger, J.P., Isachsen, C.E., Knoll, A.H., Pelechaty, S.M., Kolosov, P., 1993, Calibrating rates of Early Cambrian evolution: Science, v. 261, p. 1293-1298.

Chappell, B.W. and White, A.J.R., 1992, I- and S-type granites in the Lachlan Fold Belt, in Brown, P.E., and Chappell, B.W., eds., The Second Hutton Symposium on the Origin of Granites and Related Rocks: GSA Special Paper 272, p. 1-26.

Cook, F.A., Brown, L.D., Kaufman, S., and Oliver, J.E., 1983, The COCORP seismic reflection traverse across the southern Appalachians: AAPG Studies in Geology 14, 61 p.

Dallmeyer, R., Wright, J., Secor, D., and Snoke, A., 1986, Character of the Alleghanian orogeny in the southern Appalachians: Part II. Geochronological constraints on the tectonothermal evolution of the eastern Piedmont in South Carolina: Geological Society of America Bulletin, v. 97, p. 1329-1344.

DePaolo, D.J., 1981, Neodymium isotopes in the Colorado Front Range and crust-mantle evolution in the Proterozoic: Nature, v. 291, p. 193-196.

Fullagar, P.D. and Butler, J.R., 1979, 325 to 265 m.y.-old granitic plutons in the Piedmont of the southeastern Appalachians: American Journal of Science, v. 279, p. 161-185.

Gates, A.E., Speer, J.A., and Pratt, T.L., 1988, The Alleghanian southern Appalachian Piedmont: A transpressional model: Tectonics, v. 7., p. 1307-1324.

Hatcher, R.D., Jr., 1989, Tectonic synthesis of the U.S. Appalachians, *in* Hatcher, R.D., Jr., Thomas, W.A., and Viele, G.W., eds.: The Appalachian-Ouachita orogen in the United States (Geology of North America, Vol., F-2): Boulder, CO, GSA, p. 511-535.

Hermes, O.D. and Murray, D.P., 1988, Middle Devonian to Permian plutonism and volcanism in the N. American Appalachians, *in* Harris, A.L. and Fettes, D.J., The Caledonian-Appalachian Orogen: Geological Society Special Publication 38, p. 559-571.

Horton, J.W. Jr., Drake, A.A., Jr., and Rankin, D.W., 1989, Tectonostratigraphic terranes and their Paleozoic boundaries in the central and southern Appalachians, *in* Dallmeyer, R.D., ed., Terranes in the Circum-Atlantic Paleozoic Orogens: GSA Special Paper 230, p. 213-246.

Horton, J.W. Jr., Drake, A.A., Jr., and Rankin, D.W., 1991, Preliminary Tectonostratigraphic Terrane Map of the Central and Southern Appalachians, U.S. Geological Survey Investigations Map 2163.

Jacobsen, S.B. and Wasserberg, G.J., 1980, Sm-Nd isotopic evolution of chondrites: Earth and Planetary Science Letters, v. 41, p. 139-155.

Krogh, T.E., 1973, A low-contamination method for hydrothermal decomposition of zircon and extraction of U and Pb for isotopic age determinations: Geochimica et Cosmochimica Acta, v. 37, p. 485-494.

Leake, B.E., 1990, Granite magmas: their sources, initiation, and consequences of emplacement: Journal of the Geological Society, London, v. 147, p. 579-589.

Ludwig, K.R., 1991, PBDAT- A computer program for processing Pb-U-Th isotope data, version 1.23: USGS Open File Report 88-542, 34 pp.

Ludwig, K.R., 1990, Isoplot: a plotting and regression program for radiogenic-isotope data, for IBM-PC compatible computers, version 2.03: U.S. Geological Survey Open-File Report 88-557.

Maher, H.D., Jr., Dallmeyer, R.D., Secor, D.T., Jr., and Sacks, P.E., 1994, 40Ar/39Ar constraints on chronology of Augusta fault zone movement and late Alleghanian extension, southern Appalachian Piedmont, South Carolina and Georgia: American Journal of Science, v. 294, p. 428-448.

Maher, H.D., Jr., Sacks, P.E., and Secor, D.T., Jr., 1991, The Eastern Piedmont of South Carolina, *in* Horton, R.W., and Zullo, V., eds., The Geology of the Carolinas, Carolina Geological Society 50th Anniversary v.: University of Tennessee Press, p. 93-108.

Nelson, K.D., 1992, Are crustal thickness variations in old mountain belts like the Appalachians a consequence of lithospheric delamination?: Geology, v. 20, p. 498-502.

Nusbaum, RL., Green, J.D., Whiting, N., Stakes, D.S., and Glascock, M.D., 1992, The postmetamorphic Appling Granite, Georgia: Origin of facies and large mafic enclaves in a composite granite: Southeastern Geology, v. 33, p. 9-21.

Richard, P., Shimazu, N., and Allegre, C.J., 1976, Neodymium and strontium isotope study of ophiolite and orogenic lherzolite: Earth and Planetary Science Letters, v. 31, p. 269-278.

Sacks, P.E., Maher, H.D., Jr., Secor, D.T., Jr., and Shervais, J.W., 1989, The Burks Mountain complex, Kiokee belt, southern Appalachian Piedmont of South Carolina and Georgia: Geological Society of America Special Paper 231, p. 75-86.

Sacks, P.E. and Secor, D.T., Jr., 1990, Kinematics of Late Paleozoic continental collision between Laurentia and Gondwana: Science, v. 250, p. 1702-1705.

Samson, S.D., Coler, D.G., and Speer, J.A., 1995, Geochemical and Nd-Sr-Pb isotopic composition of Alleghanian granites of the southern Appalachians: Origin, tectonic setting, and source characterization: Earth and Planetary Science Letters, v. 134, p. 359-376.

Secor, D. T., Snoke, A.W., Bramlett, K.W., Costello, O.P., and Kimbrell, O.P., 1986a, Character of the Alleghanian orogeny in the southern Appalachians: Part I. Alleghanian deformation in the eastern Piedmont of South Carolina: Geological Society of America Bulletin, v. 97, p. 1319-1328.

Secor, D., Snoke, A., and Dallmeyer, R., 1986b, Character of the Alleghanian orogeny in the southern Appalachians: Part III. Regional tectonic relations: Geological Society of America Bulletin, v. 97, p. 1345-1353.

Sinha, A.K. and Zietz, I., 1982, Geophysical and geochemical evidence for a Hercynian magmatic arc, Maryland to Georgia: Geology, v. 10, p. 593-596.

Snoke, A.W., Kish, S.A. and Secor, D.T., 1980, Deformed Hercynian granite rocks from the Piedmont of South Carolina: American Journal of Science, v. 280, p. 1018-1034.

Speer, J.A., and Hoff, K., 1997, Elemental composition of the Alleghanian granitoid plutons of the southern Appalachians, *in* Sinha, A.K., Whalen, J.B., and Hogan, J.P., eds, The Nature of Magmatism in the Appalachian Orogen: Boulder, CO, Geological Society of America Memoir 191.

Speer, J., McSween, H., and Gates, A., 1994, Generation, segregation, ascent, and emplacement of Alleghanian plutons in the southern Appalachians: Journal of Geology, v. 102, p. 249-267.

Tera, F. and Wasserburg, G.J., 1973, A response to a comment on U-Pb systematics in lunar basalts: Earth and Planetary Science Letters, v. 19, p. 213-217.

Tera, F. and Wasserburg, G. J., 1974, U-Th-Pb systematics on lunar rocks and inferences about lunar evolution and the age of the Moon: Proceedings of the 5th Lunar Science Conference (Supp. 5): Geochimica et Cosmochimica Acta, v. 2, p. 1571-1599.

Wenner, D.B., 1981, Oxygen isotopic compositions of the late orogenic granites in the Southern Piedmont of the Appalachian Mountains, U.S.A., and their relationship to subcrustal structures and lithologies: Earth and Planetary Science Letters, v. 54, p. 186-199.

SOUTHEASTERN GEOLOGY
V. 38, No. 1, September 1998, p. 29-37

HURRICANE DANNY PRECIPITATION-INDUCED WASHOUT CHANNELS AND THEIR SUBSEQUENT REPAIR ALONG THE SOUTHEASTERN END OF DAUPHIN ISLAND, ALABAMA

CARL R. FROEDE JR.

United States Environmental Protection Agency
Region 4
Atlanta, GA 30303-3104

ABSTRACT

Hurricane Danny stalled off the southeastern end of Dauphin Island, Alabama for two days during July, 1997. The storm dropped more than one meter of precipitation across this portion of the island, and caused the formation of small- and large-scale dendritic washout channels. These channels drained ponded water and transported quartz sand from areas behind the beach scarp to the surf zone along the Gulf of Mexico. The sand within these channels probably fluidized as it flowed into the surf zone. Once transported into the shallow reaches of the Gulf of Mexico, the sand was moved either further offshore or laterally via longshore currents. Within six months following the storm, a period of natural beach replenishment had repaired the washout channels along the beach scarp to almost their original elevation. The former drainage channels located behind the repaired beach scarps remain unfilled. The lack of a vegetative cover on the now restored scarps may prove to be areas of accelerated erosion during the normal beach cycle or in subsequent storms.

INTRODUCTION

Dauphin Island, Alabama is a 25-km long micro-tidal barrier island which provides an excellent field laboratory for the study of similar barrier islands within the northern Gulf of Mexico (Campbell, 1984; Douglas, 1994; Hummell and Haywick, 1996; Knowles, 1989; Leatherman, 1988; Otvos, 1979, 1982, 1991) [Figure 1]. Information gathered by studying the island during the normal seasonal cycle and following storm events could prove valuable for coastal zone management decisions made at other barrier islands in similar settings (Alabama Department of Economic and Community Affairs, 1987; Canis, Neal, Pilkey, and Pilkey, 1985; Lins, 1980; National Research Council, 1990).

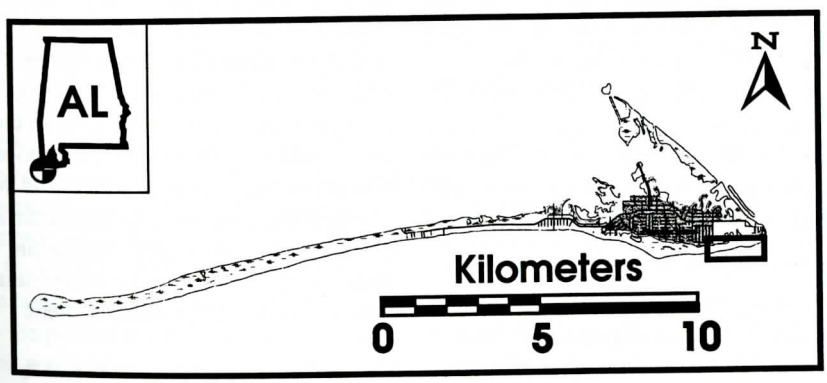

Figure 1 - Dauphin Island, Alabama showing the area covered in this investigation within the black box on southeastern end of the island. Modified from the United States Geological Survey Biloxi 1:100,000 map.

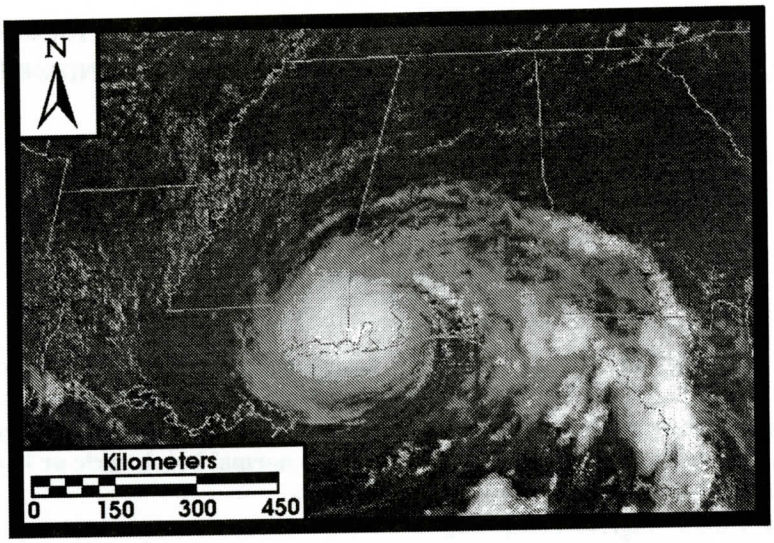

Figure 2. Visible image of Danny as seen from the GOES-8 National Weather Service satellite, taken on July 19, 1997, at 11:45 CDT. The hurricane has stalled over the eastern end of Dauphin Island, dropping over one meter of precipitation during a two-day period. Modified from Auburn University website image, 1997.

Tropical storms and hurricanes accelerate erosional processes at barrier islands which they encounter. Dauphin Island has likely experienced many such storms, since its Pleistocene origin. The most severe recent storm to impact the island was Hurricane Frederic[1], in September, 1979. Several investigators have reported on the devastating effect that this storm had across the island (Nummedal, Penland, Gerdes, Schramm, Kahn, and Roberts, 1980; Schramm, Penland, Gerdes, and Nummedal, 1980; United States Army Corps of Engineers, 1981). In July 1997, Dauphin Island experienced a much less powerful storm (Hurricane Danny[2]), but one which contributed uniquely to the rapid erosion of the southeastern section of the island.

Typically, barrier islands experience substantial erosion within the surf zone during the course of hurricanes or large storms. The combination of one or more storm surges along with high-energy waves erode and transport sand

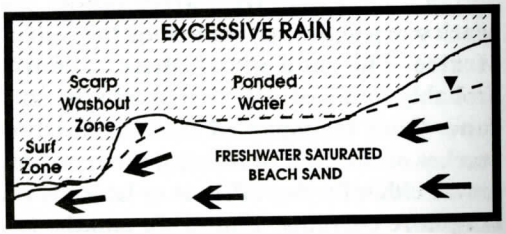

Figure 3. Precipitation associated with Hurricane Danny exceeded the quartz sand's storage capacity causing the groundwater table to rise above the ground surface in various low areas, and initiate overland flow toward the Gulf of Mexico.

away from this section of the island. However, Hurricane Danny did not impact Dauphin Island in this manner. Rather, the storm dropped a large volume of precipitation across the island with the highest levels falling on its eastern end. This article describes the formation and development of some unique small- and large-scale drainage channels created across the southeastern section of the island during the course of Hurricane Danny, and their subsequent repair in the months that followed this event.

HURRICANE DANNY

Hurricane Danny dropped more than one

1. Hurricane Frederic was a Category 3 storm, with winds ranging between 111-130 mph.
2. Hurricane Danny was a Category 1 storm, with winds ranging between 74-95 mph.

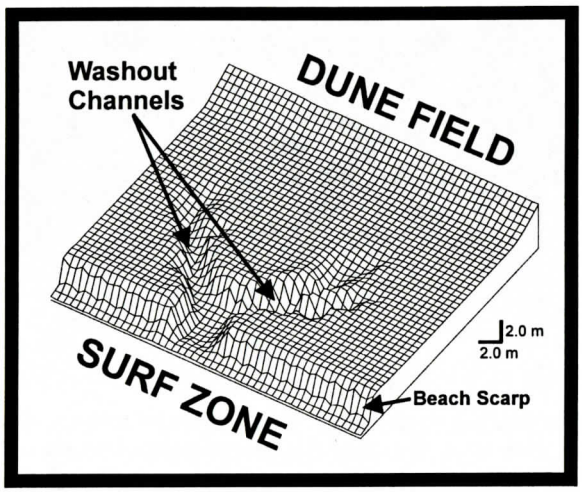

Figure 4. A generalized diagram showing the relative size and shape of one of the large washout channels in its geomorphological expression. As water accumulated at the front of the dune field, it was able to mound high enough to flow gulfward toward a low point along the beach scarp. It incised downward at the beach scarp, and intercepted the elevated groundwater table (compare with Figure 3). Rapid channel development followed, both in a headward direction and laterally.

meter of precipitation across the eastern portion of Dauphin Island (Auburn University, 1997; Pasch, 1997). This unusually large volume of water occurred because the storm stalled near the eastern end of the island from Friday, July 18, to Saturday July 19 (Pasch, 1997) [Figure 2]. Almost all of the rain readily penetrated the highly porous and permeable quartz sands. However, where rainfall exceeded the sand's ability to absorb it overland flow resulted, forming dendritic drainage channels. Two types of channels were formed, both perpendicular to the beach scarp: 1) small channels developed in the low swales of the beach scarp, and 2) large wash-out channels were created where overland flow intercepted the groundwater table along the beach scarp.

Typically, the groundwater table mirrors the topography of Dauphin Island. However, during storm events the groundwater table rapidly rises. The lateral migration of the interstitial waters from higher (i.e., dunes) to lower (i.e., surf zone) elevations accelerates with the rapid change in the potentiometric water surface. Surface water accumulates where the subsurface storage capacity is exceeded, usually in areas between the sand dune fields and the beach scarp (Figure 3). Eventually, the surface water reaches sufficient depth to initiate overland flow toward the beach scarp. As the surface water discharges over the scarp it rapidly incises downward forming a small channel. With continued development, the channel eventually intercepts the elevated groundwater table. Channel development accelerates as it deepens and moves headward with the combined flow of surface and groundwater. Concomitant cliff sapping of the channel sidewalls also occurs. All of these events result in the formation of deep, well-defined dendritic channels with steep-sided walls (Figures 4, 5, and 6). In many cases these channels extend tens of meters headward into the island (Figures 7 and 8).

FLUIDIZED SAND

The transportation of the quartz sand within the washout channels suggests that it moved initially downward and then laterally in a fluidized state. The sand particles were moved by suspension via the hydrostatic pressure within the pore spaces. This movement was not as a mass (i.e., slump); rather, the quartz particles appear to have moved individually. This interpretation is

Figure 5. A drainage channel with steep-sided walls. Note the bifurcation of the channel as it moves headward into the beach-dune zone. The channel is approximately 4 meters wide. The scale (three feet long in six-inch units) is along the left side of the channel. Brown mud lies along the bottom of the channel.

Figure 6. A drainage channel with a pine tree island. Sand remains at the former ground surface where plants roots were sufficiently close together to prevent sand loss. The sand has been removed from around the base of the pine tree with the formation of the drainage channel. The channel is approximately 8 meters wide.

Figure 7. A large washout channel which extends over 50 meters into the beach-dune zone. Note the exposed tree stumps of a paleo-maritime forest which were once buried by the sand dunes. Water stands in the bottom of the channel because it was incised below the present groundwater table.

Figure 8. A small washout channel which extends 15 meters into the beach-dune zone. The grass covered sand which formerly extended across this channel was destabilized from groundwater discharge and not from overland flow.

Figure 9. Plant roots suspended in air across a washout channel. This situation was repeated in every wash-out channel examined, and reflects the fluidized nature of sand movement within the channel. If the sand had moved as a mass then the plant roots should have been broken or abraded. The scale in the center of the channel is three feet long divided into six-inch units.

Figure 10. In certain circumstances large channels formed parallel to the elevated beach scarp. These channels reflect the combination flow of ponded water and groundwater as headward erosion of the surface channel drained both water and sand toward the opening along the beach scarp into the surf zone. The resulting channel exceeded the span of the plant roots, and they remain dangling from the sidewalls.

Figure 11. Looking toward the Gulf of Mexico, across a washout channel. Note the large pine tree root (approximately 6 cm in diameter) which still spans the channel. There is nothing left of the tremendous volume of sand which was discharged out of this channel. Natural replenishment of the surf zone has begun, but the profile fails to reflect any of the sand that passed from this area. The channel is approximately 10 meters wide at its opening.

Figure 12. Another smaller washout channel where the sand was discharged into the surf zone (same channel as Figure 8). There is no evidence of sand accumulation. Longshore currents in operation during the storm simply carried the discharged sands to the right along the shoreline, and away from the front of this channel.

based on the preservation condition of the roots and fine rootlets found suspended in air across portions of every channel examined (approximately 26 channels were inspected). The plant roots exposed within the drainage channels were perfectly preserved. They experienced no obvious physical damage as the sands moved within the channel (Figure 9). If the sand had behaved as a flowing mass, then the plant roots spanning the now empty channels should have been broken (at minimum experienced abrasion) as the sand flowed within the channel. This is not what was observed.

Vegetation within the immediate vicinity of the washout channels was impacted in various ways. In front of the dune ridge where the small channels extended headward from the large washouts at the beach scarp, the vegetation overlying the channels remained intact. Within this area fine roots were observed still spanning the empty channels. Moving toward the beach scarp the channels deepened and the overlying vegetation was generally destabilized, resulting in some cases in its lying within the channel. Larger plant roots spanned these wide empty channels with no signs of damage or abrasion. Along the beach scarp at most of the larger washouts the vegetation was completely miss-

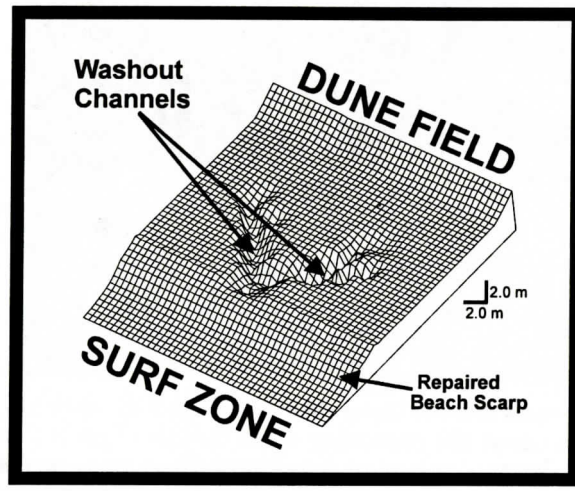

Figure 13. A generalized diagram showing the relative size and shape of a large washout channel which has experienced natural sand replenishment along the surf zone. This has almost completely repaired the washed out beach scarp to its original elevation. This addition of sand has also extended the surf zone gulfward. The drainage channels behind the repaired beach scarp remain unfilled.

ing, except for dangling plant roots along the sidewalls of the channels (Figure 10).

MISSING SAND ACCUMULATIONS

The drainage channels transported considerable volumes of sand into the surf zone. However, there was no evidence of any sand accumulation at the mouths of either the small- or large-scale washout channels (Figures 11 and 12). Hurricane Danny did not significantly raise or influence the height of the astronomical tide, and there was only a minor storm surge (Pasch, 1997). Rather, the transported sand that washed out of the channels was reworked by storm waves and longshore currents in operation during the hurricane. These currents transported the sand both offshore or along a westerly direction (due to longshore transport), thereby removing all evidence of sand accumulation.

NATURAL SAND REPLENISHMENT

In the six months following Hurricane Danny, various sections of the surf zone across the southeastern portion of Dauphin Island experienced natural sand replenishment. The sand was derived from areas immediately offshore and from the eastern end of the island (due to longshore transport). The added sand filled all of the former washout channels along the beach scarp, and extended the surf zone gulfward (Figures 13, 14, and 15). The channels behind the repaired scarp remain relatively intact, but will likely fill with sand derived from the areas immediately adjacent to them. Once filled, these former channels will have significantly lower elevations than the surrounding areas, and could create ponded-water conditions with significant precipitation. If overland flow occurs during a future storm, then washout channels could form again along the beach scarp.

The repaired beach scarps have been nearly restored to their former elevation. However, these areas lack a vegetative cover. As such, they possibly remain less stable and subject to erosion during normal weather cycles or future storms. Further investigation is required to determine if these repaired scarps will remain intact. These unvegetated areas might be susceptible to the formation of blow outs or washover fans with sufficient storm energy.

CONCLUSIONS

Dauphin Island, Alabama provides an excel-

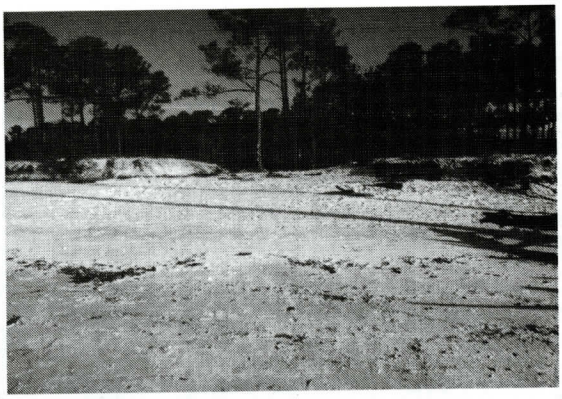

Figure 14. A former washout channel (same channel as Figure 6) which has been filled with sand almost to its original elevation. The restoration of this channel required a considerable volume of quartz sand, and high energy to wash it up on shore. The pine tree did not appear to be stressed by the loss of sand as a result of the storm or by the subsequent repair and restoration of the sand to the beach scarp in the six months which followed.

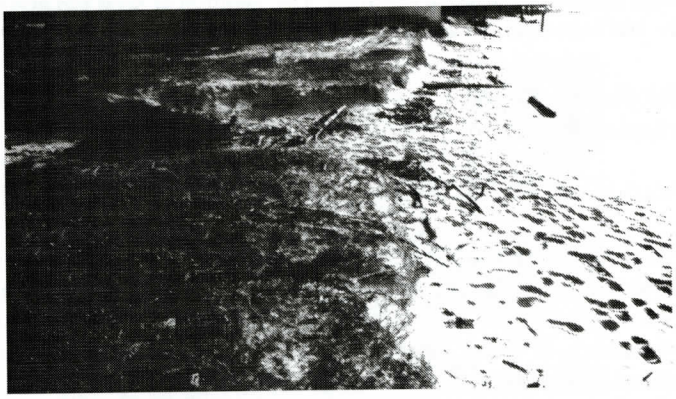

Figure 15. A smaller washout channel (same channel as Figure 5) which has had a considerable amount of sand added to restore it almost to its original elevation. Natural sand replenishment has filled the main washout channel, but the two feeder channels behind this area remain empty. The large dark area immediately behind the repaired beach scarp is seaweed.

lent laboratory for Northeastern Gulf Coast barrier island coastal management studies. The occasional island crossing tropical storm or hurricane accelerates erosion, and provides an opportunity to examine beach and near-shore dynamics. Hurricane Danny produced an unusual amount of precipitation across the eastern end of the island for two days in July 1997, and resulted in the rapid formation of small- and large-scale dendritic washout channels. These channels drained surface water and groundwater along with quartz sand from the beach-dune zone to the shallow reaches of the Gulf of Mexico.

Sand movement within the drainage channels suggests a fluidized state. This interpretation is based on excellent root and rootlet preservation (suspended in air) across the drainage channels. Considerable volumes of sand moved through these channels, but the roots were apparently unaffected. None of the exposed roots examined appear to have experienced any abrasion.

The washout channels removed significant volumes of quartz sand from the beach-dune zone to the surf zone. Areas of sand accumula-

tion are expected at the mouths of these washout channels; however, none were observed. The storm transported the sand either laterally along the surf zone via long-shore currents or immediately offshore.

Within approximately six months following Hurricane Danny, the washout channels were repaired along the beach scarp as quartz sand was washed onshore during a period of natural replenishment. The channels behind the now repaired scarps remain empty, but will likely fill with sand derived from the surrounding areas. These depressions could contribute to the formation of washout channels in the future if precipitation occurs in a manner which would initiate overland flow toward the beach scarp.

The lack of any vegetative cover across the repaired beach scarps may prove to be zones of weakness in subsequent storms, possibly increasing the opportunity for the formation of blow outs or washover fans in these areas.

ACKNOWLEDGMENTS

The author thanks Duncan Heron for his patience and guidance in helping to prepare this manuscript. The comments provided by the two reviewers were very helpful. I thank Sherryl F. Decker and Kathy Piselli for their excellent reference assistance. This article does not necessarily represent the views of the United States Environmental Protection Agency, nor was this investigation conducted in an official capacity. Any mistakes are the sole responsibility of the author.

REFERENCES

Alabama Department of Economic and Community Affairs, 1987, Alabama coastal area development guide, Office of the Governor, 48 p.

Auburn University website, 1997, Rainfall from Danny, Accessed 8/17/97: Made available from http://www.acesag.auburn.edu/department/nws/danny/dan_rain.gif; Internet.

Campbell, K.M., 1984, A geologic guide to the state parks of the Florida panhandle coast, St. George Island, St. Joseph Peninsula, St. Andrews and Grayton Beach Parks and recreation areas: Florida Department of Natural Resources, 23 p.

Canis, W.F., Neal, W.J., Pilkey, Jr., O.H., and Pilkey, Sr., O.H., 1985, Living with the Alabama-Mississippi shore: Duke University Press, 215 p.

Douglass, S.L., 1994, Beach erosion and deposition on Dauphin Island, Alabama, U.S.A.: Journal of Coastal Research, v. 10, p. 306-328.

Hummell, R.L., and Haywick, D.W., 1996, Coastal deposition and ecosystems of Alabama: Guidebook for the 33rd Annual Field Trip of the Alabama Geological Society, Tuscaloosa, 140 p.

Knowles, S.C., 1989, Analysis of barrier island dynamics for ship channel planning at Ship Island, Mississippi, *in* Stauble, D.K., ed., Barrier islands: Process and management: American Society of Civil Engineers, p. 238-252.

Leatherman, S.P., 1988, Barrier island handbook: Coastal Publications Series, Laboratory for Coastal Research, 93 p.

Lins, Jr., H.F., 1980, Patterns and trends of land use and land cover on Atlantic and Gulf Coast barrier islands: U.S. Geological Survey Professional Paper 1156, 164 p.

National Research Council, 1990, Managing coastal erosion: National Academy Press, 182 p.

Nummedal, D., Penland, S., Gerdes, R., Schramm, W., Kahn, J., and Roberts, H., 1980, Geologic response to Hurricane impact on low-profile gulf coast barriers: Transactions of the Gulf Coast Association of Geological Societies, v. 30, p. 183-195.

Otvos, E.G., 1979, Barrier island evolution and history of migration, north central gulf coast, *in* Leatherman, S.P., ed., Barrier islands, from the Gulf of St. Lawrence to the Gulf of Mexico, Academic Press, p. 291-319.

Otvos, E.G., 1982, Coastal geology of Mississippi, Alabama and adjacent Louisiana areas: Guidebook for the New Orleans Geological Society. 66 p.

Otvos, E.G., 1991, Northeastern Gulf Coast -- Quaternary Section within Dubar, J.R., Ewing, T.E., Lundelius, Jr., E.L., Otvos, E.G., and Winker, C.D., 1991, Quaternary geology of the Gulf of Mexico Coastal Plain, *in* Morrison, R.B., ed., Quaternary nonglacial geology; Conterminous U.S.: Geological Society of America, The Geology of North America, v. K-2, p. 588-594.

Pasch, R.J., 1997, Hurricane Danny, 16-26 July 1997, preliminary report, National Hurricane Center, Accessed 6/02/98: Made available from http://www.nhc.noaa.gov/1997danny.html; Internet.

Schramm, W.E., Penland, S., Gerdes, R.G., and Nummedal, D., 1980, Effect of Hurricane Frederic on Dauphin Island, Alabama: Shore and Beach, v. 48, n. 3. p. 20-25.

United States Army Corps of Engineers, Mobile District, 1981, Hurricane Frederic post disaster report, 30 August - 14 September 1979: Mobile, 312 p.

United States Geological Survey, 1982, Biloxi: MISS.-ALA.-LA., 1:100,000-scale metric map.

SOUTHEASTERN GEOLOGY
V. 38, No. 1, September 1998, p. 39-64

GEOLOGIC, GEOCHEMICAL, AND TECTONIC SETTING OF FELSIC METAVOLCANIC ROCKS ALONG THE ALABAMA RECESS, SOUTHERN APPALACHIAN BLUE RIDGE

JAMES F. TULL, PAUL C. RAGLAND, AND ROGER B. DURHAM

Department of Geology
Florida State University
Tallahassee, FL 32306

ABSTRACT

The lower greenschist facies Hillabee Greenstone metavolcanic complex occurs above the Talladega Group, at the structural top of the Talladega belt in Alabama and Georgia. The Talladega belt, an outboard part of the ancient Laurentian margin, occurs along a major structural recess (Alabama recess) in the Appalachian orogen as the southwestern extension of the western Blue Ridge province. The Hillabee Greenstone is composed of bimodal tholeiitic metabasalts and interstratified calc-alkaline felsic metavolcanic rocks (15-25%). Field studies indicate that the Hillabee Greenstone has a stratigraphic base against the Devonian to earliest Carboniferous (?) Talladega Group, but slightly discordant U/Pb zircon ages from the felsic metavolcanic rocks suggest a Middle Ordovician age, and possibly exotic origin for the Hillabee. The upper contact of the Hillabee Greenstone is the roof thrust of a major thrust duplex system, below the amphibolite-facies eastern Blue Ridge allochthon. The felsic metavolcanic rocks occur as thick homogeneous tabular sheets extending over many hundreds of km^2, and exhibit petrographic and geochemical evidence for crystal fractionation and accumulation of plagioclase and hornblende. Regional geometry, primary textural features, and chemical homogeneity indicate that these units originated as large-volume ash-flow tuffs (ignimbrites). Geochemical data from the bimodal suite suggest an arc or back-arc association. An Ordovician age interpretation indicates an exotic arc fragment accreted above the Laurentian margin, whereas interpretation of a stratigraphic base with the Talladega Group, which formed in an extensional successor basin near the southeast margin of Laurentia, suggests that the volcanic complex may represent a continental back-arc or pull-apart basin, and the possibility of middle Paleozoic A-type subduction beneath Laurentia at this latitude in the orogen. Plutonic rocks of similar age (ca. 370-470 Ma) within the tectonically overlying eastern Blue Ridge allochthon constitute a tonalite, trondhjemite, and granodiorite (TTG) suite, and the Hillabee Greenstone felsic metavolcanic rocks may be associated with one or more of these bodies.

INTRODUCTION

The Hillabee Greenstone (HG) is the youngest (early to middle Paleozoic), thickest (>2.5 km), and most laterally extensive metavolcanic unit in the western Blue Ridge province of the southern Appalachians (Figure 1). The HG occurs along the length of a major structural recess (Alabama recess) in the orogen, at the structural top of the Talladega belt in east Alabama and northwest Georgia. It extends along a sinuous trace for over 230 km, from inliers within the Gulf Coastal Plain southwest of Jemison, Alabama, to near Buchanan, Georgia (Figure 2). The Alabama recess is interpreted to have originated as a continental promontory (oceanward projection) during Neoproterozoic rifting of Laurentia (Thomas, 1993). The HG consists predominantly of metabasalt (75-85%), a significant volume of felsic metavolca-

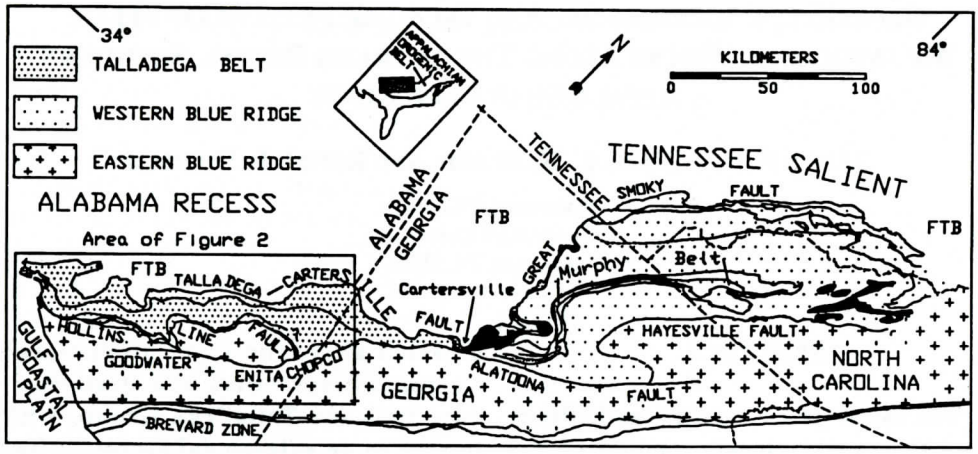

Figure 1. Generalized geologic map of the southern Appalachian Blue Ridge in the southeastern United States. Grenville Basement-black, FTB- foreland fold-thrust belt. Area of Figure 2 is outlined.

nic rock (15-25%), and minor metabasaltic andesite (Tull and Stow, 1980).

The HG and the underlying upper part of the Talladega Group are repeated by imbricate faulting in a large footwall thrust duplex, the Hollins Line fault system, which marks the terrane boundary between the eastern and western Blue Ridge (Moore and Tull, 1989; Tull, 1995). In Alabama, the HG and Talladega Group contain lower greenschist-facies mineral assemblages, but near the Georgia border, biotite and spessartine garnet are locally present in the HG (Paris and Cook, 1989; Paris, 1990).

Although the metabasalts in the HG have been examined extensively (Tull and others, 1978; Tull and Stow, 1980; Stow, 1982), little detailed geochemical work has been done on the interlayered felsic metavolcanic rocks. Accordingly, this study describes the structural and stratigraphic setting, examines the petrography and geochemistry (including major elements, trace elements, and a review of the isotopic data), and analyzes the tectonic setting of the felsic rocks of the HG. Of particular interest is the significance of the bimodal compositional nature of the interlayered mafic and felsic metavolcanic rocks.

GEOLOGIC SETTING

The Talladega belt is the southwestern extension of the western Blue Ridge allochthon. It extends from the Cretaceous unconformity of the Gulf Coastal Plain onlap in Alabama, to Cartersville, Georgia (Figure 1). The belt is bounded on the northwest by the frontal Blue Ridge thrust system. Here, the northwest-directed Alleghanian-age Talladega-Cartersville fault places the Talladega belt above unmetamorphosed to anchimetamorphic Cambrian-Mississippian rocks of the Appalachian foreland fold and thrust belt (Figure 2). The base of the Talladega belt is a >2 km thick siliciclastic unit (Kahatchee Mountain Group), correlative with the regionally extensive Lower Cambrian Chilhowee Group (Figure 2). These rocks are overlain by approximately 3 km of shallow-water carbonate rocks (Sylacauga Marble Group) equivalent to the Lower Cambrian-Lower Ordovician Shady Dolomite through Knox Group carbonate shelf (Tull and others, 1988) (Figure 2). A second major siliciclastic sequence, the Silurian (?)-Devonian (lowest Mississippian?) Talladega Group (Tull, 1982), lies above a regional low-angle unconformity that cuts both of these underlying units (Tull and others, 1988; Gastaldo and others, 1993) (Figure 2). The Talladega Group has been interpreted as a successor basin sequence >2 km thick (Tull and Telle, 1989). It contains metaturbidites and metaolistostromes in the lower part, overlain by shallow-water metasandstone, metaconglomerate,

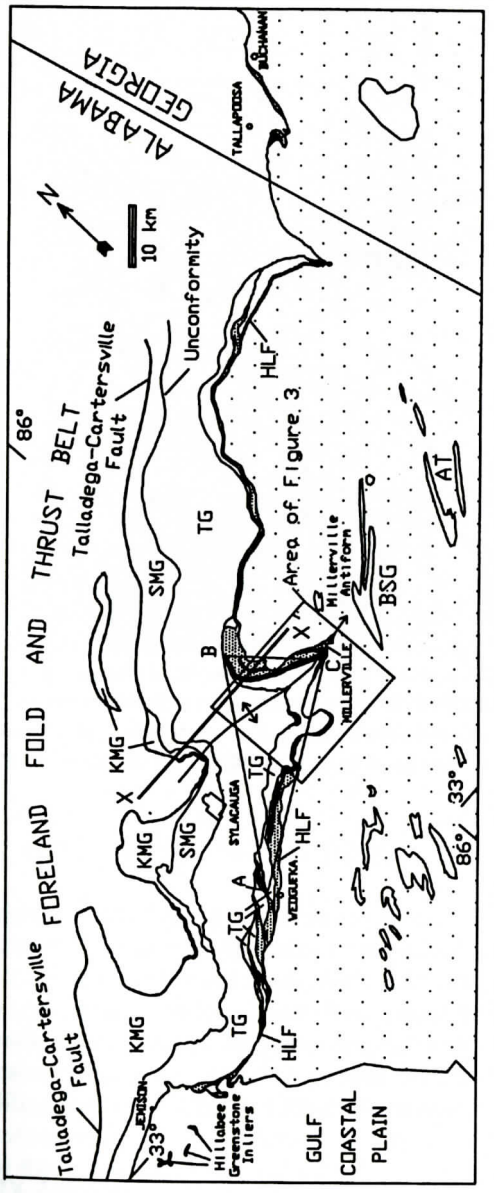

Figure 2. Generalized geologic map of the Talladega belt showing the stratigraphic and structural position of the Hillabee Greenstone (fine stipple) with felsic metavolcanic rocks (black), the trace of the Millerville cross-antiform, tonalite-trondhjemite-granite plutons (open pattern) in the Eastern Blue Ridge (AT= Almond Trondhjemite, BSG= Bluff Springs Granite), and location of Figure 3. Eastern Blue Ridge- open stipple pattern, KMG-Kahatchee Mountain Group, SMG- Sylacauga Marble Group, TG-Talladega Group, HLF- Hollins Line fault. Triangle A-B-C outlines the outcrop extent of the felsic metavolcanic rocks in Alabama. Line X-X= is line of cross-section in Figure 4.

metachert, black slate, and siliceous argillite. These sediments were derived from the underlying lower Paleozoic shelf clastic and carbonate rocks, as well as the underlying granitic Grenvillian (~1 Ga) basement. The Talladega Group is interpreted to have formed in an extensional setting above the foundered lower Paleozoic Laurentian outer shelf (Tull and Telle, 1989). The HG overlies the Talladega Group, forming the structural top of the Talladega belt. Debate exists concerning the structural/stratigraphic relationships between the HG and underlying units of the Talladega Group. Field studies suggest that the HG is younger than the Talladega Group, and occurs stratigraphically above it. Uranium/lead isotopic data (Russell, 1978), however, have been interpreted to suggest that the HG is older than the immediately underlying rocks, and thus is allochthonous relative to the rest of the Talladega belt. Discussion of age constraints is presented below.

The southeast boundary of the Talladega belt is a regional footwall thrust duplex, the Hollins Line fault system, a major Alleghanian transpressional thrust system (Moore and Tull, 1989; Tull, 1995) (Figs. 1 and 2). The roof thrust of this fault system is a major metamorphic discontinuity that is discordant to stratigraphy and structure in both its hanging and footwalls (Figure 3). Rocks above the roof thrust constitute part of a composite suspect terrane of late Neoproterozoic rocks (Jefferson Terrane of Horton and others, 1991). This fault system formed during the emplacement of the eastern Blue Ridge allochthon above the Talladega belt during the late Paleozoic Pangean collision. It consists of a floor thrust, a roof thrust, and a series of oblique imbricate thrusts that join the roof and floor thrusts and bound map-scale thrust slices (horses). The HG and upper units of the Talladega Group are repeated by thrust imbrication within the duplex. The HG locally occurs in the footwall of the floor

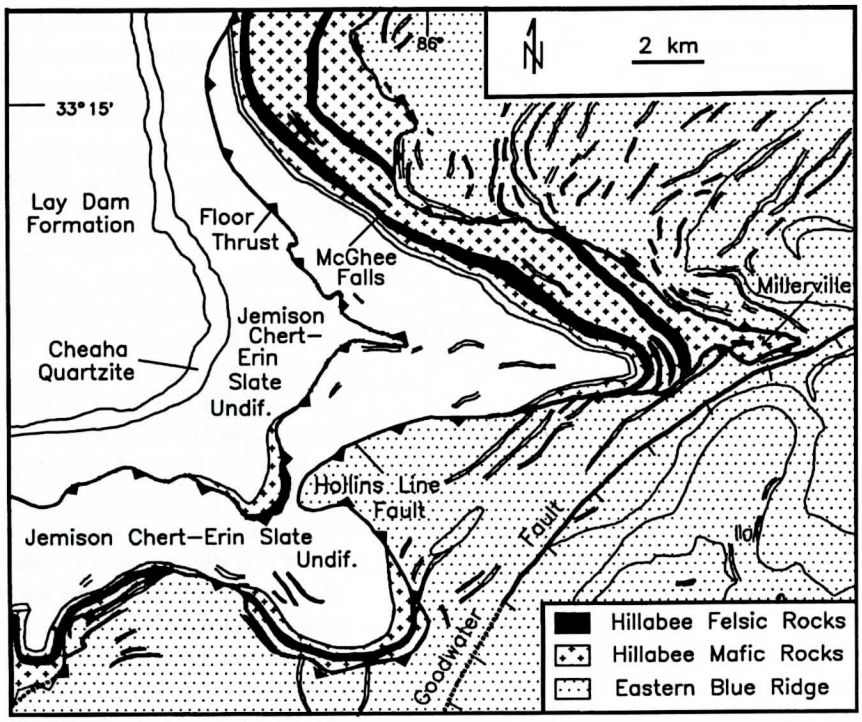

Figure 3. Geologic map of the Millerville cross-antiform area showing the interpreted structural and stratigraphic setting of the Hillabee Greenstone. Lines in eastern Blue Ridge are contacts of stratigraphic units.

thrust of the duplex, and is also found with upper units of the Talladega Group within large horses in the footwall of the roof thrust (Figures 2 and 3). The roof thrust has tectonically removed an unknown amount of the HG, and stratigraphically overlying units are absent. A generalized cross section through the Talladega belt is shown in Figure 4.

GEOMETRY OF FELSIC UNITS

Felsic metavolcanic rocks occur as discrete tabular sheets interlayered with mafic rocks of the HG. Each sheet is of relatively uniform thickness and large lateral dimensions. Six major felsic sheets mapped in the central portion of the HG outcrop belt range from approximately 50 m to 165 m thick (Griffin, 1951; Long, 1981;

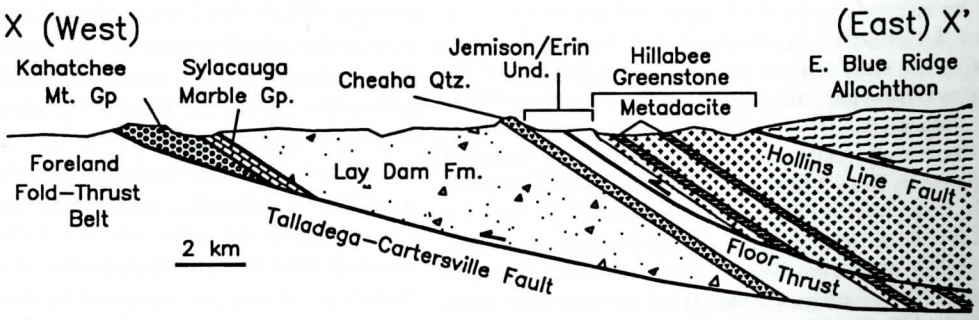

Figure 4. Generalized geologic cross-section through the Talladega belt along X-X', Figure 2.

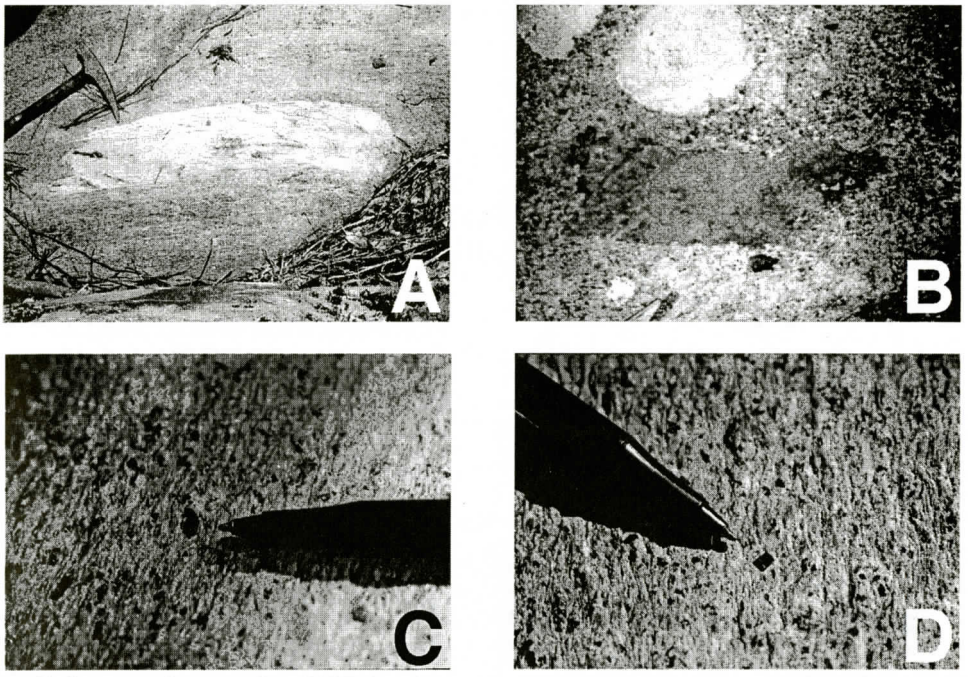

Figure 5. Outcrop photographs of Hillabee Greenstone felsic metavolcanic rocks. A-Felsic (aphyric) lithic block in metadacite. Hammer head is 18 cm long. Clast is elongated parallel to slaty cleavage and differential shear strain at end near hammer has caused interdigitation (partial transposition) with metadacite. B - rhombic metabasalt lithic fragment (6 cm × 24 cm) in metadacite. Slaty cleavage parallels long dimension of clast. Light circular areas are lichen growths. C- and D- euhedral and broken hornblende porphyroclasts (originally igneous phenocrysts) (black) embedded in phyllitic matrix. Maximum pen diameter is 8 mm.

Tull and others, 1978; Tull and others, in press) (Figure 3). Other layers of these felsic rocks are as thin as 0.5 m. Boundaries with mafic metavolcanic rocks are planar and sharp, and lack evidence of localized high shear strain, and are thus interpreted to represent un-faulted, pre-metamorphic volcanic contacts. No evidence of features suggestive of significant paleotopography on these contacts has been observed.

The lowest major felsic unit mapped in Alabama occurs approximately 300 m above the base of the HG. Along much of the outcrop trace of the HG, however, either the Hollins Line roof thrust or an imbricate thrust truncates the unit less than 300 m above the base. For this reason, felsic metavolcanic rocks are exposed along only approximately 30 percent of the 230-km outcrop trace. In Alabama, where HG sections greater than 300 m thick occur, felsic rocks are generally present. Near Tallapoosa, Georgia (Figure 2), however, cores from the Royal Vendicator mine contain zones of felsic rocks 10-50 m thick, interlayered with metabasalt, about 100 m above the base of the HG (Paris, 1990). The fact that major felsic sheets occur below the floor thrust of the Hollins Line duplex in the Talladega belt parautochthon, as well as within several imbricate thrust slices (Figs. 2 and 3), indicates that the felsic sheets also originally had considerable across-strike extent.

The structurally lowest (~165 m thick), and thus best preserved, sheet of felsic metavolcanic rocks in Alabama appears in three different structural positions in the central part of the outcrop belt (Figs. 2 and 3): 1) in the parautochthon, immediately below the floor thrust 15 km west southwest of Millerville; 2) within an imbricate slice located 4 km north of Weogufka; and 3) within the large Millerville imbricate thrust slice, which is structurally above the one

sition (see below) and thickness (140 m) occurs over much the same area. These tabular, sheet-like bodies thus display very large area-to-thickness ratios.

Contacts of the felsic sheets are planar, concordant with surrounding stratigraphic contacts, and parallel for distances of many kilometers. The units are massive at the scale of outcrop exposures. Bedding laminations were observed only at the McGhee Falls locality (Figure 3), in a 6 m-thick felsic unit exposed 6 m above the lowest major sheet of felsic metavolcanic rocks.

LITHOLOGIC DESCRIPTION

The felsic rocks are light-gray phyllite in which slaty cleavage is variably developed (Figure 5, c and d). Less foliated rocks appear gneissic. A very fine-grained (0.01-0.1 mm) matrix surrounds much larger (0.5-10.0 mm) porphyroclasts of albitic plagioclase, amphibole (edenitic hornblende/actinolite), quartz, and laminated quartz-mica fragments (Figs. 5 and 6).

Metamorphic Grade

Mafic rocks of the HG in Alabama contain the metamorphic mineral assemblage: albite+actinolite+chlorite+epidote, and HG felsic rocks contain the metamorphic assemblage: muscovite+quartz+albite+actinolite+epidote. An ACF plot (Figure 7) of HG mafic rocks places them within the albite-actinolite-chlorite zone of Winkler's (1976) lower greenschist facies. This zone is representative of conditions within P-T space approximating 300° - 350° C and 3 - 4 Kb (Bucher and Frey, 1994). Rocks within the Talladega belt beneath the HG also display lower greenschist facies mineral assemblages, and conodonts within metacarbonate rocks of the Sylacauga Marble Group have color alteration indices of 5.5, indicating temperatures of ~350° (Tull and others, 1988).

Matrix

Approximately 80 volume percent of most of the felsic rocks consists of matrix quartz+ albite+muscovite+ actinolite, ± minor chlorite and epidote, and trace zircon, apatite and titanite. The matrix commonly displays thin (0.1-3 mm), discontinuous and anastomosing layers of muscovite and chlorite that alternate with quartz-plagioclase layers (Figure 6a-c), probably reflecting metamorphic differentiation. The regional deformation appears to have been partitioned more strongly into the felsic as opposed to the mafic rocks of the HG, so that the felsic rocks commonly exhibit a mylonitic matrix fabric developed around the more rigid porphyroclasts (Figures 5, c and d, and 6, a-c). This is because quartz undergoes crystal plastic deformation under these temperatures of greenschist facies metamorphism whereas feldspar does not (Scholz, 1988).

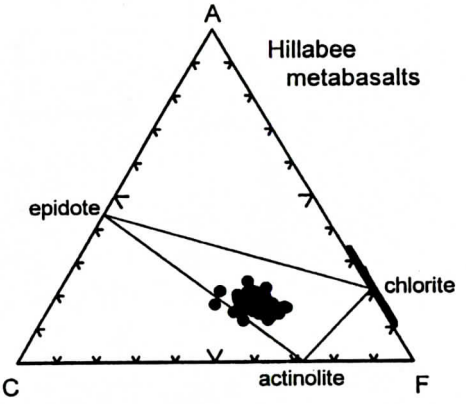

Figure 7. ACF diagram of Hillabee Greenstone mafic rocks (after Winkler, 1974).

Porphyroclasts

Porphyroclasts (0.5-10 mm in diameter) occur in all felsic metavolcanic rocks of the HG, but their proportions and relative abundances vary. Amphibole porphyroclasts are most abundant, representing up to 12% of the rock volume, followed by quartz (5 to 10%), plagioclase (<1 to 9%), and laminated fragments consisting of quartz and muscovite (<1%). Amphibole porphyroclasts are absent in some samples, but quartz and plagioclase occur in all samples.

Plagioclase and amphibole porphyroclasts consist of euhedral to angular grains that commonly are broken (Figs. 5 and 6). Some may

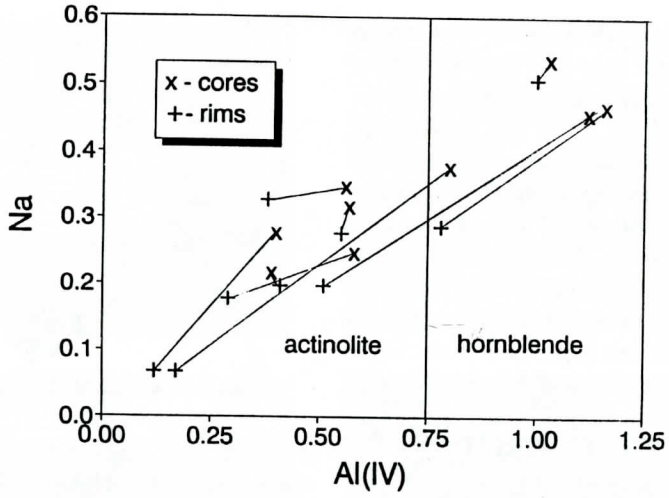

Figure 8. Molar plot of tetrahedral Al versus Na (based on 23 oxygens) showing the actinolite and hornblende fields. The four analyses in the upper right corner of diagram are representative of edenite. Tie lines connect core compositions (x) with rim compositions (+). Data from Durham (1993).

have been deposited as broken fragments. Most have clearly been broken, sheared and rotated during the superposed tectonic deformation. Both plagioclase and amphibole generally display undulatory extinction, and commonly are twinned. Quartz porphyroclasts generally have an ellipsoidal shape (Figure 6a) and are strongly polygonized. Most amphibole porphyroclasts have been altered and partially replaced by matrix phases. Laminated quartz-mica fragments are angular. Their internal laminations are folded, twisted and bent. Many porphyroclasts display strain shadows of fine-grained quartz (Figure 6,b-d).

The porphyroclasts show evidence that they predate the lower greenschist facies ductile deformation and the associated fabric-forming events. The edenitic hornblende (Durham, 1993) is in disequilibrium with the lower greenschist-facies mineral assemblage of the matrix. Such grains exhibit various stages of alteration to actinolite, with edenitic hornblende commonly occupying cores of the porphyroclasts, with rims consisting of actinolite (Figure 8). Electron microprobe (Durham, 1993) and X-ray diffraction analyses of the plagioclase porphyroclasts indicates that they are low albite, but they were probably more calcic prior to greenschist facies metamorphism. For these reasons, the amphibole, plagioclase, and quartz porphyroclasts are interpreted to represent relict igneous phenocrysts. Laminated quartz+muscovite porphyroclasts are interpreted to represent flattened, and later deformed and recrystallized pumice fragments.

GEOCHEMISTRY

Sources of Data

The geochemical database for this study consists of 52 major-oxide analyses and seven trace-element analyses of HG felsic metavolcanic rocks. The major oxides are reported in Durham (1993) (46 analyses), Paris (1990) (3 analyses), German (1990) (3 analyses), and Tull and others (1978) (2 analyses). Metabasalt data used in this study are from Tull and others (1978), Paris (1990), and German (1990). For detailed discussion of analytical methods the reader is referred to the above publications. For the analyses referenced to Durham (1993) the oxides TiO_2, CaO, and P_2O_5 were analyzed by X-ray fluorescence spectrometry (XRF). Atomic absorption spectrophotometric analyses were performed for Al_2O_3, FeO*, K_2O, MgO, MnO, and Na_2O; SiO_2 was determined by UV-VIS spectrophotometry. Loss on Ignition (LOI) was determined gravimetrically. Precision is better than 2 percent for SiO_2, and better than 3 per-

Table 1. Major-oxide analyses of the Hillabee Greenstone felsic metavolcanic rocks arranged according to increasing SiO2 (all data in weight percent).

sample	MF3A	MF3	6D	6A	MF18A	7B	9C	MF16	L1F
unit*	M	M	U	U	M	L	L	M	L
SiO_2	61.7	63.6	64.4	64.6	64.9	65.1	65.3	65.3	65.6
TiO_2	0.45	0.53	0.38	0.38	0.39	0.39	0.40	0.40	0.41
Al_2O_3	16.7	17.2	16.8	16.3	16.6	15.6	16.1	15.6	16.0
FeO*	3.75	4.05	4.11	3.82	4.12	3.90	3.55	4.00	3.60
MnO	0.09	0.09	0.09	0.08	0.07	0.09	0.08	0.08	0.08
MgO	2.31	2.11	2.45	2.27	1.78	2.36	1.94	2.05	2.20
CaO	3.76	3.87	4.96	4.84	4.44	5.25	4.16	4.23	4.83
Na_2O	2.93	3.79	3.23	3.35	2.72	3.13	2.94	2.99	3.26
K_2O	4.42	2.93	2.96	2.69	2.81	2.85	2.94	2.92	2.64
P_2O_5	0.13	0.11	0.12	0.10	0.09	--	--	0.10	0.08
LOI	1.82	1.54	1.70	1.49	2.17	1.41	2.12	1.95	1.78
Total	98.06	99.82	101.20	99.92	100.09	100.08	99.53	99.62	100.48

sample	MF2	MF2A	MF5	1B	2A	7E	9A	1E	10G
unit	M	M	L	L	L	L	L	L	L
SiO_2	65.6	65.6	65.6	65.8	65.8	65.9	65.9	66.3	66.3
TiO_2	0.35	0.37	0.35	0.40	0.36	0.35	0.32	0.38	0.33
Al_2O_3	16.2	16.2	16.2	16.3	15.8	16.2	16.2	15.7	15.5
FeO*	3.63	3.53	3.61	3.63	3.29	3.46	3.02	3.42	2.95
MnO	0.08	0.08	0.09	0.07	0.08	0.08	0.07	0.08	0.07
MgO	2.00	1.82	2.12	2.09	2.09	1.89	1.42	2.04	2.40
CaO	3.57	4.53	2.73	4.76	4.25	4.90	3.69	4.20	3.61
Na_2O	3.49	3.14	2.79	3.23	4.02	3.22	3.29	3.09	3.45
K_2O	2.88	2.88	4.00	3.23	2.38	2.84	3.08	2.90	2.96
P_2O_5	0.08	0.08	0.08	0.10	0.11	--	--	0.09	--
LOI	1.66	1.52	1.90	1.67	1.22	1.42	1.72	1.60	1.56
Total	99.54	99.75	99.47	101.28	99.40	100.26	98.71	99.80	99.13

sample	MF1	6E	G31	6H	7I	G35	10F	7A	5C
unit	M	U	U	U	L	L	L	L	U
SiO_2	66.3	66.4	66.5	66.5	66.5	66.5	66.5	66.6	67.0
TiO_2	0.35	0.37	0.33	0.37	0.34	0.36	0.38	0.39	0.35
Al_2O_3	16.0	16.0	15.3	15.9	15.8	15.1	16.3	16.1	16.0
FeO*	3.55	3.91	4.06	3.42	3.28	4.13	3.57	3.71	3.80
MnO	0.06	0.08	0.07	0.08	0.07	0.07	0.07	0.09	0.08
MgO	1.61	2.48	2.14	2.03	1.94	2.10	2.40	2.20	2.00
CaO	3.80	4.84	4.03	4.59	3.70	4.26	4.00	4.78	3.52
Na_2O	4.21	3.10	3.13	3.22	3.63	3.16	2.78	3.16	3.63
K_2O	2.04	2.84	3.01	2.63	3.16	2.81	3.28	3.01	2.74
P_2O_5	0.08	0.09	0.06	0.07	--	0.08	--	--	0.08
LOI	1.43	1.48	1.23	1.58	1.40	1.21	1.76	1.52	1.85
Total	99.43	101.59	99.86	100.39	99.82	99.78	101.04	101.56	101.05

sample	6I	7J	2C	7D	MF17	MF4A	7F	10D	10C
unit	U	L	L	L	M	M	L	L	L
SiO_2	67.0	67.1	67.1	67.1	67.1	67.1	67.5	67.5	67.6
TiO_2	0.40	0.35	0.35	0.37	0.37	0.44	0.35	0.35	0.36
Al_2O_3	16.1	14.7	15.8	15.7	15.2	16.4	16.5	15.6	15.6
FeO*	3.47	3.15	3.46	3.37	3.93	3.56	3.46	3.30	3.04
MnO	0.08	0.09	0.07	0.08	0.11	0.07	0.08	0.08	0.07
MgO	2.09	1.74	2.03	1.78	1.77	1.95	1.95	2.44	1.44
CaO	4.68	4.14	3.70	4.04	3.97	3.62	3.48	3.89	3.72
Na_2O	3.25	3.51	2.86	3.42	3.05	2.87	3.24	3.06	3.13
K_2O	2.75	2.30	3.23	3.00	2.68	3.44	3.39	2.95	3.10
P_2O_5	0.10	--	0.10	--	0.07	0.12	--	--	--
LOI	1.67	2.04	2.20	1.68	2.15	1.84	2.00	1.58	1.61
Total	101.59	99.12	100.90	100.54	100.40	101.41	101.95	100.75	99.67

sample	8A	6J	10A	5B	MF19	MF6	MF7	MF4	MF7A
unit	L	U	L	U	M	M	M	M	M
SiO_2	67.8	68.1	68.1	68.5	68.6	68.6	69.1	69.7	70.2
TiO_2	0.35	0.40	0.34	0.34	0.36	0.30	0.27	0.35	0.25
Al_2O_3	15.5	15.9	15.6	15.8	15.6	15.2	14.9	14.7	15.9
FeO*	3.19	3.50	2.80	3.35	3.84	3.38	2.86	3.12	2.53
MnO	0.07	0.07	0.06	0.08	0.11	0.05	0.06	0.07	0.04
MgO	1.68	2.06	1.22	1.81	2.11	1.57	1.32	1.42	1.15
CaO	3.97	3.98	2.73	4.56	3.11	2.62	2.79	3.59	2.10
Na_2O	3.38	3.45	3.53	4.23	2.73	3.10	2.72	4.13	3.91
K_2O	3.40	2.88	3.31	2.08	3.44	3.36	3.04	1.72	3.08
P_2O_5	--	0.10	--	0.09	0.08	0.05	0.07	0.11	0.04
LOI	1.48	1.52	1.74	1.34	2.08	1.93	1.67	1.31	1.85
Total	100.82	101.96	99.43	102.18	102.06	100.16	98.80	100.22	101.05

sample	MF8A	104-2	22-140	18-265	107-2	16-12	85-1	A T	B S G
unit	M	G	G	G	G	G	G	T(19)	T(12)
SiO_2	71.2	71.6	71.9	72.1	72.5	74.0	75.8	71.5	71.2
TiO_2	0.21	0.25	0.25	0.25	0.24	0.17	0.23	0.21	0.23
Al_2O_3	15.0	14.1	13.4	13.2	14.6	12.1	13.0	15.9	16.0
FeO*	2.19	3.12	2.34	3.10	3.05	2.34	2.38	1.43	1.60
MnO	0.03	0.06	0.04	0.07	0.07	0.03	0.06	0.03	0.04
MgO	0.95	0.90	0.68	0.83	0.81	0.39	0.51	0.43	0.48
CaO	1.89	2.60	2.40	2.30	2.50	1.69	2.00	1.96	1.83
Na_2O	3.95	4.70	4.20	4.60	4.40	4.40	5.20	5.34	4.25
K_2O	2.77	2.00	2.50	2.00	1.10	1.75	0.94	1.96	2.85
P_2O_5	0.04	0.04	--	--	0.04	--	--	0.06	0.13
LOI	1.43	1.50	1.22	1.36	1.20	2.09	1.10	0.91	1.59
Total	99.66	100.87	98.93	99.81	100.51	98.96	101.22	99.69	100.23

*Units: L - lower; U - upper; M - McGehee Falls; G - Georgia; T(n) - trondhjemitic rocks (number of analyses averaged); from Drummond and others, 1997; A T - Almond Trondhjemite; B S G - Bluff Springs Granite

Table 2. Trace-element analyses for Hillabee Greenstone felsic metavolcanic rocks (all data in ppm)

	6A	9C	10G	MF2	MF5	MF7	MF8A
La	22	15	18	23	23	17	9
Ce	40	26	36	41	47	29	15
Pr	--	--	--	5.0	4.8	2.9	1.9
Nd	29	26	26	19	20	10	6
Sm	3.4	3.2	3.9	3.3	3.9	2.2	1.6
Eu	0.87	0.86	0.97	0.70	0.50	0.53	0.72
Gd	3.2	2.8	3.3	4.4	3.7	2.2	1.5
Tb	--	--	--	--	--	0.2	0.2
Dy	--	--	--	2.7	1.9	1.3	1.6
Ho	--	--	--	0.7	0.7	0.2	0.4
Er	--	--	--	0.8	1.3	0.5	1.3
Tm	--	--	--	--	0.6	0.1	0.3
Yb	1.5	1.6	2.1	1.2	1.8	0.2	1.2
Lu	0.24	0.27	0.28	--	--	0.17	0.21
Ba	332	368	404	490	620	349	540
Hf	7.1	8.1	7.4	3.7	5.2	6.8	5.0
Nb	10	9	11	11	11	10	13
Rb	122	122	125	150	205	167	144
Sr	221	210	173	135	128	142	126
Ta	1.8	2.7	1.7	1.6	0.7	3.0	0.9
Th	6	13	13	11	11	14	14
U	7	2	3	7	6	9	6
Y	14	16	17	14	13	8	9
Zr	117	145	148	110	130	114	97

cent for the remaining oxides. Table 1 presents 52 major-element analyses of the HG felsic metavolcanic rocks arranged in order of increasing SiO_2. Trace elements (Table 2) were analyzed in commercial laboratories by XRF, neutron activation, and ICP-mass spectrometry, as reported in Durham (1993).

Evidence for Alkali Metasomatism

Because rocks of the HG are metamorphosed and this study is concerned with the geochemistry of the igneous protoliths, a brief discussion of the possibility that the felsic rocks were metasomatically altered is necessary. Drummond and others (1986) have shown that a trend with a slope of -1 on a molar Na-K plot is good evidence for metasomatic exchange of alkalies between the rocks and a metamorphic fluid. Such a trend can be seen on Figure 9 for the HG felsic rocks. Samples from Georgia are the most sodic, so including them in the database gives a stronger correlation and thus a smaller error on the calculated regression slope (m on Figure 9). The slope of -1 required for the exchange process, however, is within the calculated error limits (95 percent confidence) for m regardless of whether the Georgia samples are included. As explained below, in the light of other chemical patterns shown on subsequent figures, this negative correlation between Na and K cannot be readily explained by any primary igneous process, such as crystal fractionation.

Thus alkali metasomatism apparently affected the felsic rocks, but whether the analyzed rocks experienced primarily potash or soda metasomatism, or both, is impossible to know. Moreover, whether this metasomatism took place during post-emplacement alteration of the ash-flow tuffs (e.g., Roddy and others, 1988; Hollocher and others, 1994) or metamorphism (e.g., Drummond and others, 1986) also cannot be resolved. Two interesting observations stem from the probability of this exchange alkali metasomatism, however. First, the Na_2O/K_2O ratio is obviously sensitive to metasomatic alteration. Figure 10 is a plot of Na_2O/K_2O for the HG felsic rocks, subdividing them into rocks of the main upper and lower units from Alabama, and the Georgia samples. Although the Georgia samples are more sodic (also more silicic; compositionally they are soda rhyolites), on this and subsequent figures there is no significant difference in average compositions of samples from the upper and lower Alabama units. In addition, within either the samples from Alabama or Georgia, there is no correlation between Na_2O/K_2O and any other oxide. This observation is taken as evidence that only the alkalies were involved in the metasomatism.

Second, the implication of Figure 9 is that total alkalies (molar Na+K) should remain con-

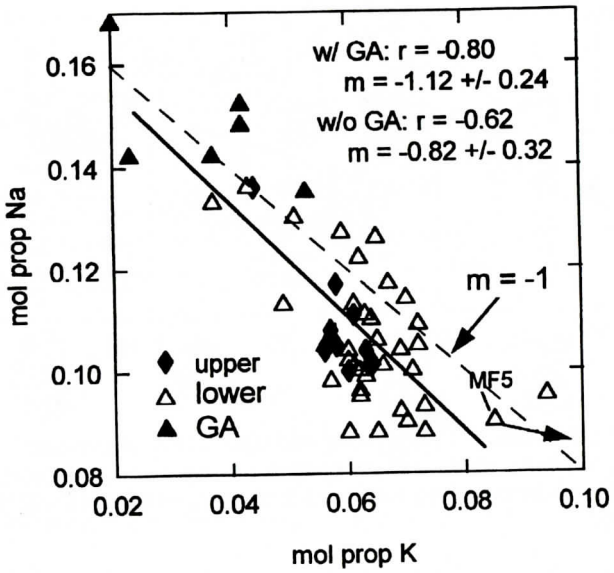

Figure 9. Plot of mol proportion Na versus mol proportion K for felsic metavolcanics from the Hillabee Greenstone (modified after Drummond and others, 1986). Slope of reference line with m = -1 (dashed) is within error limits (95 percent confidence) of slope for regression best-fit line (dark), regardless of whether samples from Georgia are included. Intercept for the reference line is not critical. See text for further explanation.

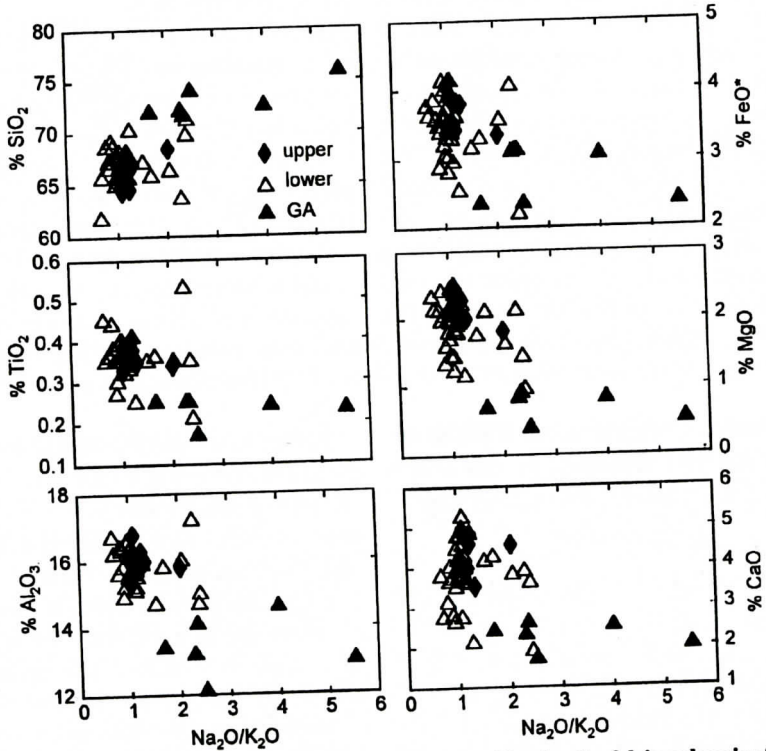

Figure 10. Plots of the Na_2O/K_2O ratio versus several major oxides for the felsic volcanics from the Hillabee Greenstone. All data are in weight percent.

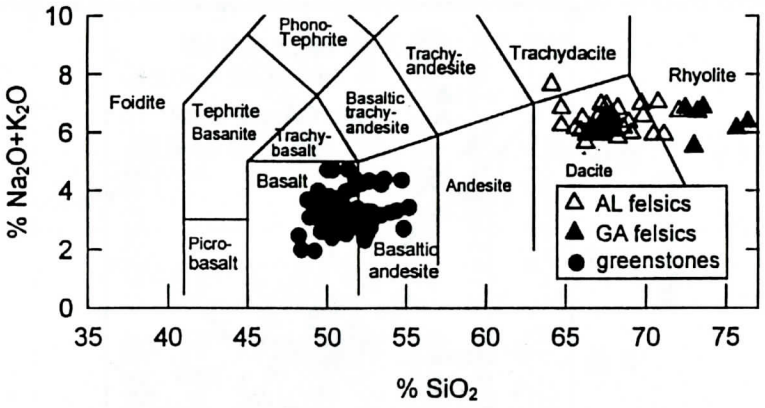

Figure 11. Total alkali-silica diagram (from LeBas and others, 1986) illustrating bimodality of Hillabee Greenstone metavolcanic rocks (mafic rocks or greenstones -closed circles, Alabama felsic rocks- open triangles, Georgia felsic rocks-closed triangles) and their volcanic classification. Mafic rocks are from Tull and others (1978).

stant during the alkali-exchange metasomatism. Figure 11 is a TAS (total alkalies-silica; LeBas and others, 1986) plot of the interlayered HG felsic and mafic metavolcanic rocks. Although Na+K will remain constant during alkali exchange, Na_2O+K_2O will vary slightly, because of the conversion from molar to weight units. In this case, the very weak negative correlation between Na_2O+K_2O and SiO_2 on Figure 10 becomes a weak positive correlation when molar Na+K is plotted versus SiO_2 (not shown). For rocks of this composition, a positive correlation between total alkalies and silica is more common. Thus, despite the fact that these rocks may have undergone alkali metasomatism, the total alkalies, in addition to the remainder of the analyses, are useful in describing the igneous protolith of these felsic metamorphic rocks.

Major Element Comparisons of Hillabee Greenstone Metavolcanic Rocks and Evidence for Crystal Fractionation/ Accumulation

As required for the TAS plot (Figure 11), all analyses were recalculated to 100 percent on a volatile-free basis. With one exception, all analyses of the felsic metavolcanic rocks plot in the dacite and rhyolite fields, whereas the mafic rocks plot as basaltic andesite and basalt. Tull and Stow (1980) concluded that the metabasalts are tholeiitic and the dacites are calc-alkaline. An AFM diagram (not shown) supports this conclusion. The bimodal nature of this suite is apparent; a compositional gap of almost 9 percent SiO_2 is present and no rocks of intermediate composition exist.

Harker diagrams for analyses of the HG suite, including both the mafic and felsic rocks, are given in Figure 12. Felsic rocks from Alabama and Georgia are plotted separately for comparison. On this and subsequent plots involving major oxides, analyses were not recalculated to 100 percent so that the plotted points will agree with the analyses in Table 1. The bimodal nature of the suite is again immediately apparent; a number of oxides in addition to silica exhibit compositional gaps between the mafic and felsic rocks (e.g., FeO*, MgO, and CaO).

Although no trends are apparent between silica and the other oxides for the metabasalts, every plot of felsic rocks in Figure 12 exhibits a strong linear or near-linear trend; all oxides except Na_2O are negatively correlated with silica. The felsic rocks from Georgia, which as reported above are at a different stratigraphic level from those in Alabama, plot on the silica-rich end of the trends. Allowing that these negative correlations are enhanced by closure, the trends still have some petrogenetic significance. A question arises, however, as to whether or not,

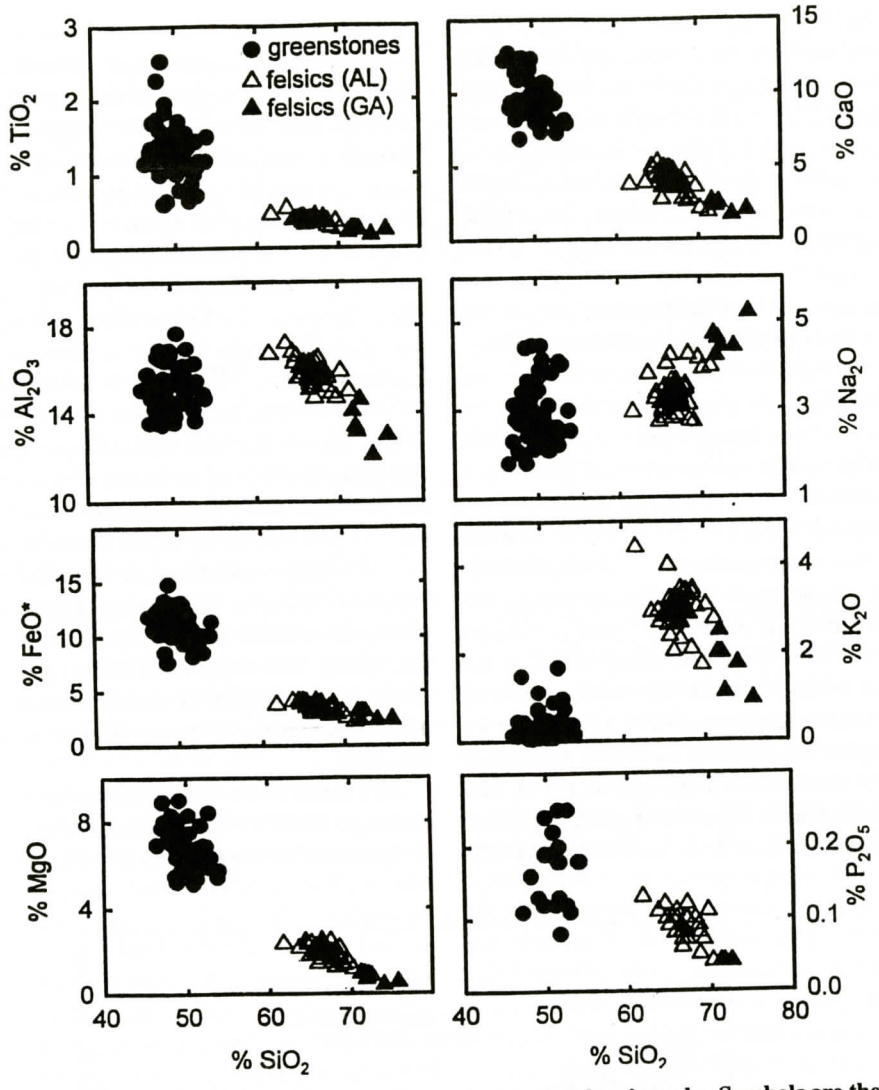

Figure 12. Harker diagrams for the Hillabee Greenstone metavolcanic rocks. Symbols are the same as in Figure 5. Mafic rocks ("greenstones") are from Tull and others (1978).

for purposes of mixing calculations, felsic rocks from Georgia and Alabama should be treated together as one cogenetic group, or treated separately. When all samples are considered together, correlation coefficients (r values) for all the oxides are quite significant and range from -0.65 for K_2O to -0.86 for Al_2O_3 and MgO. When only the Alabama samples are used in the calculation, r values are less (ranging from -0.59 for CaO to -0.74 for TiO_2), but are still quite significant. The exception is the alkalies, where r = +0.30 for Na_2O and -0.26 for K_2O for the Alabama samples. Moreover, the slopes of the best-fit regression lines are not significantly different if all samples are considered together or the Alabama samples are considered separately. Nevertheless, we adopt the more conservative approach; for purposes of mixing calculations described below, only the Alabama samples were used.

The possibility that magma mixing between end-member HG basalts and rhyolites might explain the range of dacite compositions is precluded by some of the patterns, especially those

involving Al_2O_3, K_2O, FeO*, and MgO. Note, for example, that a best-fit line for Al_2O_3-SiO_2 (not shown) through the trend for the felsic rocks would not pass through the metabasalt field. Likewise, for similar reasons, these four major-element plots preclude the possibility of contamination of a basaltic magma from a lower crustal source to explain the dacites.

Although it provides no unique solution, a least-squares mixing calculation (Bryan and others, 1969) to test the possibility of simple crystal fractionation/accumulation is informative. The two major porphyroclastic phases (interpreted to have been originally phenocrysts) in the felsic rocks are hornblende, partially to totally altered to metamorphic actinolite, and metamorphic albite (Durham, 1993). Durham has estimated compositions for these premetamorphic phenocrysts (plagioclase: An_{40}; amphibole: $Fe_{31.5}$, $Mg_{35.0}$, $Ca_{27.6}$, $Na_{5.8}$). Amphibole estimates were made based on microprobe analyses of the cores of amphibole porphyroclasts (Durham, 1993); plagioclase estimates are from literature values for plagioclases in calc-alkaline dacites (Durham, 1993). This calculation is fairly robust; using slightly different mineral compositions does not drastically change the results.

Using these mineral compositions for the Alabama data, a least-squares mixing calculation demonstrates that a possible daughter magma (sample MF8A) can be derived from a possible parent (sample MF3) by 32-36 percent fractional crystallization of an extract assemblage comprising 68-72 percent plagioclase, 22-28 percent hornblende, and 4-5 percent Fe-Ti oxides. The reason for these ranges is that the calculations were performed in three ways, as explained below. This result is based on a simple model of fractional crystallization; it will be shown below that this crystallization was accompanied by crystal accumulation. As a result, the 32-36 percent crystallization should be considered as a maximum value. Some models for AFC (combined assimilation-fractional crystallization; DePaolo, 1981) were attempted, but produced no lower sums of squares of the residuals (SSR) than those cited below. As the fractional crystallization is simpler than the AFC model, we chose to go no further with AFC modeling.

As a result of the discussion above regarding exchange alkali metasomatism, a question arises regarding how to treat the alkalies in the mix-

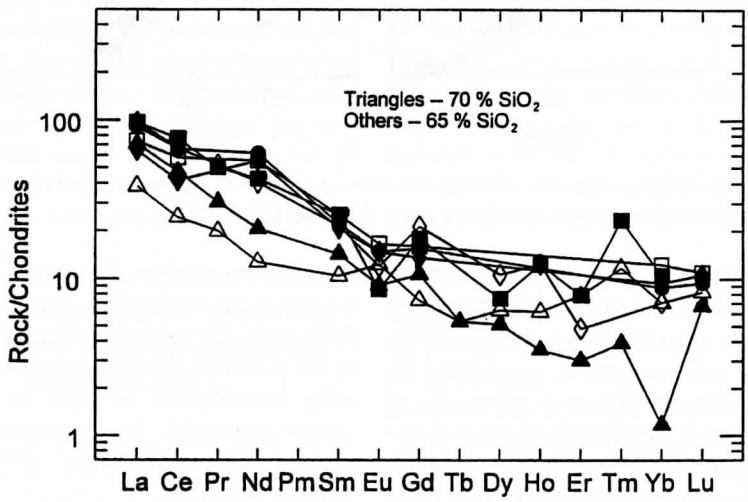

Figure 13. Chondrite-normalized rare-earth elements for seven samples from the felsic volcanics of the Hillabee Greenstone. Data are from Table 2. Samples are: open triangle - MF8A, closed triangle - MF7, open square - 10G, closed square - MF5, open diamond - MF2, closed diamond - 9C, open circle - 6A. Silica contents are: MF8A - 71.2%, MF7 -69.1%, 10G - 66.3%, MF5 - 65.6%, MF2 - 65.6%, 9C - 65.3%, 6A - 64.6%.

ing calculation. All r-values for the Alabama felsic rock trends on Figure 12 are significant except those for K_2O and Na_2O. Moreover, assuming the weak negative correlation between K_2O and SiO_2 for the Alabama rocks represents a primary igneous process, it obviously cannot be explained by fractionation of amphibole and plagioclase. Relative goodness of fit is determined by SSR. The least squares calculation was done three ways: 1) summing and including the alkalies as a single variable (SSR = 1.457), 2) omitting the alkalies (SSR = 0.538), 3) and including the alkalies separately (SSR = 1.803). Clearly, the main contribution to SSR in this case is from the alkalies. Fortunately, percentages of minerals in the extract assemblage and percent crystallization are quite similar for the three solutions, and the ranges given in the previous paragraph are based on all three calculations. Durham (1993) has offered additional evidence for hornblende and plagioclase fractionation. In igneous rocks of this composition, the REE in hornblende are commonly compatible (Nagasawa and Schnetzler, 1971; Arth and Barker, 1976). Thus, with increasing fractional crystallization, the overall chondrite-normalized REE patterns are lowered with increasing degree of fractionation. This general relationship holds for the HG felsic rocks, as shown in Figure 13. In addition, several negative and one positive Eu anomalies are present in these REE patterns, suggesting plagioclase fractionation and accumulation, respectively. Any attempts to quantify this fractionation model for the REE using reasonable KD's to calculate D (bulk partition coefficient based on proportions of fractionating minerals cited above) however, have difficulties. Although the proportion of plagioclase is reasonable to explain the negative Eu anomalies, the proportion of amphibole is too low to explain why the more silicic samples are more REE depleted. Apatite and zircon are accessory phases in these rocks. Assuming they are relict, perhaps they were also involved in the fractionation, which would certainly lower the overall REE concentrations during fractionation. This possibility is admittedly speculative.

Analyses of felsic rocks labeled G in Table 1 (104-2 to 85-1) are from Georgia (Paris, 1990; German, 1990). Compared to the Alabama samples, on average the Georgia samples are enriched in SiO_2 and Na_2O, and depleted in Al_2O_3, MgO, CaO, and K_2O. On Figure 11 the Georgia samples plot in the rhyolite field, whereas most of the Alabama samples plot in the dacite field. The Georgia rocks can be characterized as soda rhyolites and their major-element compositions are similar to those of some similar age trondhjemitic rocks (Almond Trondhjemite and Bluff Springs Granite; Figure 2 and Table 1) in the Alabama eastern Blue Ridge (Russell, 1978; Drummond and others, 1997) discussed below. Thus, these soda rhyolites may be the volcanic equivalents of some eastern Blue Ridge trondhjemitic rocks, or their high Na contents may be the result of alkali metasomatism.

Chemical Homogeneity Within and Among Hillabee Greenstone Felsic Metavolcanic Rocks

Evidence presented above suggests that the HG felsic rocks have been affected by crystal fractionation/accumulation. When major-oxide compositions are plotted along vertical profiles within either the lower or upper major felsic sheets, however, no significant compositional correlations exist with stratigraphic position. Additionally, when major-oxide compositions are compared between these sheets, no significant compositional correlations exist either. Lastly, when major-oxide compositions are plotted along southeast-northwest lateral profiles which extend over distances of 5 and 10 km within the upper and lower major felsic sheets respectively, no significant compositional correlations exist. The absence of trends indicates a high degree of homogeneity both within and among the felsic sheets.

DISCUSSION

Age Constraints

The age of the HG is controversial because of conflict between field interpretations of the nature of its basal contact and results of isotopic

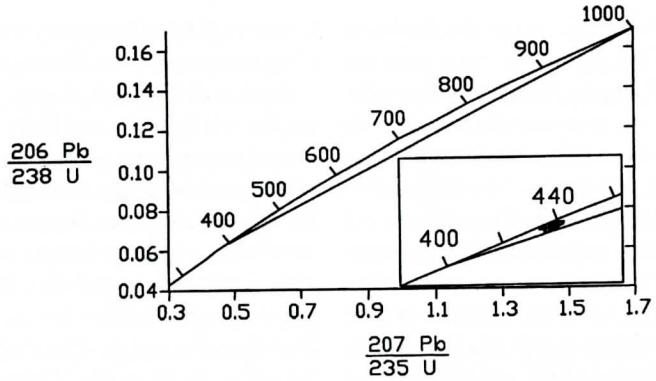

Figure 14. Pb^{206}/U^{238} - Pb^{207}/U^{235} concordia plot of zircons from Hillabee Greenstone felsic rocks (modified from Russell (1978) and Russell and others (1984). Reference isochron is from 400 Ma to 1000 Ma.

studies of the felsic units. The conflicting arguments relative to the age of the HG are reviewed below.

Age Interpretation Based on Field Studies

Several geologists (Tull and others, 1978; Tull and Stow, 1980; Paris and Cook, 1989; Paris, 1990; German, 1990) have argued that the lowermost units of the HG are stratigraphically interlayered volcanic, volcaniclastic, and epiclastic rocks that grade into metasedimentary rocks of the underlying Talladega Group which are as young as Devonian (earliest Mississippian?). Interlayering of quartz-rich epiclastic rocks with laminated mafic phyllites over an interval of several meters can be observed at a number of localities at the base of the HG. At other localities, however, this contact locally corresponds with an imbricate fault.

A second feature of the basal HG contact that supports a stratigraphic interpretation is its concordancy with stratigraphic units within both the HG and the underlying Talladega Group. For example, on a regional scale, the lower felsic metavolcanic unit maintains a concordant position within approximately 300 m of the basal contact along a strike length of >30 km, and for a minimum of 16 km across strike (Figs. 2 and 3). Other stratigraphic features internal to the HG are also concordant with the lower contact. These include primary stratabound massive sulfide deposits within a few tens of meters of the basal contact, extending concordantly for distances of at least 27 km (Tull and Stow, 1982), and magnetite-bearing quartzite (banded iron formation) about 100 m from the basal contact (Prouty, 1923; Paris and Cook, 1989; Paris, 1990; Heuler, 1993). Units of quartz-rich metasedimentary rocks (metachert, siliceous argillite, and metasandstone) form a sharp ridge immediately below the basal HG contact throughout its 230-km strike length (Tull and Stow, 1980; Paris and Cook, 1989; Paris, 1990; German, 1990; Heuler, 1993). The locally fossiliferous Lower to Middle Devonian Jemison Chert (Butts, 1926; Tull and others, 1988) and the Upper Devonian-Mississippian (?) Erin Slate (Gastaldo and others, 1993) underlie the HG. A rare plant species reported to occur near the Devonian/Mississippian boundary has been found in the Erin Slate (Gastaldo and others, 1993), but no other Carboniferous fossils have been documented from the Talladega belt. The Jemison Chert and Erin Slate fossils argue that the HG is no older than middle Paleozoic, if the interpretation of a stratigraphic contact is correct.

Age Based on Isotopic Studies

Zircons from the lower felsic unit of the HG are slightly discordant on a U/Pb concordia diagram (Figure 14) and have been interpreted as indicating an Early Ordovician age (Russell, 1978; Russell and others, 1984). Because this date is older than the rocks immediately under-

lying the HG, it has been interpreted to imply that the basal contact is tectonic (Russell, 1978). Russell (1978) obtained two zircon splits (magnetic and non-magnetic) that were slightly discordant, giving minimum Pb 207/206 ages of 444 and 458 Ma, which she suggested "are probably very close to the age of crystallization of the zircons." Additional U/Pb zircon analyses from the HG based upon size splits, are consistent with the earlier U/Pb determinations (Russell and others, 1984). The euhedral shapes suggest that the zircons are unlikely to have gone through a sedimentary cycle (Russell, 1978).

At least three zircon populations can be identified from the felsic metavolcanic rocks based upon morphology. These include: a) small, elongate, clear zircons (avg. 0.13 mm × 0.05 mm, axial ratio = 2.6) (Figure 15 b), b) larger, elongate, commonly concentrically zoned zircons, with both clear and clouded cores (avg. 0.285 mm × 0.08 mm, axial ratio = 3.56) (Figure 15 a and b), and c) equant, commonly concentrically zoned, some slightly rounded zircons, some with rounded and clouded cores (avg. 0.196 mm × 0.102 mm, axial ratios = 1.91) (Figure 15 a-g). The analyses of Russell (1978) and Russell and others (1984) involved large volumes of zircons (5-50 g^3), and thus likely homogenized the various fractions described above. Attempts to obtain U/Pb ages of small volumes (10-20 g^3) of the separate fractions described above, in order to test the interpretation of the earlier conventional U/Pb data, are currently in the initial stages.

Because of common zoning and the presence of rounded and clouded cores, the slightly discordant zircons of Russell (1978) and Russell and others (1984) can also be interpreted as falling on a mixing line between younger zircons with magmatic rims, representing the stratigraphically determined age (~400 Ma), and older inherited components, possibly including Grenvillian crust (~1000 Ma) (Figure 14). Units in the Talladega Group contain Grenville (U/Pb zircon ages ~1000 Ma) basement boulders (Telle and others, 1979), so that if the interpretation that the HG stratigraphically overlies this group is correct, it probably intruded through Precambrian crust and may have incorporated a xenocrystic zircon component.

Other isotopic techniques may approximate the time of greenschist facies metamorphism, and provide a minimum age of the HG. Russell (1978) obtained a K/Ar age of 382 ± 14 Ma from hornblende porphyroclasts in the lower felsic unit. Durham (1993) obtained a seven-point Rb/Sr whole-rock isochron from the 6-m thick McGehee Falls felsic unit of 395 ± 20 Ma (one sigma), with an initial 87Sr/86Sr value of 0.7082 ± 0.0010. Sr-isotopic ratios in volcanic rocks are particularly susceptible to rehomogenization during thermal metamorphism (Faure, 1986; Asmerom and others, 1991). The K/Ar hornblende and Rb/Sr ages from HG felsic metavolcanic rocks are within the range of K/Ar whole-rock slate ages (399 ± 17 Ma) reported by Kish (1990) from the underlying Talladega Group, which are interpreted as the age of regional metamorphism (Kish, 1990). The fossil discovery from the Erin Slate (Gastaldo and others, 1993), however, requires a post-Devonian regional metamorphism.

Origin as Pyroclastic Ash-flow Deposits

Our interpretations of the origin of the HG felsic rocks are based on the thickness and areal extent of the units, their internal textures and fabrics, and their whole-rock geochemistry. The observed sheet geometries are characteristic of pyroclastic flows erupted over subdued flat or gently sloping topography. The large volume (> 50 km^3) of individual sheets implies eruption from large stratovolcanoes, or possibly even more extensive sources associated with large caldera systems (Fisher and Schmincke, 1984).

The lack of significant vertical or lateral chemical or mineralogical compositional contrasts within either the lower or upper major felsic sheet also suggests ejection from large-volume systems of 102-10^3 km^3, in contrast to small volume systems that tend to show stronger compositional contrasts (Fisher and Schmincke, 1984). The homogeneity among the major felsic sheets suggests that the same eruptive center may have been responsible for many of the individual felsic sheets, and that

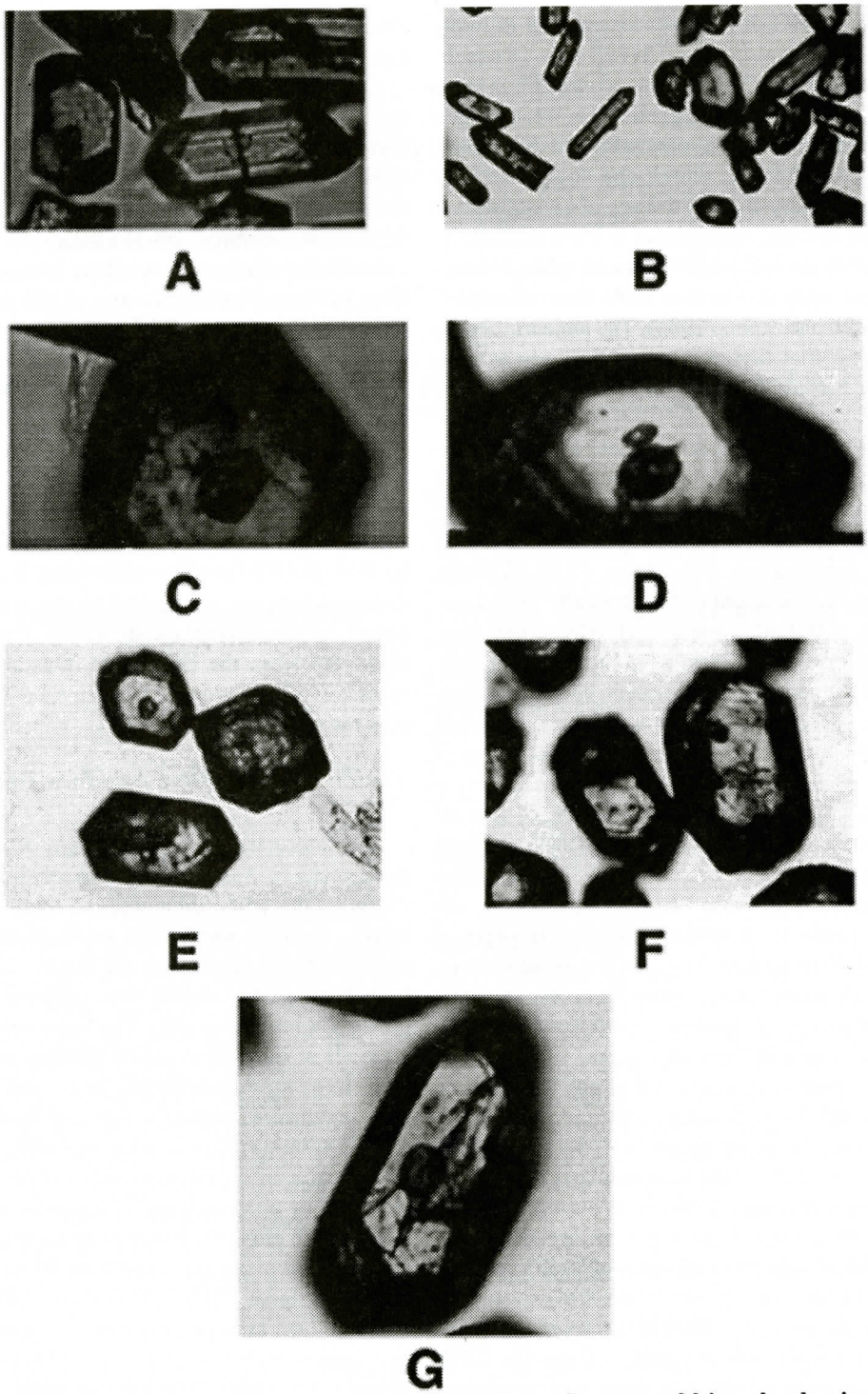

Figure 15. Photomicrographs of zircon populations from Hillabee Greenstone felsic rocks, showing evidence of inheritance with common zoning and cores. A, C, D, E, and F show zircons of population c, A and D show zircons of population b, and D shows all three populations (see text). Approximate long dimensions of photos are: C, D, and G = 0.3 mm; A, E, and F = 0.6 mm; B = 1.0 mm.

only a small volume of the magma chamber may have emptied during each eruption. HG felsic rocks, like pyroclastic flow deposits, generally form massive thick beds, without visible internal laminations. These features stand in contrast to subaerial fallout deposits (Fisher and Schmincke, 1984). The only known occurrence of nonmassive felsic rocks is a 0.5-m laminated interval near the top of the 6-m section at McGhee Falls, consisting of alternating clast-rich and clast-poor laminae a few cm thick. This layered zone may represent a pyroclastic surge deposit, although internal structures characteristic of surge deposits cannot be identified in these deformed rocks. Some of the angular porphyroclasts observed in the felsic units may have originally been broken during eruption and transport, as well as during deposition, also characteristic of ash-flow tuffs (Fisher and Schmincke, 1984). Although the nature of the original matrix of the HG metafelsites is obscure, it is interpreted as having originally been a very fine-grained felsic material, probably representing recrystallized glass shards and broken pumice fragments. Subsequent low-grade metamorphic recrystallization of the matrix did not result in the matrix exceeding the volcanic ash size range (<2 mm).

Lithic fragments (blocks) of cognate and accidental origin within the HG felsic rocks are rare. They have been observed at only one well exposed locality near McGhee Falls, within 10 m of the base of the lowermost major felsic unit. An angular fine-grained mafic (metabasalt) clast (6 cm × 24 cm) (Figure 5b) and an angular aphyric felsic lithic clast (8 cm × 24 cm) (Figure 5a) occur within homogeneous unbedded pyroclast-rich felsic metavolcanic rocks. The observation that this flow incorporated and transported fragments from the underlying metabasalt, as well as large pumice blocks, implies the ability to erode and transport large clasts. The mafic clast appears little deformed relative to the matrix, whereas the felsic clast has been flattened and elongated parallel to the slaty cleavage in the felsic rock (Figure 5a and b). These features support the observation that shear strain was differentially partitioned into the felsic relative to the mafic lithologies of the HG, but the magnitude of the strain was not great enough to significantly distort the lithic fragments. Importantly, block-size fragments apparently occur only at the base of the felsic sheets, implying that they may have been segregated by gravity from within a turbulent ash flow.

We suggest from the features described above that HG felsic metavolcanic rocks were transported via particulate flow as large-volume pyroclastic flows. Because they show no evidence of reworking or subsequent erosion, it is likely that they formed as densely welded tuffs (ignimbrites).

The question arises as to whether the HG is marine or non-marine. Interpretation of depositional setting as marine or non-marine rests upon examination of hundreds of exposures of both felsic and mafic rocks. No textures or structures, such as pillows or pillow fragment breccias, have been found that would suggest subaqueous deposition. Because the upper contact of the HG is tectonic and is coincident with the Hollins Line thrust and associated imbricate thrusts, no overlying metasediments are known. If the interpretation is correct that this volcanic sequence has a stratigraphic base at most localities, then the HG overlies shallow-water marine rocks, as indicated by fossil assemblages in the underlying Jemison Chert (Tull and others, 1988) (Figure 2). Assuming that formation of the volcanic sequence was relatively rapid, it is likely that the underlying shallow water sediments were quickly covered, and that the vast majority of the greater than 2 km-thick HG is subaerial. The rarity of metasediments intercalated within the metavolcanic sequence above the basal few tens of meters supports this contention. Only one such occurrence of a possible metasediment, a quartz sericite phyllite 5 m thick and traceable for 3 km, has been mapped (Tull and others, 1978) within the HG.

Tectonic Setting

In this section we examine the geologic and geochemical evidence bearing on the tectonic setting of the HG. Two scenarios are presented. The first assumes that the HG is Ordovician

based upon interpretation of the U/Pb ages and is exotic to the underlying Talladega Group, and possibly to Laurentia. The second assumes stratigraphic linkage of the HG to the Talladega Group based upon field relationships.

Exotic Setting of The Hillabee Greenstone

Acceptance of an Ordovician age based upon U/Pb zircon analyses for the HG requires a fault at the base of the metavolcanic sequence. As pointed out above, the structural top of the HG is either an imbricate thrust or the roof thrust of the Alleghanian Hollins Line fault. Therefore, an Ordovician age implies that the HG is entirely fault bounded, and may represent only a fragment (up to 2.5 km thick and 230 km long) of a more extensive volcanic complex. The imbricate and roof thrusts are discordant to units and metamorphic fabrics in both hanging and footwalls, and the roof thrust is a major metamorphic discontinuity. However, the basal HG contact is concordant to stratigraphy both in the HG and underlying units in the Talladega Group, and no metamorphic break occurs between the HG and the Talladega Group (see above).

Lower Ordovician micritic marbles occur in the lower Talladega belt within the Sylacauga Marble Group (Tull and others, 1988). There is no evidence for volcanic activity in this part of the stratigraphy. Silurian (?)-Devonian Talladega Group successor basin rocks deposited unconformably above the underlying Cambrian-Lower Ordovician shelf-facies rocks contain no volcanic detritus (Tull and Telle, 1989). Therefore, an Early Ordovician age of the HG would imply that the volcanic complex was originally located distally from equivalent-age rocks in the Talladega belt, which represent the most outboard portion of the Laurentian continental margin exposed in this portion of the orogen, and later obducted onto the Laurentian shelf prior to regional metamorphism. In this scenario, the metavolcanic complex must have been thrust atop the lower Paleozoic Laurentian shelf and the middle Paleozoic successor basin deposits of the Talladega Group before lower greenschist facies regional metamorphism, in order to be at the same metamorphic grade as the footwall rocks. Thus, this thrust must predate the imbricate faults which involve both the HG and upper Talladega Group stratigraphy. Such an exotic origin for the HG requires that understanding its tectonic setting rests entirely upon petrologic and geochemical interpretations. These interpretations are presented below.

Stratigraphic Linkage of the Hillabee Greenstone to the Talladega Group

Interpreting the metavolcanic rocks as occurring stratigraphically atop the Talladega Group implies linkage to the southeastern margin of Laurentia, and extrusion of the HG through continental crust along the Alabama continental promontory. The underlying Talladega Group is interpreted to have been deposited in an extensional basin formed above the foundered Laurentian lower Paleozoic shelf (Tull and Telle, 1989). Interpreting the HG to be at the stratigraphic top of this successor-basin sequence suggests that these volcanic deposits may have also formed within an extensional ensialic basin, such as a back-arc or pull-apart basin, suggesting A-type subduction beneath the Alabama Laurentian continental promontory. This interpretation, which is also compatible with a xenocrystic interpretation of the zircon data, is the one that the authors believe to be most likely.

Tectonic Discrimination Based Upon Petrology and Geochemistry

The HG metabasalts are clearly tholeiitic (Tull and Stow, 1980; Stow, 1982), but their tectonic setting based on tectonic discrimination diagrams is somewhat equivocal. Various trace-element tectonic discrimination diagrams used by Tull and Stow (1980), and Stow (1982) place the mafic rocks in the overlap region between island-arc tholeiites, calc-alkaline basalts, and ocean floor basalts (N-MORB to volcanic arc fields). This ambiguity for the metabasalt compositions extends to tectonic discrimination di-

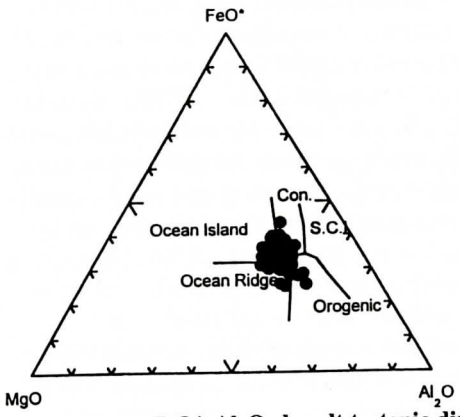

Figure 16. MgO-FeO*-Al_2O_3 basalt tectonic discrimination plot (from Pearce and others, 1977) showing positions of Hillabee Greenstone metabasaltic rocks. Data are from Tull and others (1978).

agrams for major elements (Figs. 16-17). On Figure 16 (after Pearce and others, 1977) the centroid of points falls near the intersection of four fields: orogenic, ocean ridge, ocean island, and continental. Figure 17.(after Mullen, 1983) is more definitive, suggesting that the metabasalts are similar in composition to island-arc tholeiites. This discriminator, however, is primarily applicable to oceanic basalts.

Rare-earth patterns for the HG metabasalts are linear and horizontal, with small positive Eu anomalies (suggesting plagioclase accumula-

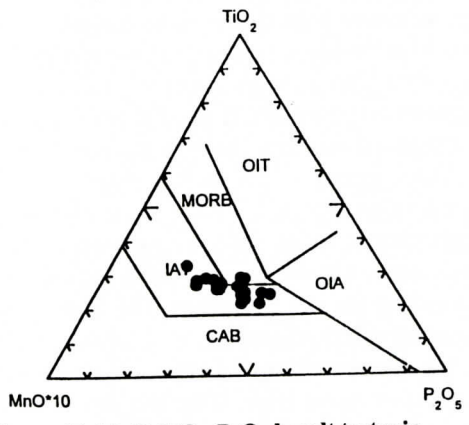

Figure 17. MnO-TiO_2-P_2O_5 basalt tectonic discrimination plot (from Mullen, 1983) showing field for Hillabee Greenstone metabasaltic rocks. Data are from Tull and others (1978).

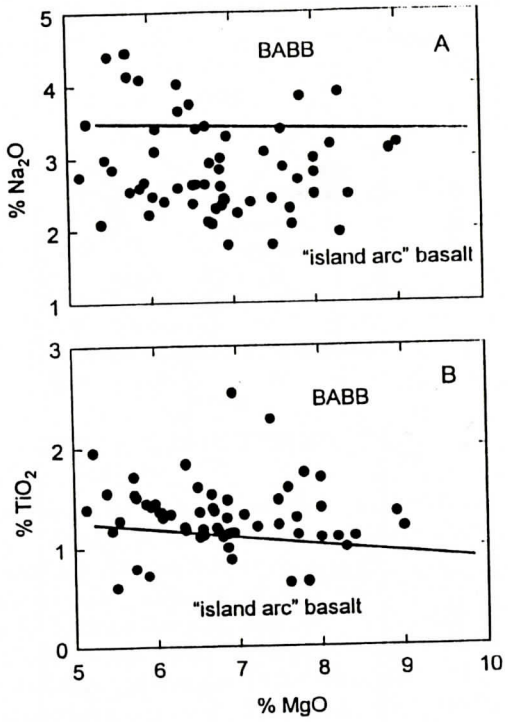

Figure 18. Tectonic discrimination diagrams (from Gamble and Wright, 1995) differentiating back-arc basin basalts and island arc basalts showing the positions of Hillabee Greenstone metabasaltic rocks: A) MgO-Na_2O, B) MgO-TiO_2. Data are from Tull and others (1978).

tion, as discussed above) and chondrite-normalized values ranging between 10 and 20 (Durham, 1993). Such patterns are typical of a variety of tholeiites, such as some back-arc basin basalts, arc (high-K) tholeiites, continental-rift tholeiites, and enriched mid-ocean basalts (E-MORBs). Figure 18 (from Gamble and Wright, 1995) illustrates additional ambiguity; the top graph (Figure 18a) suggests that most of the metabasalt samples are similar to island-arc basalts, whereas the bottom graph (Figure 18b) suggests a more likely affinity with back-arc basin basalts. Although Na is commonly more mobile during metamorphism, it can increase during such events, so that the plot in Figure 18a may have validity for these rocks. For more definitive conclusions, a more extensive geochemical database for the metabasalts, including isotopes and many more trace-element analy-

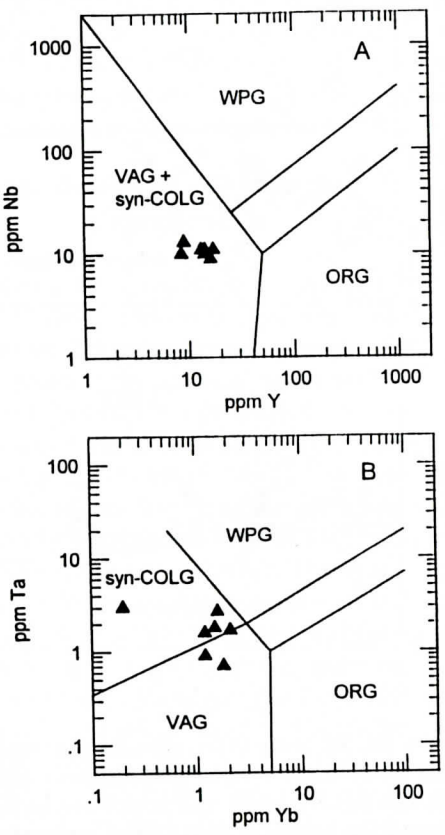

Figure 19. Trace-element tectonic discrimination plots from Pearce and others (1984) for Hillabee Greenstone felsic metavolcanic rocks. Source regions are designated as follows: VAG=volcanic-arc granite; WPG=within-plate granite; ORG=ocean-ridge granite; syn-COLG=syn-collisional granite.

ses, is needed.

Other important tectonic information, however, can be gained from the presence of the intercalated felsic rocks and their trace-element composition (Table 2). Based on certain trace elements, felsic rocks of the HG are similar in composition to volcanic-arc or syn-collisional granites (Figure 19, from Pearce and others, 1984). Such an origin could imply that the felsic metavolcanic rocks were erupted from the continentward flank of an arc and emplaced as ash flows within a back-arc basin, which was simultaneously erupting tholeiitic basalt. This scenario could explain the rarity of a bimodal suite, like the HG, consisting of tholeiitic basalt and calc-alkaline dacite in an extensional setting. Examples of coexisting basalts and dacites in apparent bimodal suites have been reported (e.g., Wharton and others, 1995), but unlike the HG, they are generally not tholeiitic and calc-alkaline, respectively. Bimodal suites in modern continental rifts, such as east Africa, usually involve basaltic and felsic alkaline rocks (e.g., Davies and Macdonald, 1987). Most dacites and rhyodacites are calc-alkaline rocks that are associated with compressional rather than extensional tectonics. It is informative however, to compare trace-element compositions of the felsic metavolcanic rocks of the HG with dacites and rhyodacites from extensional settings, including back-arc basins. Figure 20, a double chondrite-normalized spidergram (normalized to chrondites and the recalculated so that all patterns have the same Yb content), makes the comparison between five dacite and rhyodacite suites associated with back-arc basins or rifts. The samples can be divided into two groups: continental (Taos, Chios, Peru) and oceanic (Fiji, New Hebrides). The differences between these two groups are striking; approximately horizontal patterns for the oceanic samples, in comparison to relatively steep negative slopes for the continental samples. Unfortunately, there are gaps in the data for some samples (e.g., Chios). The HG felsic rock average (based on data in Table 2) is clearly similar to compositions for the other continental samples, in agreement with the stratigraphic arguments presented in the second scenario above that the HG was extruded through Laurentian crust. The agreement is particularly good between the HG average and the Peruvian back-arc sample.

Thus, geochemical tectonomagmatic discrimination diagrams of the felsic and mafic metavolcanic rocks, although somewhat equivocal, suggest an arc or continental back-arc basin setting for HG volcanism. The felsic rocks may have either originated in the former setting, or been emplaced into the latter setting from the flank of an adjacent arc. If the HG metavolcanic rocks formed in association with an arc or extensional continental back-arc setting, then the main body of the arc must now reside to the southeast. The tectonically overlying eastern

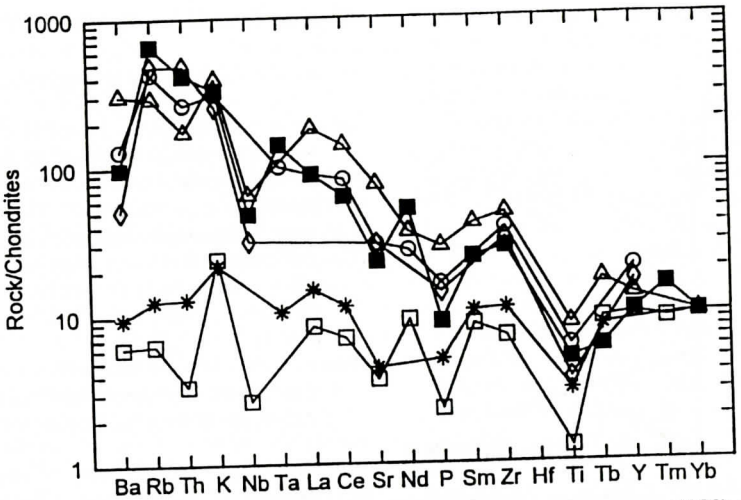

Figure 20. A double chondrite-normalized spidergram (values from Thompson, 1982) comparing the average Hillabee Greenstone felsic metavolcanic rock to five dacite and rhyodacite suites associated with extension in back-arc basins or rifts. The five dacite and rhyodacite suites were chosen based on their SiO_2 contents matching the average of the Hillabee samples (about 66 percent) as closely as possible (they range from 64 to 72 percent SiO_2). Data for the Hillabee samples are in Tables 1 and 2. Symbols are: closed squares -- Hillabee Greenstone felsic metavolcanic rocks (average of seven samples; open triangle -- Taos Plateau, northern New Mexico (McMillan and Dungan, 1988); open square -- Fiji (Wharton and others, 1995); open diamond -- island of Chios, Greece (Pe-Piper and others, 1995); open circle -- Peruvian Andes (Petford and Atherton, 1995); star -- New Hebrides (Maillet and others, 1995).

Blue Ridge allochthon contains Late Proterozoic metasedimentary and metavolcanic sequences. Thus, any Paleozoic arc complex must either be covered by this allochthon or have formed above it, and any volcanic superstructure has been eroded. A series of tonalitic, trondhjemitic, and granodioritic plutons ranging from 1-160 km^2 however, are distributed throughout much of the southern Appalachian eastern Blue Ridge allochthon (Miller and others, 1997), including Alabama, where tonalites and trondhjemites are common (Drummond and others, 1997) (Figure 2). There are no mafic or intermediate rocks associated with these plutons. The plutons range from ~470 to ~380 Ma (Miller and others, 1998), roughly the age of the HG based upon either U/Pb zircon or stratigraphic arguments. Zircons from this plutonic suite are euhedral, with magmatic rims, but contain almost ubiquitous inherited cores of highly variable age, including a predominance of Grenvillian ages (Miller and others, 1998). The possibility exists that the HG felsic metavolcanic rocks, which we interpret to be of generally similar age, could be genetically related to some of the plutons from this suite, and thus could have been sourced from within this allochthon. If so, HG zircons may record inheritance from an older source, including Grenville crust, but may also include xenocrysts from younger batholiths (e.g., the ~500 Ma Elkahatchee batholith [Russell, 1978]).

One possible origin of such a tonalite-trondhjemite-granodiorite (TTG) association is as a result of island-arc or continental-margin magmatism associated with subduction zones (Barker and others, 1976; Barker, 1979; Drummond and Defant, 1990), although a direct origin as slab melts for these rocks is debated (Kay and others, 1993; Miller and others, 1997). Figure 21 (adapted after Miller and others, 1997) shows that the HG felsic rocks are similar to typical arc volcanics and granites, and we infer that some of the eastern Blue Ridge tonalites

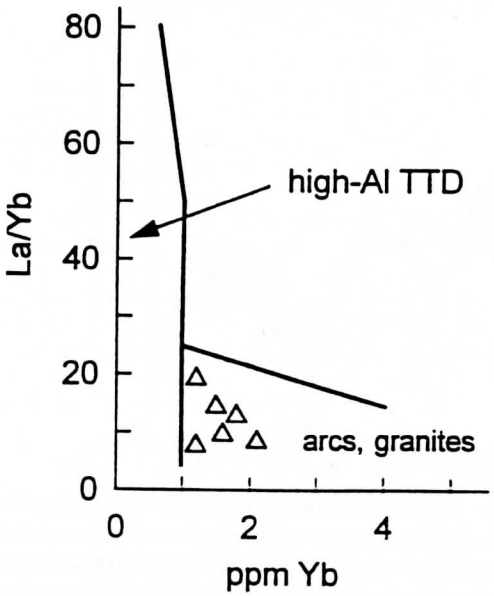

Figure 21. La/Yb vs. Yb plot (modified from Miller and others, 1997) showing positions of Hillabee Greenstone felsic metavolcanic rocks vs. the fields for arc granites and high-Al tonolite-trondhjemite-dacite (high-Al TTD) rocks.

and trondhjemites of similar age may be tectonically related to the HG.

ACKNOWLEDGMENTS

During our studies of the Hillabee Greenstone felsic metavolcanic rocks we have worked with several geologists who have given valuable assistance, insight, and advice. These include: Bert Hayes-Davis, Mark Drummond, Lamar Long, Roy Odom, Gail Russell, and Steve Stow. We are most appreciative to them for this. We are also indebted to Steve Kish for his contribution of some unpublished analyses and his aid with isotopic data, all of which are tabulated in Durham (1993). Erick Lockner preformed X-ray diffraction analyses on albite porphyroclasts. The manuscript was improved by reviews R. F. Dymele, R. D. Hatcher, Jr., E. McClellan, N. Rogers, S. Seaman, J. W. Shervais, S. Sorensen, and R. P. Tollo. Partial funding for this work was provided by the University of Alabama Mineral Resources Institute, the Alabama Geological Survey, and the National Science Foundation (EAR-8109056).

REFERENCES

Arth, J. G., and Barker, F., 1976, Rare-earth partitioning between hornblende and dacitic liquid and implications for the genesis of trondhjemitic-tonalitic magmas: Geology, v. 4, p. 534-536.

Asmerom, Y., Damon, P., Shafigullah, M., Dickinson, W.R., and Zartman, R.E., 1991, Resetting of Rb-Sr ages of volcanic rocks by low-grade burial metamorphism: Chemical Geology (Isotope Geoscience Section), v. 87, p. 167-173.

Barker, F., 1979, Trondhjemite: definition, environment, and hypotheses of origin, *in* F. Barker (ed.), Trondhjemites, Dacites, and Related Rocks, New York, Elsevier, p. 1-12.

Barker, F., Arth, J.G., Peterman, Z. E., and Friedman, I., 1976, The 1.7- to 1.8-b.y. old trondhjemites of southwestern Colorado and northern New Mexico: Geological Society of America Bulletin, v. 87, p. 189-198.

Bryan, W.B., Finger, L. W., and Chafes, F., 1969, Estimating proportions in petrographic mixing equations by least squares approximation: Science, v. 163, p. 926-927.

Bucher, K., and Frey, M., 1994, Petrogenesis of Metamorphic Rocks, New York, Springer-Verlag, 318 p.

Butts, C., 1926, The Paleozoic rocks, *in* G.I. Adams, C. Butts, L. W. Stephenson, and W. Cooke, Geology of Alabama: Geological Survey of Alabama Special Report 14, p. 40-223.

Davies, G. R., and Macdonald, R., 1987, Crustal influences in the petrogenesis of the Naivasha basalt-rhyolite complex: combined trace element and Sr-Nd-Pb isotope constraints: Journal of Petrology, v. 28, p. 1009-31.

DePaolo, D.J., 1981, Trace element and isotopic effects of combined wallrock assimilation and fractional crystallization: Earth and Planetary Science Letters, v. 53, p. 189-202.

Drummond, M.S., and Defant, M. J., 1990, A model for trondhjemite-tonalite-dacite genesis and crustal growth via slab melting: Archean to modern comparisons: Journal of Geophysical Research, v. 95, no. B13, p. 21,503-21,521.

Drummond, M.S., Nielson, M. J., Allison, D.T., and Tull, J. F., 1997, Igneous petrogenesis and tectonic setting of granitic rocks from the eastern Blue Ridge and Inner Piedmont, Alabama Appalachians, *in* Sinha, A. K., Whalen, J. B., and Hogan, J. P., eds., The Nature of magmatism in the Appalachian orogen: Boulder, Colorado, Geological Society of America Memoir 191, p. 147-164.

Drummond, M.S., Ragland, P.C., and Wesolowski, D., 1986, An example of trondhjemite genesis by means of alkali metasomatism, Rockford Granite, Alabama Appalachians: Contributions to Mineralogy and Petrology, v. 93, p. 98-113.

Durham, R. B., 1993, Petrochemistry of metadacite units in the Hillabee metavolcanic sequence, Talladega slate

belt, Alabama [M.S. thesis]: Tallahassee, Florida, Florida State University, 239 p.

Faure, G., 1986, Principles of isotope geology, 2nd edition: New York, John Wiley and Sons, 589 p.

Fisher, R.V., and Schmincke, H.-U., 1984, Pyroclastic rocks: New York, Springer-Verlag, 472 p.

Fridich, C.J., and Mahood, G.A., 1987, Compositional layers in the zoned magma chamber of the Grizzly Peak Tuff: Geology, v. 15, p. 299-302.

Gamble, J. A., and Wright, I. C., 1995, The Southern Havre Trough: geological structure and magma petrogenesis of an active backarc rift complex, *in* Taylor, B., ed., Backarc basins: tectonics and magmatism: New York, Plenum Press, p. 29-62.

Gastaldo, R.A., Guthrie, G.M., and Steltenpohl, M.G., 1993, Mississippian fossils from southern Appalachian metamorphic rocks and their implications for late Paleozoic tectonic evolution: Science, v. 262, N. 5134, p. 732-733.

German, J. M., 1990, Stratigraphic implications from core drilling in the vicinity of the Royal-Vindicator Gold Mine, Haralson County, Georgia: Georgia Geological Survey Information Circular 84, 19 p.

Griffin, R.H., 1951, Structure and petrography of the Hillabee sill and associated metamorphics of Alabama: Geological Survey of Alabama Bulletin 63, 74 p.

Heuler, G. F., 1993, Geology of the Talladega belt of Haralson County, Georgia and its boundary with the northern Piedmont [M.S. thesis]: Tallahassee, Florida, Florida State University, 168 p.

Hollocher, K., Spencer, J., and Ruiz, J., 1994, Composition changes in an ash-flow cooling unit during K metasomatism, west-central Arizona: Economic Geology, v. 89, p. 877-888.

Horton, J. W., Jr., Drake, A. A., Jr., Rankin, D. W., and Dallmeyer, R. D., 1991, Preliminary tectonostratigraphic terrane map of the central and southern Appalachians: U.S. Geological Survey Miscellaneous Investigations Series, Map I-2163.

Kay, S. M., Ramos, V. A., and Marquez, M., 1993, Evidence in Cerro Pampa volcanic rocks for slab melting prior to ridge-trench collision in southern South America: Journal of Geology, v. 101, p. 703-714.

Kish, S.A., 1990, Timing of middle Paleozoic (Acadian) metamorphism in the southern Appalachians- K-Ar studies in the Talladega belt, Alabama: Geology, v. 18, p. 650-653.

LeBas, M. J., LeMaitre, M. J., Streckeisen, R. W., and Zanettin, B., 1986, A chemical classification of volcanic rocks based on the total alkali-silica diagram: Journal of Petrology, v. 27, p. 745-750.

Long, A. L., 1981, Relationship between the structure and geochemistry of the copper deposits of the Hillabee Greenstone in the Millerville region, Clay County, Alabama [M.S. thesis]: Tuscaloosa, Alabama, University of Alabama, 233 p.

Maillet, P., Ruellan, E., Gerard, M., Person, A., Bellon, H., Cotten, J., Joron, J., Nakada, S., and Price, R. C., 1995, Tectonics, magmatism, and evolution of the new Hebrides backarc troughs (southwest Pacific), *in* Taylor, B., ed., Backarc basins: tectonics and magmatism: New York, Plenum Press, p. 177-235.

McMillan, N. J., and Dungan, M. A., 1988, Open system magmatic evolution of the Taos Plateau volcanic field, northern New Mexico: 3. Petrology and geochemistry of andesite and dacite: Journal of Petrology, v. 29, p. 527-557.

Miller, C. F., Fullagar, P. D., Sando, T. W., Kish, S. A., Solomon, G. C., Russell, G. S., and Wood Steltenpohl, L. F., 1997, Low-potassium, trondhjemitic to granodioritic plutonism in the eastern Blue Ridge, southwestern North Carolina-northeastern Georgia, *in* Sinha, A. K., Whalen, J. B., and Hogan, J. P., eds.,The nature of magmatism in the Appalachian orogen: Boulder, Colorado, Geological Society of America Memoir 191, p. 235-254.

Miller, C. F., Ayers, J. C., Hatcher, R. D., Jr., Coath, C. D., and Harrison, T. M., 1998, Age and inheritance of eastern Blue Ridge plutons, SW North Carolina-NE Georgia, by high-resolution ion microprobe: Geological Society of America: Abstracts with Programs, v. 30, no. 4, p. 51.

Moore, W.B., and Tull, J. F., 1989, Results of geologic mapping along the Hollins Line duplex terrane boundary, southern Appalachians: Geological Society of America Abstracts with Programs, v. 21, no. 3, p. 51.

Mullen, E.D., 1983, MnO/TiO2, P2O5: a minor element discriminant for basaltic rocks of oceanic environments and its implications for petrogenesis: Earth and Planetary Science Letters, v. 62, p. 53-62.

Nagasawa, H., and Schnetzler, C. C., 1971, Partitioning of rare earth, alkalic and alkaline earth elements between phenocrysts and acidic igneous magma: Geochimica et Cosmochimica Acta, v. 35, p. 953-968.

Paris, T. A., 1990, The Royal-Vindicator gold deposit, Haralson County, Georgia: A metamorphosed epithermal hot springs type gold deposits, *in* Cook, R. B., ed.: Proceedings of symposia on the economic mineral deposits of the southeast: metallic ore deposits: Georgia Geologic Survey Bulletin 117, p. 50-84.

Paris, T. A., and Cook, R. B., 1989, Exploration geology of selected gold prospects traditionally related to the Hillabee Greenstone, Alabama and Georgia, *in* Lesher, C.M. and others, eds.: Gold Deposits of Alabama: Geological Survey of Alabama Bulletin 136, p 33-59.

Pearce, J. A., Harris, N. B. W., Tindle, A. G., 1984, Trace element discrimination diagrams for the tectonic interpretation of granitic rocks: Journal of Petrology, v.25, n.4, p.956-983

Pearce, T. H., Gorman, B. E., and Birkett, T. C., 1977, The relationship between major element chemistry and tectonic environment of basic and intermediate volcanic rock: Earth and Planetary Science Letters, v. 36, p. 121-132.

Pe-Piper, G., Piper, D. J. W., Kotopouli, C. N., and Panagos, A. G., 1995, Neogene volcanics of Chios, Greece: the relative importance of subduction and back-arc exten-

sion, *in* Smellie, J. L., ed., Volcanism associated with extension at consuming plate margins: Geological Society of London Special Publication 81, p. 213-231.

Petford, N., and Atherton, M. P., 1995, Cretaceous-Tertiary volcanism and syn-subduction crustal extension in northern central Peru, *in* Smellie, J. L., ed., Volcanism associated with extension at consuming plate margins: Geological Society of London Special Publication 81, p. 233-248.

Prouty, W.F., 1923, Geology and mineral resources of Clay County with special reference to the graphite industry: Alabama Geological Survey Special Report 12, 190 p.

Roddy, M. S., Reynolds, S. J., Smith, B. M., and Ruiz, J., 1988, K-metasomatism and detachment-related mineralization, Harcuvar Mountains, Arizona: Geological Society of America Bulletin, v. 100, p. 1627-1639.

Russell, G. S., 1978, U/Pb, Rb-Sr, and K-Ar isotopic studies bearing on the tectonic development of the southernmost Appalachian orogen, Alabama [Ph.D.dessert.]: Tallahassee, Florida, Florida State University, 197 p.

Russell, G. S., Russell, C. W., and Golden, B. K., 1984, The Taconic history of the northern Alabama piedmont: Geological Society of American Abstracts with Programs, v. 16, no. 3, p. 191.

Scholz, C. H., 1988, The brittle-plastic transition and the depth of seismic faulting: Geologische Rundschau, v. 77, p. 319-329.

Stow, S. H. 1982, Igneous petrology of the Hillabee Greenstone, northern Alabama Piedmont, *in* Bearce and others, eds., Tectonic studies in the Talladega and Carolina slate belts, southern Appalachian orogen: Geological Society of America Special Paper 191, p. 79-92.

Telle, W. R., Tull, J. F., and Russell, C. W., 1979, Tectonic significance of the bouldery facies of the Lay Dam Formation, Talladega slate belt, Chilton County, Alabama: Geological Society of America Abstracts with Programs, v. 11, p. 215.

Thomas, W. A., 1993, Low-angle geometry of the late Precambrian-Cambrian Appalachian-Ouachita rifted margin of southeastern North America: Geology, v. 21, p. 921-924.

Thompson, R. N., 1982, Magmatism of the British Tertiary volcanic province: Scottish Journal of Geology, v. 18, p. 49-107.

Tull, J. F., 1982, Stratigraphic framework of the Talladega slate belt, Alabama Appalachians, *in* Bearce, D. N., Black, W. W., Kish, S. A., and Tull, J. F., eds., Tectonic studies in the Talladega and Carolina slate belts, southern Appalachian orogen: Geological Society of America Special Paper 191, p. 3-18.

Tull, J. F., 1984, Late Paleozoic deformation in the southeastern foreland and northwestern Piedmont of the Alabama Appalachians: Journal of Structural Geology, v. 6, no. 3, p. 223-234.

Tull, J. F., 1995, Hollins Line transpressional duplex: eastern-western Blue Ridge terrane boundary, Geological Society of America Abstracts with Programs, v. 27, no. 2, p. 93.

Tull, J. F., Allison, D. T., and Drummond, M. S., in press, Geology of the Millerville 7.5 minute Quadrangle, Clay County, Alabama: Alabama Geological Survey Quadrangle Series Map.

Tull, J. F., Harris, A. G., Repetski, J. E., McKinney, F. K., Garrett, C. B., and Bearce, D. N., 1988, New paleontologic evidence constraining the age and paleotectonic setting of the Talladega slate belt, southern Appalachians: Geological Society of America Bulletin, v. 100, p. 1291-1299.

Tull, J. F., Stow, S. H., 1980, The Hillabee Greenstone: A mafic volcanic complex in the Appalachian Piedmont of Alabama: Geological Society of America Bulletin, v.91, p. 27- 36.

Tull, J. F., and Stow, S. H., 1982, Geologic setting of the Hillabee metavolcanic complex and associated stratabound sulfide deposits in the Appalachian Piedmont of Alabama: Economic Geology, v. 77, p. 318-327.

Tull, J. F., Stow, S. H., Long. A. L., and Hayes-Davis, B., 1978, The Hillabee Greenstone: stratigraphy, petrology, structure, geochemistry, and mineralization: University of Alabama, Mineral Resources Inst. Research Report, No. 1, 100 p.

Tull, J. F., and Telle, W. R., 1989, Tectonic setting of olistostromal units and associated rocks in the Talladega slate belt, Alabama Appalachians, *in* Horton, J. W., and Rast, N., eds., Melanges and olistostromes of the Appalachians: Geological Society of America Special Paper 228, p. 247-269.

Wharton, M. R., Hathway, B., and Colley, H., 1995, Volcanism associated with extension in an Oligocene-Miocene arc, southwestern Viti Levu, Fiji: *in* Smellie, J. L., ed., Volcanism associated with extension at consuming plate margins, Geological Society of London Special Publication 81, 95-114.

Winkler, H. G. F., 1976, Petrogenesis of Metamorphic Rocks, New York, Springer-Verlag, 334 p.